LSU Doctoral Dissertations   Graduate School

2013

Development of Soluble Dietary Fiber Based Nanofiber Delivery System for Alpha-Tocopherol

Juan Li
Louisiana State University and Agricultural and Mechanical College

Follow this and additional works at: https://repository.lsu.edu/gradschool_dissertations

Part of the Life Sciences Commons

Recommended Citation

DEVELOPMENT OF SOLUBLE DIETARY FIBER BASED NANOFIBER DELIVERY SYSTEM FOR ALPHA-TOCOPHEROL

A Dissertation

Submitted to the Graduate Faculty of the
Louisiana State University and
Agricultural and Mechanical College
in partial fulfillment of the
requirements for the degree of
Doctor of Philosophy

in

The Department of Food Science

by
Juan Li
B. S., Hunan Agricultural University, 2007
M. S., Hunan Agricultural University, 2010
December 2013

TABLE OF CONTENTS

LIST OF TABLES

LIST OF FIGURES

ABSTRACT

The bioactive compound vitamin E is essential for human health. It has been reported to reduce the risk of cancer, cardiovascular disease, diabetes and aging. One of the main concerns about the availability of vitamin E is the stability, or lack thereof, associated with the processing and storage of it. Degradation could occur when vitamin E is exposed to light, temperature or oxygen, which results in the loss of efficacy. Also, the application of vitamin E is limited because of its poor solubility in aqueous media. Among the tocopherols contained in the vitamin E family, α-tocopherol (α -TOC) has the highest biological activity. Thus, development of a suitable delivery system for α -TOC which overcomes problems of solubility and stability is meaningful.

In the present study, development of a highly protective delivery system for α-tocopherol was conducted. The delivery system contemplated was based on soluble dietary fiber (SDF) based nanofibers. The first step in the development was fabrication of the nanofibers. They were fabricated by using electrospinning. Homogenous, smooth and bead-free nanofibers were electrospun from spinning solutions containing 3% SDF. SDF based nanofibers with an average diameter of 171.45 nm were observed. Then, α -TOC was encapsulated into SDF based nanofibers either by emulsion electrospinning or loading α -TOC into particles and subsequent incorporation into SDF nanofibers. High encapsulation efficiency and slow release of α-TOC in vitro were obtained for both loading forms of α-TOC in nanofibers. Stability tests of encapsulated α-TOC as a function of heat, UV irradiation and storage time were conducted. The SDF based nanofiber carrier protected α-TOC from degradation and maintained the most α-TOC during storage. The effect of SDF based nanofiber carried α-TOC on the lifespan of *C. elegans* was investigated. Increased lifespan was observed for both N2 and TK22 strains. Also,

significant increases of pharyngeal pumping rates were exhibited by TK22. The results suggested

SDF based nanofiber delivery system not only protected α-TOC from severe conditions, but also

enhanced its bioavailability.

CHAPTER 1   INTRODUCTION

Vitamin E is an important hydrophobic antioxidant which interacts with peroxyl radicals in cell membranes to prevent the propagation of free radical reactions. It has been reported that the consumption of vitamin E can help reduce the risk of several diseases, such as cancer, cardiovascular disease, diabetes and aging (Herrera and Barbas 2001). Natural vitamin E includes four tocopherols (α, β, γ, and δ) and corresponding tocotrienols (α, β, γ, and δ) of which α-tocopherol (α-TOC) has the highest biological activity (Herrera and Barbas 2001). Thus, daily supplementation of vitamin E is necessary. However, α-TOC has poor water solubility and is biologically unstable. α-TOC may be exposed to light, temperature, and/or oxygen during processing and storage, which results in degradation or isomerization and loss of its beneficial effects on human health.

Nanotechnology is an emerging technology that shows great potential in nutritional and functional foods production (Chen, Weiss and Shahidi 2006). Nano scale materials have numerous benefits such as faster intestinal absorption, higher cellular uptake, targeted delivery, and maximized in vivo effect. Nano-encapsulation is a significant technology that can preserve sensitive bioactive compounds by entrapping nutrients in a core structure within a protective shell. The nano-encapsulation of bioactive compounds not only protects them from severe processing and storage conditions, but can also achieve controlled release of encapsulated nutrients to a specific site (Luo et al. 2011).

Nanofibers are fibers with diameter ranging from 5 to 500 nm (Deitzel et al. 2001). Nanofibers have high surface area to volume ratio, tunable porosity, and malleability to form a variety structures for desired properties and applications (Sadri et al. 2012, Xu et al. 2012). They have been widely used for filtration, drug delivery, food texture alterations, encapsulation of

food additives, wound dressings and tissue engineering (Torres-Giner, Gimenez and Lagarona 2008). As a protective carrier, nanofibers shield from environmental oxygen, heat, and light. This could increase the stability of entrapped nutrients. Moreover, a bioactive compound can easily be loaded into nanofibers through an electrospinning process without severely influencing the compound's bioactivity. Also, the release profile can be precisely controlled through modulating the morphology, porosity and composition of the nanofibers.

Various materials including natural and synthetic polymers have been studied for use in the fabrication of nanofibers. Due to the biocompatible, biodegradable, and non-toxic property, biopolymers like food proteins and polysaccharides are ideal materials for nano-encapsulation of bioactive compounds for food applications. Polysaccharides have a wide variety of sources in nature. They are stable, non-toxic, and can be easily modified to produce a variety of derivatives. What's more, hydrophilic groups such as hydroxyl, carboxyl and amino groups contained in polysaccharides could interact with biological tissue, for example, in bio adhesion with epithelia and mucous membranes and thus increase the absorbance of encapsulated bioactive compounds (Liu et al. 2008).

Soluble dietary fiber is soluble in water. It includes pectin, β-glucan, guar gum and psyllium, which can be separated into viscous and non-viscous fibers. Abundant epidemiological studies have shown that high soluble dietary fiber intake could effectively reduce serum cholesterol and thus reduce the risk of cardiovascular disease. Soluble rice bran fiber (SDF) extracted from defatted rice bran with dilute alkali retains cholesterol lowering activity (Aoe et al. 1993a). The main components of hemicelluloses extracted from rice bran are arabinose and xylose with small amounts of galactose and glucose (Aoe et al. 1993a, Scheller and Ulvskov

2010). Hemicelluloses as coating materials have exhibited low oxygen permeability (Wan et al. 2011). These characteristics make SDF an ideal delivery system for bioactive nutrients.

In order to fabricate SDF nanofibers with sufficient protection, effective absorption and controlled release of encapsulated nutrients, cospinning polymers is required for nanofiber formation. Polyethylene oxide (PEO) is the simplest hydrophilic polymer. Due to the balanced hydrophobic and hydrophilic interactions of its chemical structure, it is soluble in water over a broad range of temperature (Branca et al. 2013). Because of its biocompatibility, non-immunogenicity and low toxicity, PEO has been widely used in the biomedical field (Bianco, Calderone and Cacciotti 2013). Besides, PEO is permitted by FDA as a food additive for direct addition to food for human consumption (FDA 2012).

The overall goal of this dissertation was to develop a highly protective and safe delivery system for α-TOC. A SDF based nanofiber delivery system should not only improve α-TOC stability but also enhance the bioavailability and controlled release property of α-TOC in vivo. Dietary fiber with its concurrent health benefits will also be consumed with the consumption of the α-TOC supplement. The SDF based nanofiber delivery system will not only be applied to α-TOC, but also can be applied to other hydrophobic nutraceuticals.

CHAPTER 2   LITERATURE REVIEW

2.1   Encapsulation and Nanotechnology

Encapsulation as a novel technology has gained increased interest in recent years. Encapsulation is the technology that incorporates core material into wall material. Core materials such as bioactive compounds, nutrients, and drugs are immobilized in a wall material or shell material such as polymers to achieve the desired purpose, i.e., protection or enhanced bioavailability. A number of encapsulation studies have been conducted in pharmaceutical and medical research for drug delivery, cancer treatments, and gene therapy. Encapsulation has shown a protective effect of encapsulated bioactive materials against changes in the environment, enzyme activity, extreme pHs, temperatures, and ionic strengths (Mozafari et al. 2008). The application of encapsulation technology in the food area has become popular in recent times. Sensitive bioactive components such as proteins, enzymes, vitamins, antioxidants and flavors are protected from severe environmental conditions or extreme processing conditions. The stability can be increased during processing and storage, and undesired interactions with the food matrix can also be prevented. More importantly, a controlled release of bioactive compounds can be achieved by specifically designed wall materials and to enhance bioavailability.

Nanotechnology as an emerging technology shows great potential in its application for production of nutritional and functional foods (Chen et al. 2006). Nano scale food materials prepared by physical and chemical energy have increased surface area to volume ratio, and are endowed with new outstanding characteristics that bulk materials do not have (Zhu et al. 2010). Compared with bulk materials, nano materials have tremendous advantages such as faster intestinal absorption, higher cellular uptake, target delivery and increased bioavailability (Feng et al. 2009).

2.2   Nanofiber Delivery System

Generally, the delivery system for encapsulated bioactive components can be solid or liquid, spherical or non-spherical particles, fibers or tubes and networks with gel-like or sponge-like characteristics (Arecchi, Mannino and Weiss 2010). Due to the unique properties, nanofiber delivery systems have attracted an increasing interest in recent years.

Several factors should be considered when creating a delivery system for nutrients for food applications: 1) all ingredients must be non-toxic with low cost; 2) the delivery system must be stable during processing and storage under different temperatures, light, oxygen, and mechanical forces; 3) the addition of a delivery system should not affect the characteristics of food products, such as appearance, texture, and flavor; and 4) controlled release of incorporated bioactive compounds (Ziani, Fang and McClements 2012).

2.2.1   Introduction of Nanofiber

Nanofibers are continuous filaments with a diameter ranging from several nanometers to one micrometer. They have very high surface area-to-volume ratios, high porosity, and are easy to use to fabricate different structures. Due to their unique properties, nanofibers have been widely used in the biomedical field for drug delivery, tissue engineering, wound dressing, as a biocatalysis and for biosensing (Xie, Li and Xia 2008), environmental protection such as filtration, metal ion adsorption and recovery, carriers for catalysts and enzymes, sensors, energy harvesting and storage (Fang 2011). As a delivery system, the release rate of encapsulated drugs or bioactive compounds can be controlled by modifying the structure, porosity, diameter and composition of nanofibers, as well as loading dosage and incorporation method of drugs or bioactive components (Qi et al. 2010).

2.2.2 Electrospinning for Nanofibers Production

Different methods have been developed to fabricate nanofibers, such as drawing, template synthesis, self-assembly, phase separation, melt-blowing, and electrospinning. Electrospinning is the simplest, most cost-effective and most capable method for large scale production of nanofibers (Fang 2011, Baba et al. 2013). Electrospinning technique was started in 1897, patented in 1934, and received much attention in the early 1990s (Kriegel et al. 2008). A basic set-up of electrospinning includes a high voltage power supply, a syringe pump, a syringe with a flat-end metal needle, and an electrically conductive collector (Figure 2.1). Spinning solutions are stored in a syringe and fed by a syringe pump. A needle is fixed to a bracket with adjustable height. An electrode of power supply is connected to the needle, and another one is attached to the grounded collector. During electrospinning, a DC voltage is applied on the needle containing the spinning solution, and the surface of the spinning solution is charged. Mutual charge repulsion and the contraction of the surface charges to the counter electrode cause an opposite force to the surface tension (Huang et al. 2003). The increase in intensity of the electric field, a conical shape known as the Taylor cone is formed on the surface of a drop at the needle tip in order to balance the repulsion and the surface tension of the drop. A liquid jet of solution is generated from the cone tip once the critical voltage is achieved, and the jet is accelerated towards the grounded collector by electrical potential in a whipping motion to form continuous thin fibers (Fung, Yuen and Liong 2011). Solvent is evaporated during the process and leaves behind a charged fiber.
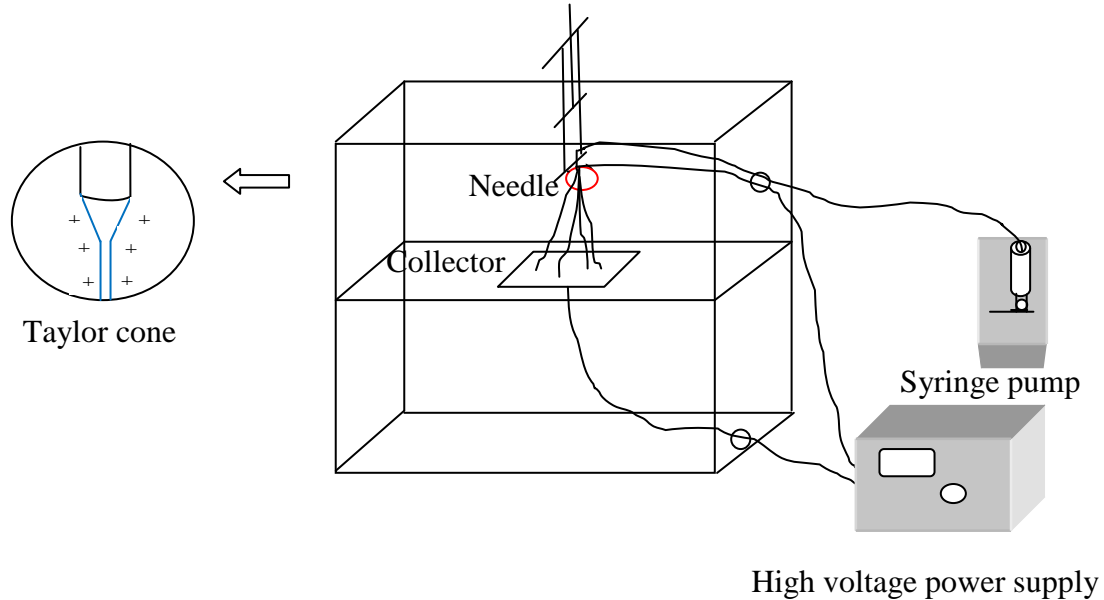
Figure 2.1 Schematic diagram of a basic set-up of electrospinning system

Spinning solution properties and processing parameters affect the electrospinning process (Yu 2009, Kriegel et al. 2008), with molecular weight, structure of polymer such as branched or linear, viscosity, conductivity, dielectric constant and surface tension as main factors that influence the electrospinning process. Viscosity of the polymer solution as a key parameter in electrospinning has a significant effect on the morphology of nanofibers. On one hand, low viscosity means low concentration of the polymer, in which finer nanofibers may result. On the other hand, lower viscosity means lower viscoelastic force, where the jet is more likely to break up and form droplets. Thus the viscosity of polymer solution should be high enough to prevent the jet from breaking apart into droplets. For processing parameters, voltage, distance between the tip and collector, temperature, humidity and air velocity in the chamber, and the flow rate, impact the electrospinning, which voltage as the most important factor. A high voltage is required to form a stable Taylor cone, thus the jet can be ejected. Also, the nanofiber diameter is affected by the voltage (Kriegel et al. 2008). When the solution conditions and the process

conditions are not ideal, the jet may break apart into little droplets and particles will be collected in the collector rather than fibers.

Electrospinning techniques, including conventional, coaxial and emulsion electrospinning, have been used for bioactive components entrapped nanofibers production. For conventional electrospinning, bioactive components are entrapped within using polymers, and for coaxial and emulsion electrospinning, bioactive components and drugs are encapsulated within nanofibers. Conventional electrospinning is easier than coaxial and emulsion electrospinning due to the preparation process of spinning solutions. However, an apparent initial burst release of embedded drugs or bioactive compounds is formed (Qi et al. 2010). Coaxial electrospinning is used to fabricate core-sheath nanofibers (Ji et al. 2013, Maleki et al. 2013, Chang et al. 2013, Huang et al. 2013, Thuy et al. 2012, Kriel, Sanderson and Smit 2012, Pakravan, Heuzey and Ajji 2012). Even though the initial burst release can be reduced in core-sheath nanofibers, the electrospinning setup is complicated and the process is challenged. In coaxial electrospinning, there are two different solutions, one is supplied to the inner capillary and another is supplied to the outer capillary. Thus, a double-compartment syringe with a core-shell nozzle or two separate syringe pumps for supplying two polymer solutions and pipelines leading to a core-shell nozzle are required. In order to synthesize high quality nanofibers, the solvent for the inner solution and the electrospinning conditions should be optimized. Emulsion electrospinning is developed to fabricate core-sheath nanofibers with a conventional elestrospinning setup (Xu et al. 2006). Emulsion electrsospinning differs from conventional electrospinning, an emulsion is used as electrospinning solution instead of polymer/nutrient blend.

2.2.3 Application of Nanofiber in Nutraceutical Delivery

The application of nanofiber for biomedicine and drug delivery has attracted substantial interest and has been summarized in recent reviews (Goh, Shakir and Hussain 2013, Sridhar et al. 2013, Pillay et al. 2013, Leung and Ko 2011, Cui, Zhou and Chang 2010, Chakraborty et al. 2009, Yoo, Kim and Park 2009, Li, Mauck and Tuan 2005, Xie et al. 2008). Due to their unique properties, the application of nanofibers for nutraceutical delivery and food science is getting popular recently.

Food ingredients such as vitamins, probiotics, functional lipids and amino acids serving as bioactive components play an important role in human health. Even though they have functional ability, they are sensitive and unstable when expose to extreme environments. Utilization of nanotechnology on nutraceuticals can protect them during processing, storage and gastrointestinal transit before they reach the target. Nanofibers can be used for nutrients delivery and to protect encapsulated bioactive compounds against heat, pH, moisture and light (Konwarh, Karak and Misra 2013). Also, controlled release can be achieved and the bioavailability of nutraceuticals can be improved. The application of nanofibers as carriers of bioactive nutrients was summarized below.

2.2.3.1 Polyphenol

Curcumin was incorporated into electrospun cellulose acetate fibers with average diameters ranging from 314 to 340 nm (Suwantong et al. 2007). The release assay of curcumin showed that almost all of the curcumin incorporated in nanofibers was released into the medium. Curcumin retained its antioxidant activity after electrospinning with a high electrical potential. Other studies of incorporation of curcumin into electrospun fibers have been conducted (Suwantong, Ruktanonchai and Supaphol 2010, Brahatheeswaran et al. 2012).

In the study by Li et al. (2009), an electrospun zein nanofiber was used as a carrier for tea polyphenol (-)-epigallocatechin gallate (EGCG) to improve its stability. They found that EGCG loaded nanofiber, after aging at 0% relative humidity for at least 1 day, had better protection and recovery (>98%) of polyphenol than freshly spun nanofibers (82% recovery).

Raspberry extract was incorporated into electrospun soy protein isolate-based fibers (Wang et al. 2013). The study showed that the addition of anthocyanin-rich red raspberry extract (ARRE) affected the electrical conductivity of electrospinning solutions, which decreased with increasing ARRE. ARRE addition did not change the fibers morphology significantly. Also, the spinning solution had a higher level of anthocyanins when ARRE was added after soy protein isolate denaturation, and a greater antibacterial activity was observed in ARRE loaded electrospun fibers.

2.2.3.2 Vitamin

Fernandez et al. (2009) successfully encapsulated light sensitive antioxidant β-carotene in zein electrospun fibers. The cross-section diameter of β-carotene encapsulated zein fibers ranged from the micro to nano scale. β-carotene was widely dispersed inside the fibers and was stable. Also, the encapsulated β-carotene had a significantly increased light stability when exposed to UV-vis irradiation.

Electrospun cellulose acetate nanofibers were used as delivery carriers for Vitamin A and vitamin E to the skin (Taepaiboon, Rungsardthong and Supaphol 2007). Smooth fibers with average diameters ranging from 247 to 265 nm were obtained. Compared with vitamin loaded cast films, vitamin loaded electrospun fibers exhibited a gradual increase without a burst release of vitamins.

2.2.3.3 Enzyme

Electrospun fibers can be used as a delivery system for enzymes. Superoxide dismutase (SOD) was loaded into PLLA electrospun fibers and its antioxidant activity was investigated (Chen et al. 2010). The study reported that no obvious initial burst release of SOD from electrospun fibers was observed. The antioxidant activity of SOD remained stable during electrospinning and the release process, and the released SOD had high antioxidant activity.

2.2.3.4 Probiotics

Probiotic *B. animalis* Bb12 was encapsulated into poly(vinyl alcohol) electrospun nanofibers by coaxial electrospinning (Lopez-Rubio et al. 2009). The electrospun fibers had an average diameter of 150 nm. It was reported that the melting point and crystallinity of nanofibers decreased and the glass transition temperature was increased with the incorporation of probiotics. Encapsulated *B. animalis* Bb12 remained viable for 40 d at room temperature and 130 d at 4 °C, while a significant decrease was observed in non-encapsulated bacteria.

2.2.3.5 Other functional compounds

The extracts from the fruit hull of mangosteen was successfully incorporated into electrospun poly (vinyl alcohol) fibers (Opanasopit et al. 2008). The average diameter of extract-loaded fibers was 197.3 nm with clear and smooth surfaces. An initial burst release of extracts was observed on extracts-loaded fibers compared with extracts-loaded cast films.

Antioxidant ferulic acid was also encapsulated in zein fibers using coacial electrospinning (Yang et al. 2013). A higher quality of ferulic acid loaded fibers with a rounder morphology, more homogeneous structures, smaller diameters and narrow size distribution were obtained compared to fibers prepared by the single-fluid electrospinning process. Ferulic acid was encapsulated into zein fibers by hydrogen bonding and presented in an amorphous state. The in vitro release tests showed that ferulic acid encapsulated in zein fibers produced by coaxial

electrospinning had better sustained release profiles with a smaller initial burst effect and less tailing-off release than those fabricated by the single process.

Gallic acid, a naturally antioxidant, was encapsulated into zein nanofibers with cross-section diameters ranging from 327 to 387 nm (Neo et al. 2013). It was reported that gallic acid had retained DPPH scavenging activity before and after incorporation in zein nanofibers. A different thermal stability of gallic acid loaded zein fibers was shown because of the incorporation of gallic acid. The incorporation of gallic acid into ploy(L-lactic acid) electrospun fibers was also studied (Chuysinuan et al. 2009).

Electrospun nanofibers can be a carrier for emulsions containing lipophilic bioactive compounds. An antimicrobial phytophenol (eugenol) was encapsulated into poly (vinyl alcohol) nanofibers and the mean diameter of fiber ranged from 57 to 126 nm with a broad distribution (Kriegel et al. 2009). The diameter of nanofibers decreased with increased surfactant content and decreased eugenol concentration. Eugenol droplets were homogenously dispersed in the nanofibers.

2.2.4   Nanofiber Materials

Polymers, including synthetic and natural, have been successfully electrospun into nanofibers. Synthetic polymers, such as polylactide (Zhang et al. 2012), polyglycolide acid (PGA) (You et al. 2005), and polycaprolactone (PCL) (Song et al. 2013), polyglycolic acid (PGA) (Aghdam et al. 2012), polylactic acid (PLA) (Hu et al. 2013a), polyethylene oxide (PEO) (Jacobs, Patanaik and Anandjiwala 2011), and polyvinylacetate (PVA) (Park, Lee and Bea 2008) are commonly used for nanofiber fabrication because of their low cost, high availability, and they have more choices of well-defined molecular and functional characteristics. Biopolymers have gained increased interest especially in the application of nanofibers in the food industry due to the safety concern. They are biocompatible, biodegradable, nontoxic and renewable. What's

more, additional value is added when using biopolymers as raw material for nanofiber fabrication. Polysaccharides and proteins are two large groups of biopolymers that are used for nanofibers fabrication, they are generally recognized as safe (GRAS). Many biopolymers have been investigated for nanofiber production. For instance, polysaccharides include chitosan (Dogan et al. 2013), alginates (Bonino et al. 2012), cellulose and cellulose derivatives (Xiang et al. 2013, Konwarh et al. 2013), and dextran (Unnithan et al. 2012); proteins include collagen (Kobayashi et al. 2013), gelatin (Hu et al. 2013b), casein (Xie and Hsieh 2003), wheat protein (Woerdeman et al. 2005), zein (Yao, Li and Song 2009), eggshell membrane proteins (Xiong et al. 2012), egg albumen (Rathna, Jog and Gaikwad 2011), bovine serum albumin (Zhang et al. 2006), and silk fibroin (Sheng et al. 2013).

However, the fabrication of nanofibers from biopolymers is limited by the properties of polymers. Usually, the preparation of biopolymers is time consuming, and sometimes purification is required, which is high-cost. Also, since they have a relatively high level of crystallinity or polarity, biopolymers have low solubility in most organic solvents. What's more, because of the strong hydrogen bonds, many biopolymer solutions may have a high viscosity or form gel, which may not be good for electrospinning. The poor mechanical properties of biopolymer fibers is also one concern (Kriegel et al. 2008). Thus, synthetic polymers are usually used together with natural polymers to overcome the limitations. It is considered that synthetic polymers have more flexible chains, which can wrap themselves around the more rigid biopolymers, therefore the required linkages and entanglements are provided and the blend solution can be successfully electrospun into nanofibers (Duan et al. 2004). In addition, the biocompatibility of nanofibers can be improved and good mechanical properties can be reached when blending biopolymers and synthetic polymers for nanofiber production (He et al. 2005).

2.3   Soluble Rice Bran Dietary Fiber

2.3.1   Dietary Fiber

According to American Association of Cereal Chemists (AACC 2001), dietary fiber is the edible parts of plants or analogous carbohydrates that are resistant to digestion and absorption in the human small intestine with complete or partial fermentation in the large intestine. It includes polysaccharides such as cellulose and hemicellulose, oligosaccharides, lignin, and associated plant substances such as waxes, cutin, and suberin. Epidemiological studies have shown that high dietary fiber intake effectively prevents colon cancer (Fechner, Fenske and Jahreis 2013), breast cancer (Li et al. 2013), atherosclerosis (Eussen et al. 2011) and development of non-insulin dependent diabetes mellitus (Moore, Park and Tsuda 1998, Cho et al. 2013), as well as reduces serum cholesterol and thus reduces the risk of cardiovascular disease (Hu and Yu 2013, Viuda-Martos et al. 2010).

Dietary fiber can be divided into soluble and insoluble fibers. Soluble dietary fiber is soluble in water (Doleyres, Fliss and Lacroix 2002). It includes some hemicellulose, pectin, β-glucan, gums, psyllium and storage polysaccharides, which can be separated into viscous and non-viscous fibers. For soluble viscous but relatively non-fermentable fibers, a gel is formed that binds bile acids in the small intestine and thus increases their excretion in the feces. For soluble non-viscous fibers, fermentation takes place in the caecum and colon to produce short chain fatty acids (e.g. acetate, propionate, and butyrate), which may indirectly reduce blood cholesterol through inhibition of hepatic cholesterol synthesis (Gunness and Gidley 2010).

2.3.2   Soluble Rice Bran Dietary Fiber

Dietary fiber can be obtained from cereals, legumes, fruits, vegetables, nuts, and seeds. Cereals as a primary source of dietary fiber contribute 50% of the fiber intake in western countries (Lambo, Oste and Nyman 2005). Rice bran is a by-product during rice milling, and

consists of 10% of the grain composition together with germs. Rice bran can be a good source of dietary fiber (Randall et al. 1985). Rice bran contains high amounts of dietary fiber ranging from 25.5% to 40%, and soluble dietary fiber ranging from 2.3 to 4.3% (Aoe et al. 1993a, Abdul-Hamid and Luan 2000, Sudha, Vetrimani and Leelavathi 2007).

Soluble rice bran fiber (SDF) is extracted from defatted rice bran with dilute alkali solution. SDF primarily contains hemicelluloses, which are a heterogeneous group of polysaccharides with β- (1→4)-linked backbones. The main monosaccharide components of soluble hemicelluloses extracted from rice bran are arabinose and xylose with small amounts of galactose and glucose (Aoe et al. 1993a, Scheller and Ulvskov 2010, Wan, Prudente and Sathivel 2012).

2.3.3   Health Benefits of Soluble Rice Bran Fiber

SDF extracted from rice bran exhibited health benefits, such as antioxidant activity, cholesterol lowering capacity, immune modulation and antitumor properties, which are summarized below.

2.3.3.1 Antioxidant activity

It has been reported that polysaccharides from rice bran have strong antioxidant properties. Zha et al. (2009b) tested the antioxidant properties of polysaccharide extract from rice bran with hot-water. They found that the polysaccharides composed of 54.1% of Glu, 10.5% of Man, 21.7% of Gal, 7.4% of Rib and 6.3% of Ara had good capability of scavenging superoxide radical, hydroxyl free radical and anti-lipid peroxidation at concentration of 1.0 mg/mL. They also compared the antioxidant activity of water extracted polysaccharides and NaOH extracted polysaccharides (Zha et al. 2009a). The results showed that 5% (w/v) NaOH extracted polysaccharides had higher hydroxyl free radical scavenging capability of 84.8% than water at a with the concentration of 1.0 mg/mL.

The antioxidant activity of xylo-oligosaccharides (XO) obtained from rice bran was also evaluated (Veenashri and Muralikrishna 2011). This study showed that XO from rice bran had antioxidant activity of 60% with XO concentration of 1000 µg/mL by DPPH and ferric reducing anti-oxidant power (FRAP) assays, and had a better antioxidant activity co-efficient compared with XO from ragi, maize and wheat brans. Another study was also conducted by the same authors on the antioxidant activities of soluble hemicellulosic saccharides extracted from rice bran (Rivas et al. 2013). The results demonstrated that hemicellulose-derived saccharides had radical scavenging capacity and protected the emulsion against oxidation, and these capacities were dependent on the concentration.

2.3.3.2 Antitumor activity

Antitumor activity is another health benefit of SDF. Takeshita et al. (1992) examined the antitumor activity of rice bran polysaccharides, and reported that they prevented the reduction in immunocompetence, suppressed carcinogenesis and prolonged the survival rate of rats with gastrointestinal cancer. Aoe et al. (1993b) examined the effect of rice bran hemicellulose on intestinal carcinogenesis of rats, and found that hemicellulose fed rats had significantly lower incidence and number of colon tumors than those fed with the basal control diet. Wang et al. (2009) evaluated the antitumor activities of polysaccharides obtained from defatted rice bran. They reported that sulfated polysaccharides showed strong antitumor activities in vitro. Even though antitumor activities of soluble rice bran fiber are reported, the relationship between the structure and activity still needs to be verified.

2.3.3.3 Cholesterol lowering capacity

Many studies have verified the cholesterol lowering and bile acid binding capacity of rice bran in vitro/vivo over the last two decades (Newman et al. 1992, Kahlon et al. 1992, Rouanet, Laurent and Besancon 1993, Kahlon et al. 1993, Gerhardt and Gallo 1998, Kahlon and Woodruff

16

2003, Cheng et al. 2010). Water soluble fiber or water soluble hemicellulose plays an important role in lowering cholesterol capacity. It is reported that feeding dietary fibers rich in soluble fiber produces lower serum and liver cholesterol concentrations than does feeding commonly water-insoluble fiber (Anderson, Jones and Riddellmason 1994). Similar results were reported by Hu et al. (2013), they investigated the cholesterol and bile acid scavenging ability of rice bran hemicellulose. This study confirmed that rice bran hemicellulose has high cholesterol and bile acid binding capacity, while insoluble dietary fiber has poor binding ability. Soluble rice bran fiber extraction does not influence its functional capacities. It also confirmed that SDF extracted from defatted rice bran with dilute alkali retains cholesterol lowering activity (Aoe et al. 1993a).

2.3.4 Application of SDF in Food Field

Due to the health benefits, SDF can be added to various food products as a functional ingredient. Besides physiological functions, water-holding capacity, viscosity, gel-forming ability and fat-binding capacity of dietary fiber can be provided to foods. Thus, food properties are improved (Abdul-Hamid and Luan 2000, Sudha et al. 2007). The application of dietary fiber in food products has been reviewed (Kim and Paik 2012, O'Shea, Arendt and Gallagher 2012, Havrlentova et al. 2011). SDF can be explored as a novel potential antioxidant and for protecting sensitive compounds against oxidation. Wan et al. (2011) applied SDF on microencapsulation of fish oil, and the study demonstrated that SDF effectively inhibited fish oil oxidation.

2.4 Vitamin E

2.4.1 Introduction of Vitamin E

Vitamin E is an important hydrophobic antioxidant in the human body, which interacts with peroxyl radicals in cell membranes to prevent the propagation of free radical reactions. It has been reported that the consumption of vitamin E can help people reduce the risk of several diseases, such as cancer, cardiovascular disease, diabetes and aging (Herrera and Barbas 2001).

17

Natural vitamin E includes four tocopherols (α, β, γ, and δ) and corresponding tocotrienols (α, β, γ, and δ), and the structures are shown in Figure 2.2 (Sabliov et al. 2009). α-tocopherol (α-TOC) has the highest biological activity (Herrera and Barbas 2001), one α-TOC molecule can trap two peroxyl radicals.

α-TOC is light yellow oil that is soluble in oils, fats, and organic solvents, including acetone, ether, alcohol and chloroform. α-TOC are abundant in wheat germ, sunflower seeds, extra virgin olive oil, peanut oil, corn oil and soybean oils (Sabliov et al. 2009). Although the deficiency of vitamin E is rare in humans, the susceptibility to free radical damage could be increased due to the minute deficiency, especially in premature infants and hypercholesterolemic individuals, which results in neuromuscular abnormalities, myophthies, and neurological diseases (Luo et al. 2011). The daily recommended intake of α-TOC is 22.7 mg/day for adults, and 600-800 mg/day for patients with cancer, artherosclerosis and coronary heart diseases (Shukat, Bourgaux and Relkin 2012). Thus, daily supplementation of vitamin E is necessary.

However, α-TOC is not soluble in water and is biologically unstable. When α-TOC is exposed to light, temperature, and oxygen during processing and storage, it may degrade and thus lose its health benefits. Sabliov et al. (2009) reported that the free form of α-TOC had the highest degradation rate when heated at 180 °C, but no degradation happened when it was exposed to UV light for 6 hours. The dissolved form of α-TOC in both methanol and hexane degraded significantly after being exposed to UV light, but a smaller degradation rate was observed than the free form at high temperatures. Since α-TOC has poor water solubility, it is very difficult to mix in aqueous media and it limits the application of VE in a food system. So it is important to select an ideal delivery system for α-TOC. Different delivery systems have been studied for vitamin E and are discussed below.
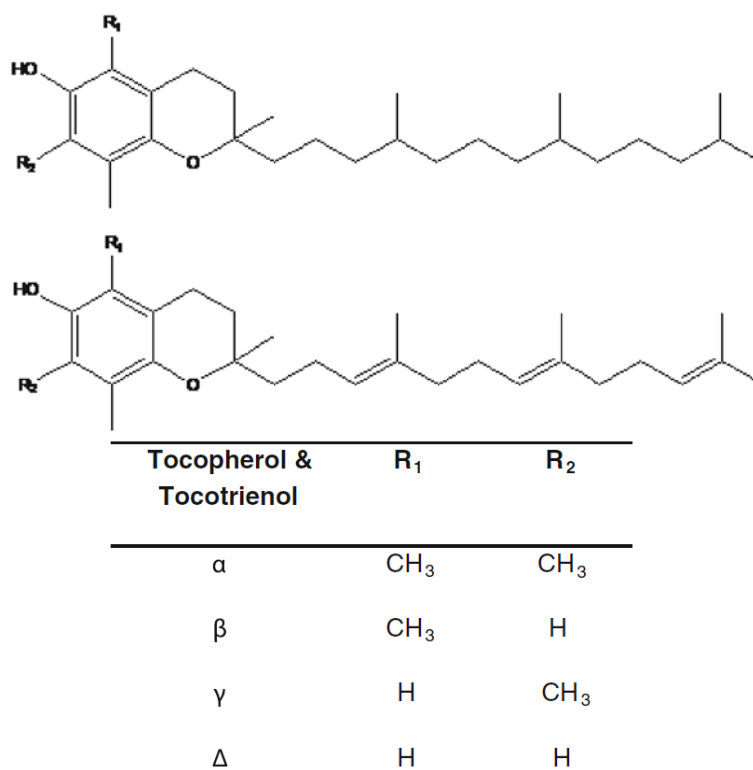
Figure 2.2 Structure of vitamin E. Source: Sabliov et al. (2009)

2.4.2 Delivery Systems for Vitamin E

2.4.2.1 Emulsion delivery system

For lipophilic bioactive compounds, the commercial way is to incorporate them into an aqueous matrix which is suitable for oral consumption. An emulsion delivery system is a convenient way to do this. Feng et al. (2009) used oil-in-water microemulsions as delivery systems for vitamin E. They reported that vitamin E had a lower release ratio in a microemulsion system compared with free vitamin E solutions, and no cell toxicity was observed.

A nanoemulsion system was also evaluated for vitamin E delivery. Laouini et al. (2012) prepared a nanoemulsion delivery system for α-TOC by the membrane emulsification method. They selected Tween80 and Brij35 (polyoxyethylene glycol dodecyl ether) as surfactants and medium chain triglyceride (MCT) as the oil phase due to the solubility of α-TOC. The results

showed that stable nanoemulsions (zeta potential = -22.9 mV) were produced using a 0.9 μm SPG membrane with 1400 rpm stirring speed at 25 °C. Encapsulation efficiency reached 99.7 ±0.4%. Another study is conducted by Saberi et al. (2013), they prepared a vitamin E nanoemulsion delivery system by the spontaneous emulsification method. VE was mixed with medium chain triglyceride (MCT) oil first to get different compositions of the oil phase. The results showed that 10% oil phase containing 8% VE mixed with 10% Tween80 and 80% aqueous phase resulted in the smallest droplets with a diameter around 55 nm, but nanoemulsions with droplets of 158 nm were formed when the oil phase containing 10% VE. The effect of surfactant type and concentration on particle size also was tested. In contrast to Tween 20, 40, 60, and 85, smallest droplets with narrow distribution (55nm, PDI=0.12) were formed by using 10% of Tween 80. Preparation conditions, including temperature and stirring speed, were tested for small droplet size formation. Higher temperature was reported to facilitate the formation of smaller droplets, and stirring may provide mechanical energy to breke down droplets. The stability test showed that the droplet size was increased after two months due to flocculation, coalescence and Ostwald ripening.

A water/oil/water double emulsion system was also investigated. Li et al. (2011) studied water/oil/water double emulsion system prepared from whey protein isolate (WPI) and polysaccharides (Ps) guar gum (GG) or gum arabic (GA) as a delivery system of α-tocopherol (VE) and riboflavin (VB2). They found that WPI-GG system had higher VE encapsulation efficiency (EE) (88%) than in the WPI-GA system when they had the same ratio (5:0.5). The particle size of the WPI-GG system was bigger than the WPI-GA system. The in vitro release study of VE showed that the release rate in the WPI-GG (5:0.5) system was slower than in the WPI-GA (5:0.5) system at pH 1.2 w/without pepsin and pH 7.4, but there was a slight difference

between WPI-GA and WPI-GG systems at pH 7.4 with pancreatin. Similar phenomena were observed for the VB2 in vitro release process. This study showed that the WPI-GG system had better protective ability for VE for simulated gastric conditions. Another delivery system prepared by whey protein isolate/polysaccharide (low methoxyl pectin (LMP)/κ-carrageenan (KCG)) complexes was also evaluated by the same authors (2012). The study showed that the WPI-LMP system had higher encapsulation efficiency (93%) for vitamin E than the WPI-KCG system (80%) when the weight ratio of WPI to LMP was more than 5:0.1. Similar results were observed for vitamin B2. The droplet size varied from 18.8 to 83.4 μm with the ratio of WPI to LMP ranging from 5:0 to 5:0.5. The droplet size increased from 18.8 to 69.8 μm with the increased ratio of WPI to KCG from 5:0 to 5:0.5. Controlled release of incorporated vitamins was observed in both WPI-LMP and WPI-KCG complex delivery system under simulated gastric conditions. The study demonstrated that LMP had better synergistic effects than KCG with WPI.

Oil-in-water emulsion system was also used for vitamin E acetate delivery (Yang and McClements 2013a). The emulsion formation characteristics of a natural emulsifier Q-Naturale which was extracted from the bark of the Quillaja saponaria Molina tree was studied and compared with synthetic food-grade surfactant Tween 80. Vitamin E acetate was mixed with medium chain triglyceride (MCT) oil to reduce the viscosity and form small droplets. Oil-in-water emulsions were formed by both Q-Naturale and Tween 80 with small droplet sizes (<400 nm). The droplet size was decreased with decreased vitamin E acetate contents. Compared with Tween 80, Q-Naturale could form relatively small droplets when the oil phase contained high vitamin levels (60 -80%). This study demonstrated that Q-Naturale could be used for the formation of vitamin E delivery systems which can be applied in the food field.

The effect of surfactant type on the vitamin emulsion was investigated as well. Ziani et al. (2012) studied the effect of surfactant type on the formation and properties of vitamin oil emulsions. They found that there was no significant difference between food-grade nonionic surfactants Tween 20, Tween 60 and Tween 80 on vitamin oil emulsions formation, and the emulsions were relatively stable once they were formed.

2.4.2.2 Liposome delivery system

Liposomes are closed, continuous vesicles composed of lipid bilayer with abilities to dissolve, protect, and deliver hydrophilic, lipophilic or amphiphilic materials. The application of liposomes on vitamin E delivery has been investigated. Xie et al. (2008) encapsulated VE and Vitamin C (VC) into methyl linoleate small unilamellar vesicle (SUV) liposomes and reported that the antioxidant activity of vitamins was increased when VE and VC were co-encapsulated in liposomes. The result also means VE and VC can be used against lipid oxidation of liposomes. Another study on encapsulated VE and VC was conducted by Marsanasco et al. (2011b) in which liposomes were known to maintain antioxidant activity of encapsulated VE and VC in orange juice during pasteurization. The liposome particle size ranged between 0.5 to 400 μm. In addition, the addition of liposomes in orange juice did not change the appearance of products.

Zhao et al. (2011) investigated a polyethylene glycol (PEG) coated liposome delivery system for VE. VE containing liposome was produced by the thin-film evaporation method and then lyophilized. The results showed that PEG coating increased encapsulation efficiency of liposomes from 87.53 to 91.03%, and the zeta potential was decreased from -25.9 to -35.8 mV. The particle size of VE loaded liposome was increased from 96.7 nm to 111.3 nm after coating. After freeze drying, the size was increased to 164.2 nm. Higher VE retention (78.94%) was observed in PEG coated liposomes than conventional liposomes (62.05) after exposure to UV irradiation for 60 min. Also, lower storage temperature (4 °C) resulted in higher VE retention

than higher temperatures (25 and 40 °C) after 15 days. Controlled release (17.4% released after 6 h) of VE was observed on PEG coated liposomes, while 80% of VE was released from free samples during the first 2 h in simulated intestinal fluid (SIF). In phosphate buffered saline (PBS) solution (pH 6.8), only 35.6% of VE was released from PEG coated liposomes after 6 h, but 42% of VE was released from uncoated liposomes.

Laouini et al. (2013) prepared liposomes using an ethanol injection method and applied it to vitamin E encapsulation. Liposomes preparation conditions were optimized and the mean particle size of POPC (1-palmitoyl-2-oleoyl-sn-glycero-3-phosphocholinee) liposomes was 59 nm, and Lipoid E80 liposomes had mean size of 84 nm. After encapsulation of vitamin E, the mean size was increased to 96 nm with a zeta potential around -28 mV. High encapsulation efficiency of vitamin E was observed in Lipoid E80 liposomes, which was 99.87 ±1.14%. The stability test showed that vitamin E loaded liposomes were very stable, and there was no significant decrease in the encapsulation efficiency, which was changed from 99.87±1.14% to 98.81±1.20% after 2 months of storage at 5±3 °C.

2.4.2.3 Nanoparticle delivery system

Varied nanoparticles have been developed for vitamin E delivery. Trombino et al. (2009) tested the ability of stearyl ferulate-based solid lipid nanoparticles (SF-SLNs) as a carrier for α-tocopherol and β-carotene. Results showed that α-tocopherol loaded SF-SLNs had an average diameter of 175.7 nm and β-carotene loaded nanoparticles had average diameter of 169.8 nm. Antioxidants encapsulated in SF-SLNs were very stable during 3 months storage when exposed to sunlight and showed strong antioxidant capacity.

Luo et al. (2011) used chitosan-zein as a carrier for α-TOC. Zein concentration, zein/chitosan weight ratio, and α-TOC content were investigated. Nanoparticles with an average size of 200 to 800 nm were produced. They reported that zein/chitosan encapsulated α-TOC had

prolonged release in a simulated gastrointestinal tract (SGI) compared with control (without chitosan coating). Higher zein concentration (20 mg/ml), higher α-TOC loading percentage (30%), and lower zein/chitosan weight ratio (5/1) reduced initial burst effect and prolonged release process in PBS medium. Similar results were observed for the release profile of encapsulated α-TOC in SGI. However, the authors reported that much less α-TOC was released in SIF compared with the release content in SGF. They proposed that zein was hydrolyzed and adsorbed to TOC droplets which resulted in slow release of α-TOC in SIF.

Khayata et al. (2012a) produced VE loaded nanocapsules by the nanoprecipitation method and scaled up the production from lab scale to pilot scale. The formulation was optimized at the lab scale, and the size and encapsulation efficiency of nanocapsules did not change too much after being scaled up to pilot scale. The results were 165 nm and 98% for lab scale, 172 nm and 97% for pilot scale, respectively. The stability of VE loaded nanocapsules prepared at either lab scale or pilot scale was also investigated (Khayata et al. 2012b). After different storage times (3 and 6 months) at high temperature (40 ±2 °C) and relative humidity (75±5%) conditions, the encapsulation efficiency of lab made nanocapsules was decreased from 98% to 96% after 3 months and 89% after 6 months of storage. Pilot scale made VE loaded nanocapsules had significant change in encapsulation efficiency, which decreased from 97% to 59% after 6 months of storage. The effect of lyophilization on nanocapsules was evaluated as well. The authors found that sucrose could be an ideal cryoprotectant to avoid aggregation of nanocapsules.

2.4.2.4 Nanofibers delivery system

The application of nanofiber as a delivery system for vitamin E in the food field is still lacking in the literature. There only two reported studies are delivering VE as photoprotection dressing. Taepaiboon et al. (2007) produced a cellulose acetate nanofibers delivery system for

vitamin E and vitamin A. Vitamin E loaded nanofibers had an average diameter of 253±41 nm, and Retin-A load nanofibers had a mean diameter of 247±31 nm. Around 78-83% of vitamin E was loaded into nanofibers, which was higher than that of Retin-A (45-53%). VE in nanofibers had very high stability, no significantly change (97% of VE was retained) was observed after 24 h incubation in B/T/M releasing media (acetate buffer solution containing 0.5 vol % Tween 80 and 10 vol % methanol) at 37 °C. The release test of entrapped vitamins was conducted in B/T/M media at 37 °C. Initial burst release was observed on cast-film samples during the first 20 min, while VE loaded nanofiber samples exhibited controlled release during the 24 h testing period. In B/T/M media, VE loaded nanofibers showed gradual release and reached 95% after 24 h.

Wu et al. (2011) produced both α-tocopherol acetate (α-TAc) and magnesium L-ascorbic acid 2-phophate (MAAP) incorpotated polyacrylonitrile (PAN) nanofibers by coaxial electrospinning method. PAN and poly(lactic-co-glycolic acid) (PLGA) were shell and core carrying materials, respectively. Results showed that α-TAc and MAAP were successfully incorporated into PAN nanofibers with smooth and uniform structure (average diameter was 200±15 nm) that spun from 8% PAN spin solution. Compared to PAN nanofibers that produced by normal electrospinning, nanofibers produced by the coaxial spinning method had controlled in vitro release. The initial burst release of entrapped α-TAc and MAAP from core-shell PAN nanofibers was alleviated and sustainable release was provided.

2.4.2.5 Hydrogel delivery system

Hydrogen is another delivery system for vitamin E. The ability of hydrogel β-lactoglobulin (BLG) and hen egg white protein (HEW) were examined as a delivery system for α-TOC (Somchue et al. 2009). The study found that salt played an important role in TOC encapsulation. α-TOC could not be entrapped in BLG aggregates without addition of $CaCl_2$, but

it was encapsulated in HEW particles without the addition of ZnCl$_2$. Besides inducing protein gel formation, salts were hardening agents for the alginate coating to achieve controlled release goals. The authors also reported that the encapsulation efficiency of α-TOC in BLG and HEW was increased with increased concentration of α-TOC in protein solutions, but it was limited by the amount of BLG and HEW. Release profiles of encapsulated α-TOC were determined under simulated gastric and intestinal digestion conditions. The authors found that BLG and HEW themselves as carriers were not enough to achieve controlled release of α-TOC, since 86.4% and 93.4% of entrapped α-TOC were released in SGF from BLG and HEW carriers, respectively. However, with the alginate coating, both BLG and HEW showed controlled release rate in SIF, as well as increased encapsulation efficiency of α-TOC (from 32% increased to 85% in HEW).

CHAPTER 3   FABRICATION OF SOLUBLE DIETRY FIBER BASED NANOFIBER BY ELECTROSPINNING

3.1   Introduction

Nanotechnology as an emerging technology has attracted many attentions in recent decades. Nanofibers are fibers with cross section diameter ranging from 5 to 500 nm and length for several micro meters (Deitzel et al. 2001). Nanofibers have high ratios of surface area to volume, tunable porosity, and malleability to form a variety of structures for desired properties and applications (Sadri et al. 2012, Xu et al. 2012). Nanofibers have been widely used in the field of filtration, drug delivery, food texture alterations, encapsulation of food additives, active and bioactive packaging elements, separation membranes, reinforcement in composite materials, biomaterials for wound dressings and scaffolds for tissue engineering (Torres-Giner et al. 2008).

Fabrication methods, for instance, drawing, template synthesis, phase separation, self-assembly and electrospinning, have been used to produce nanofibers (Huang et al. 2003). Electrospinning is the most common technology for nanofibers fabrication. Compared to electrospinning, the other methods have a number of disadvantages: time-consuming, complicated processing procedures, requiring equipments, and limitation on nanofiber materials (Yu 2009). Electrospinning is simple, versatile and capable to form nanofibers from various polymers (Tong, Zhang and Wang 2012). Polymer blends can be co-processed and cross-linked during electrospinning process, therefore, the chemical composition of nanofibers can be controlled. In addition, other particles or fillers can be encapsulated into nanofibers for various purposes (Yu 2009).

In a typical electrospinning process, a high power direct current (DC) voltage is applied to a polymer spinning solution. Upon charging, a conical shape known as the Taylor cone is formed on the surface of a drop at the needle tip in order to balance the repulsive force and the

27

surface tension of the drop. A stable jet of solution is generated from the cone tip when the critical voltage is achieved, and the jet travels to the grounded collector by electrical potential in a whipping motion to form continuous fibers (Fung et al. 2011).

Various materials including natural and synthetic polymers have been studied for nanofiber fabrication. Synthesized polymers, e.g., polyethylene oxide, polyacrylonitrile, polyvinyl alcohol, polyvinyl acetate, polyacrylamide, polystyrene, and so on, have been used to produce nanofibers (Crespy, Friedemann and Popa 2012). Due to the biocompatible, biodegradable, and non-toxic property, biobased materials and food hydrocolloids, such as DNA, cellulose, chitin, chitosan, alginate, dextran, collagen, gelatin, silk, casein, wheat protein and zein, showed a potential in nanofiber fabrication and grabbed most research interests in recent years (Xu et al. 2012). Polysaccharides contain hydrophilic groups such as hydroxyl, carboxyl and amino groups, they can interact with biological tissues such as in bio adhesion with epithelia and mucous membranes, and thus increase the absorbance of encapsulated bioactive compounds (Liu et al. 2008). However, the formation of nanofibers not only depends on parameters such as electric potential, distance between the tip of needle and the collecting plate, flow rate of polymer solution, but also on viscosity, elasticity, conductivity, and surface tension of the polymer solution (Doshi and Reneker 1995). Due to the limitation of biopolymers, synthesized polymers are usually used together with biopolymers for helping nanofiber fabrication (Dogan et al. 2013, Aliabadi et al. 2013, Yao et al. 2009). Flexible chains of synthetic polymers wrap themselves around rigid biopolymers to provide required linkage and entanglement for spinning solution, thus electrospun nanofibers can be produced successfully (Duan et al. 2004). The improved biocompatibility and mechanical properties of nanofibers can be obtained (He et al. 2005).

Dietary fibers are non-starch plant polysaccharides and are resistant to digestion and absorption in the human gastrointestinal tract (Brennan, Tudorica and Kuri 2002). Extensive epidemiological studies have shown that high dietary fiber intake effectively prevents colon cancer, breast cancer, atherosclerosis and development if non-insulin dependent diabetes mellitus (Moore et al. 1998). Soluble dietary fiber is soluble in water (Doleyres et al. 2002). It includes pectins, β-glucan, gums and storage polysaccharides, which can lower absorption of nutrients in intestine which results in a consequent decrease in insulin levels (Moore et al. 1998). Some research reported that soluble dietary fiber has antioxidant capacity, immune-modulation and anti-tumor activities (Aoe et al. 1993a, Wan et al. 2011, Saunders 1990, Cummings et al. 1992, Wang et al. 2008, Zha et al. 2009b). Soluble dietary fiber as a functional ingredient has been added to various food products to improve their biological activity and physical properties (Kim and Paik 2012, O'Shea et al. 2012, Havrlentova et al. 2011, Abdul-Hamid and Luan 2000, Sudha et al. 2007).

Soluble dietary fiber has the potential to produce nanofibers. However, only few study is reported to used soluble dietary fiber for nanofiber fabrication (Fung, Yuen and Liong 2010). In addition, little is known about the concentration of dietary fiber in spinning solutions, and how the dietary fiber affects the formation is still lacking in the literature.

Soluble dietary fiber (SDF) extracted from purple rice bran was selected to fabricate a novel type of electrospun nanofibers in this study due to its functional properties. In order to fabricate SDF nanofibers with sufficient protection, effective absorption and controlled release of encapsulated nutrients, cospinning polymer is used for nanofiber formation. Polyethylene oxide (PEO) is the simplest hydrophilic polymer. Due to the balanced hydrophobic and hydrophilic interactions of its chemical structure, it is soluble in water over a broad range of temperature

29

(Branca et al. 2013). Because of its biocompatibility, non-immunogenicity and low toxicity, PEO has been widely used in the biomedical field, agricultural engineering, the pharmaceutical and food industries (Bianco et al. 2013). Besides, PEO is permitted by FDA as a food additive for direct addition to food for human consumption (FDA 2012).

The objective of this chapter was to develop SDF based functional nanofibers. The effect of SDF concentrations on nanofibers fabrication was investigated. Characterizes, e.g., size, morphology, and thermal analysis of SDF based nanofibers were evaluated. The chemical interaction of SDF and PEO in nanofibers was studied as well.

3.2 Materials and Methods

3.2.1 Extraction of Soluble Dietary Fiber from Purple Rice Bran

SDF was extracted from purple rice bran by a modified method (Wan et al. 2011) of Aoe et al. (1993a). Fifty grams of defatted purple rice bran was mixed with 500 mL of distilled water and 0.5 mL of heat stable α-amylase solution (13083 units/mL, Sigma-Aldrich, St Louis, MO, USA) was added to the mixture. pH of the mixture was adjusted to 6.9 and the starch was digested for 15 min at 90 °C. Then starch-free defatted purple rice bran was separated by centrifugation at 12,000 g and washed with distilled water four times. For soluble dietary fiber extraction, a solution with 3% $Ca(OH)_2$ was added to starch-free defatted rice bran at a ratio of 30:1 (V/W) and was stirred for 1 h at 84 °C by a Talboys laboratory 134-1 stirrer (Troemner LLC, Thorofare, NJ). The extract was separated from the solid fraction by centrifugation (Beckman J2-HC centrifuge, GMI, Inc., Ramsey, MN, USA) at 12,000 g for 30 min at 4 °C, and then the soluble fraction was neutralized with concentrated acetic acid (99.85%). Furthermore, the neutralized soluble fraction was purified by a Millipore stirred ultrafiltration cell unit (Model 8400, Millipore Co., Bedford, MA) with 10 kDa molecular weight cut-off (MWCO) membrane

(Millipore Corp, Bedford, USA) at 100 kPa Nitrogen gas pressure. The resulting purified SDF retained on the ultrafiltration cell unit was freeze dried and stored at 4 °C.

3.2.2 Fabrication of Nanofiber from SDF

The effect of SDF concentrations on the nanofiber formation was examined using 3 different concentrations. Spinning solutions were prepared by dissolving 0.1, 0.3, or 0.5 g of SDF powder and 0.5 g of polyethylene oxide (PEO, 400,000MW; Sigma-Aldrich, St. Louis, MO, United States) in deionized water and stirred by a magnetic stirrer until homogeneous. The finial concentration of SDF in the spinning solutions were 1%, 3%, and 5%, respectively. And a 5% PEO was kept consistent in each spinning solution based on the preliminary test, which showed that a low PEO content ($\leq$4%) in spinning solutions was ineffective for nanofiber production. A 5% of PEO spinning solution that prepared by dissolving 0.5 g of PEO powder in 9.5 g deionized water without SDF adding was used as a control. The formulations of spinning solution were listed on Table 3.1. The freshly prepared spinning solutions were characterized by determining their flow properties and electrical conductivities. Flow properties of spinning solutions were measured by an AR 2000 ex Rheometer (TA Instruments, New Castle, De, USA) with 40 mm diameter steel plate, where a gap of 200 μm was used and shear rate was from 10 to 200 s^{-1} at 25 °C. The viscosity at 200 s^{-1} was reported. The powder law (Equation 3.1) was used to characterize the flow properties of the spinning solutions.

$$\sigma = K\dot{\gamma}^{n} \qquad\qquad (3.1)$$

where σ = shear stress (Pa), $\dot{\gamma}$ = shear rate (s^{-1}), K = consistency index (Pa•s^{n}), and n = flow behavior index.

Electrical conductivities of spinning solutions were measured using an Orion 4-Star pH/Conductivity meter (Thermo Scientific, Beverly, MA, United States) with 013605MD conductivity cell at 25°C.

Table 3.1 Formulations of spinning solution containing SDF

Spinning solutions	SDF (%)	PEO (%)	Deionized water (%)
A1	1	5	94
A2	3	5	92
A3	5	5	90
A4 (Control)	0	5	95

The solutions were electrospun from a 3 mL syringe with a 23 gauge (0.35 mm) needle at room temperature. A 30A24-P30 single output high voltage power supply (Ultravolt, Ronkonkoma, NY, United States) was used, and flow rate was controlled by a KDS-100 syringe pump (KD Scientific, Hayward, CA, United States). Electrospinning conditions were set as follows: flow rate of 0.2 mL/h, voltage of 20 kV, and the distance between tip and collector was 15 cm. Aluminum foil was used as a collector. The electrospun fibers were dried in a vacuum oven at room temperature for 24 h to remove residual moisture and then were stored in desiccators for further analyses.

3.2.3 Characterization of Nanofibers

3.2.3.1 Morphology and size distribution of nanofiber

The morphology of nanofiber was observed using scanning electron microscopy (SEM). Nanofiber sample was placed on a SEM stub and coated with platinum for 4 min using an EMS 550X sputter coating machine (Electron Microscopy Sciences, Hatfield, PA, United States). Then the morphology of sample was observed by a JSM-6610LV scanning electron microscope (SEM, JEOL, Peabody, MA, United States). Size distribution of nanofibers was calculated through measuring the diameter of 200 randomly selected nanofibers.

3.2.3.2 Thermal properties of nanofiber

Thermal properties of four nanofiber samples, pure PEO powder, and SDF powder were determined using differential scanning calorimetry (DSC) and thermogravimetric analysis (TGA). For TGA measurements, five micrograms of samples were heated in a Hi-Res Modulated TGA 2050 Thermogravimetric Analyzer (TA Instruments, New Castle, DE, United States) to 600 °C at a rate of 10 °C/ min in a N_2 atmosphere to evaluate the thermal stability of SDF containing nanofibers. The degradation time were obtained from TG curves. For DSC measurements, five micrograms of samples were heated in a DSC 2920 Modulated DSC (TA Instruments, New Castle, DE, United States) from -30 °C to 120 °C at a rate of 10 °C/ min, and then was cooled down to -30 °C at a rate of 5 °C/min. After maintaining the temperature for 5 min, the sample was reheated from -30 °C to 120 °C at a rate of 10 °C/ min and the data were collected.

3.2.3.3 Molecular interaction of nanofiber

The molecular interaction between SDF and PEO in nanofibers was evaluated by attenuated total reflectance infrared spectroscopy (ATR-FTIR). Samples were placed on a diamond ATR cell and measured by ALPHA Platinum ATR QuickSnap (Bruker, Billerica, MA, United States). The spectra were recorded at 600-4000 cm^{-1} with the resolution of 4 cm^{-1}, and 8 scans were used. The spectra data were collected and analyzed using OPUS 7.2 data collection program.

3.2.4   Statistical Analysis

Mean values and standard deviation of triplicate measurements were reported. Analysis of variance (ANOVA) was conducted to test the significant differences ($p<0.05$) among different treatments using the SAS safeware (SAS Inst. Inc., Cary, N.C., USA.).

3.3   Results and Discussion

3.3.1   Characteristics of Spinning Solutions

The rheology properties of spinning solutions containing SDF were shown in Table 3.2. Apparent viscosity of the control spinning solution (A4) was significantly lower compared to solutions A1, A2 and A3, which indicated that the addition of SDF increased the apparent viscosity of spinning solutions. Solution A3 (containing 5% SDF) had a significantly higher apparent viscosity (2.34 Pa.s) compared to A1 (1.60 Pa.s) and A2 (1.61 Pa.s), which indicated the concentration of SDF in spinning solution affected the apparent viscosity, a higher SDF concentration resulted in a higher apparent viscosity in the spinning solution. The flow behavior index n values were less than 1.0, which indicated that the spinning solutions A1, A2, A3 and A4 were non-Newtonian fluids (shearing thinning). The consistency index K value of A4 was significantly lower than those of spinning solutions A1, A2 and A3 containing SDF.

Table 3.2 Electric conductivity and flow properties of PEO spinning solutions containing SDF

Spinning solutions	Electrical conductivity (mS/cm)	Apparent viscosity (Pa.s)	n	K (Pa. s^n)
A1	1.91 ± 0.01^C	1.60 ± 0.01^B	0.62 ± 0.00^B	12.29 ± 0.15^B
A2	5.09 ± 0.01^B	1.61 ± 0.00^B	0.63 ± 0.00^B	11.74 ± 0.12^B
A3	6.25 ± 0.03^A	2.34 ± 0.01^A	0.62 ± 0.00^B	18.54 ± 0.15^A
A4 (Control)	0.092 ± 0.00^D	1.323 ± 0.01^C	0.73 ± 0.02^A	6.29 ± 0.54^C

Values are means ± SD of triplicate determinations. ^{ABCD}means with the same letter in the columns are not significantly different (P>0.05). n=flow behavior index; K=consistency index.

Viscosity is an important determinant of the size and quality of nanofibers. It is related to the extent of polymer molecule chain entanglement within the solution, which is critical to nanofiber formation (Kriegel et al. 2008). Viscosity is required to be high enough, so nanofibers can be formed without beads. Otherwise, the jet breaks up into droplets or beads rather than fibers in a low viscosity polymer solution due to the limited entanglement of polymers (Deitzel et al. 2001). Therefore, an increase in polymer concentration is beneficial for nanofiber

formation. Viscosity impacts the diameter of nanofibers as well. Thus, it is necessary to determine the suitable polymer concentration. Different polymer solutions have different required viscosities for nanofiber fabrication. The apparent viscosity of spinning solution A3 was 2.34 Pa.s in this study, which was higher than the reported viscosity range of PEO solution by Fong, Chun and Reneker (1999). Authors reported that ethanol/water PEO solution with viscosities ranging from 0.1 to 2 Pa.s could be used for nanofibers formation, while the electrospinning was unsuccessful once the viscosity was over 2 Pa.s or less than 0.1 Pa.s (Fong, Chun and Reneker 1999).

Spinning solutions A1, A2 and A3 had significantly higher electrical conductivities than the control spinning solution A4, which were 1.91, 5.09, 6.25 and 0.092 mS/cm, respectively (Table 3.2). The higher the SDF concentration, the higher the electrical conductivity in the spinning solution. This may be due to the minerals in the SDF, since minerals including calcium and iron can be extracted out and stay in SDF portion (Fung et al. 2010). Also, calcium hydroxide was used to extract SDF in this study, and 6.85% of calcium was contained in SDF powder, which was the main source of calcium. Electrical conductivity is another factor that impacts nanofiber formation. Higher conductivity of spinning solution results in enough electric force to stretch the jet from the Taylor cone and form thinner fibers. Thus inorganic salts are used to generate a high electrical conductivity of spinning solution (Barakat et al. 2009).

3.3.2   Morphology of Nanofibers

Nanofibers were smooth without visible beads (Figure 3.1). Defects such as junctions were found on nanofibers produced from solution A4. The junctions did not appear on nanofibers produced from spinning solutions A1, A2 and A3, which contained 6%, 8% and 10% of SDF/PEO polymers, respectively. These polymer solution concentrations were higher than the reported PEO polymer concentration (5%) by Deitzel et al. (2001). The presence of junctions in

35

nanofibers was due to the slow solidification effect of polymer fibers that produced from low

polymer concentration spinning solution.
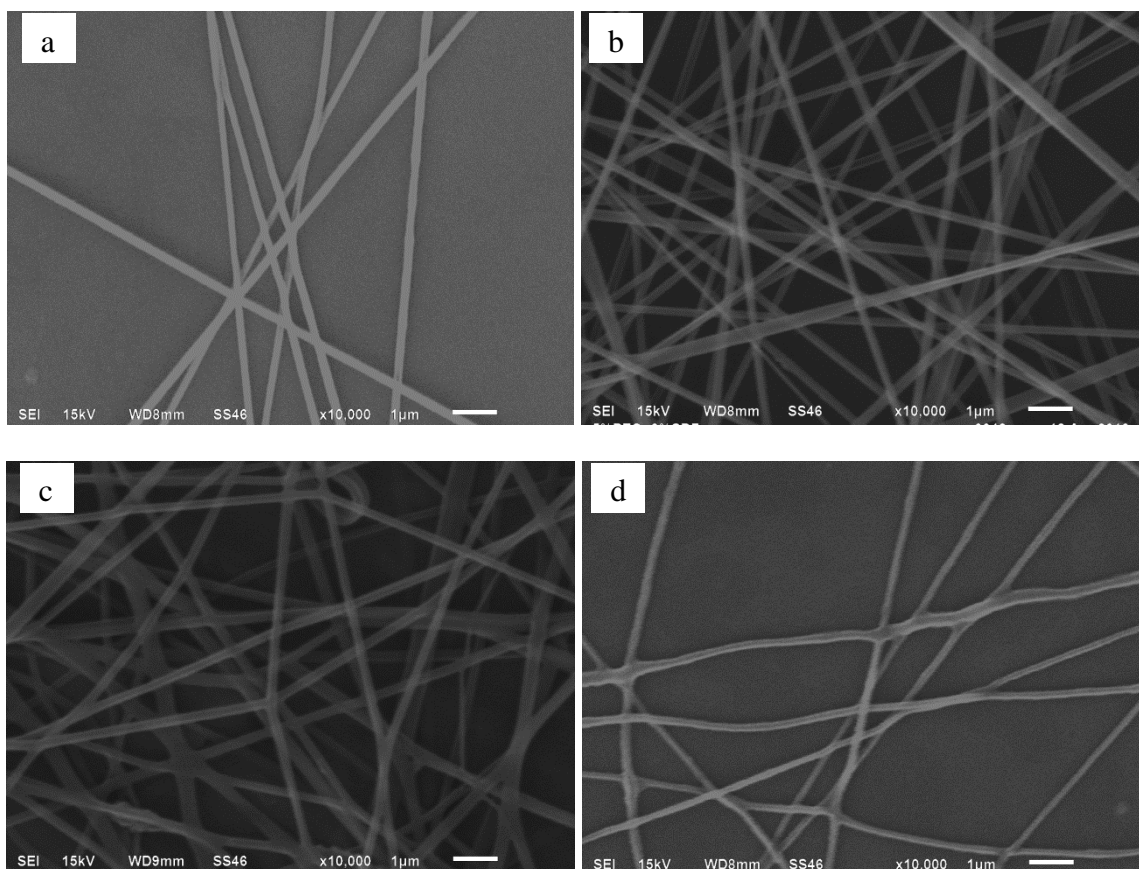
Figure 3.1 SEM of nanofibers
(a) A1, 1% SDF+5% PEO; (b) A2, 3% SDF+5%PEO; (c) A3, 5% SDF+5% PEO; and (d) A4,
5% PEO.

With increased SDF content, the average diameters of nanofibers were increased (Table

3.3). Nanofibers that produced from spinning solution A3 had the highest average diameter of

198.19 nm, and the lowest average diameter (155.05 nm) was found in nanofibers that produced

from spinning solution A4. The nanofiber average diameter was kept consistent with the result of

viscosity, the higher spinning solution concentration, the higher viscosity, and the larger

nanofiber diameter. The nanofiber size found in this study was lower than the reported nanofiber

diameter (5 µm) by Doshi and Reneker (1995), which was produced from 7% PEO solution.

Also, it was lower than the previous reported nanofiber average diameter (250 nm) by Fong et al.

(1999), which was produced from 4.5% PEO solution.

Table 3.3 Cross section diameter of nanofibers

Spinning solutions	Nanofiber average diameter (nm)
A1	174.54 ± 26.92
A2	171.45 ± 37.19
A3	198.19 ± 41.82
A4	155.05 ± 24.49

The size distribution of diameters in nanofibers was shown in Figure 3.2. Nanofibers

produced from spinning solution A1 has a narrow cross section diameter distribution ranging

from 102 to 280 nm. Nanofibers electrospun from A2 and A3 had broad diameter distributions,

which ranged from 102 to 328 nm and from 122 to 365 nm, respectively. A4 had a narrow cross

section diameter distribution which ranged from 100 to 253 nm. These values were lower than

the size distribution of diameters in nanofibers produced from 7% PEO solution, which ranged

from 130 to 430 nm (Deitzel et al. 2001). Deitzel et al. (2001) also reported that bimodal

diameter distribution was exhibited in nanofibers electrospun from PEO solutions with

concentration over 7%. The similar result was reported by Xu et al. (2012), they found branching

was significant in nanofibers that produced from high concentration spinning solution containing

8% soy protein isolate and 0.5% PEO. However, no obvious bimodal diameter distribution was

found in all four nanofiber samples in this study, which indicated the spinning solution was

homogenous and the charge was evenly distributed on the jet during electrospinning, and thus

resulted in the smooth and uniform nanofibers. It also indicated that the concentration of SDF

had minor effect on nanofiber fabrication.
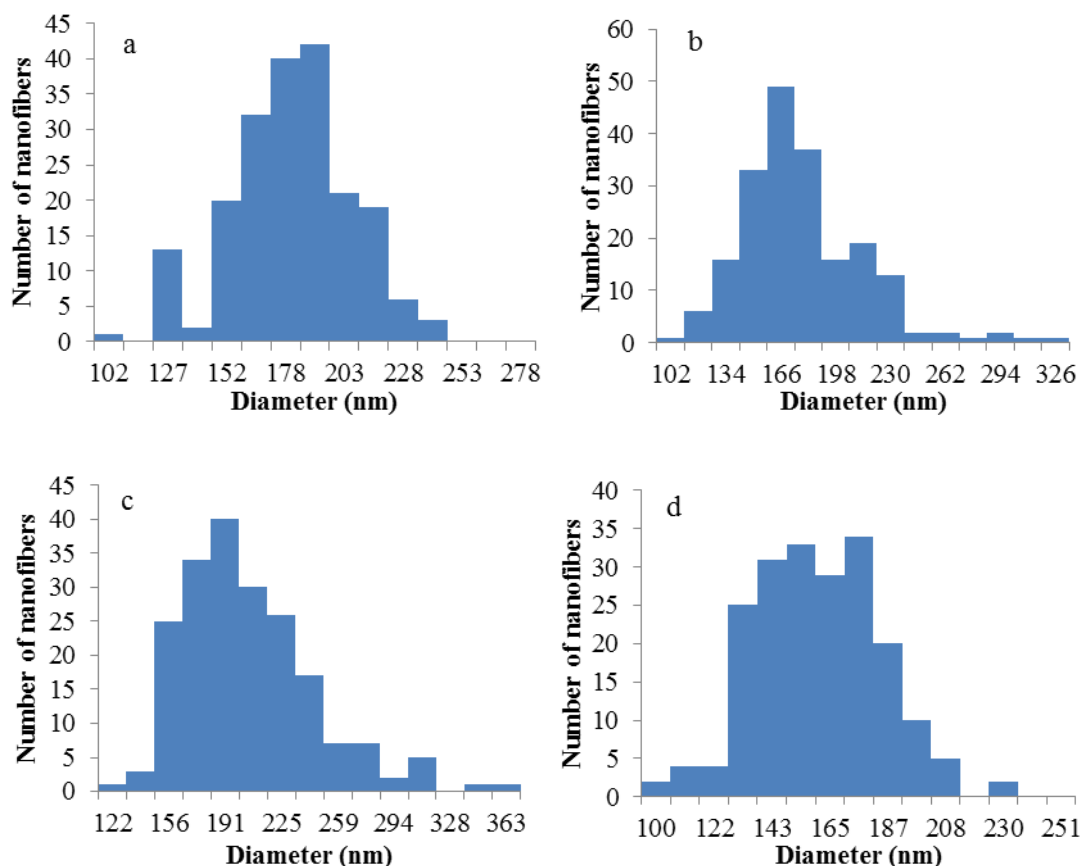
Figure 3.2 Size distribution of diameters in nanofibers
Nanofibers produced from (a) A1 (1% SDF+5% PEO), (b) A2 (3% SDF+5%PEO), (c) A3 (5% SDF+5% PEO), and (d) A4 (5% PEO).

3.3.3 Thermal Properties of SDF Based Nanofiber

TGA thermogram of nanofibers was shown in Figure 3.3. Pure PEO powder had a T_{onset} of 372.04 °C, and nanofibers produced from 5% PEO had a T_{onset} of 376.13 °C. Two regions of weight loss were observed in SDF based nanofibers. SDF had one weight loss at 243.0 °C. T_{onset} of nanofibers with the addition of SDF decreased with increased content of SDF. Nanofibers produced from solutions A1 had two onset temperatures around 240.8 °C and 386.2 °C. Nanofibers produced from A2 and A3 solutions had onset temperatures at 241.5 and 388.7 °C, and 234.5 and 387.1 °C, respectively. The first weight loss may be caused by the decomposition of SDF, and the second resulted from the decomposition of PEO.
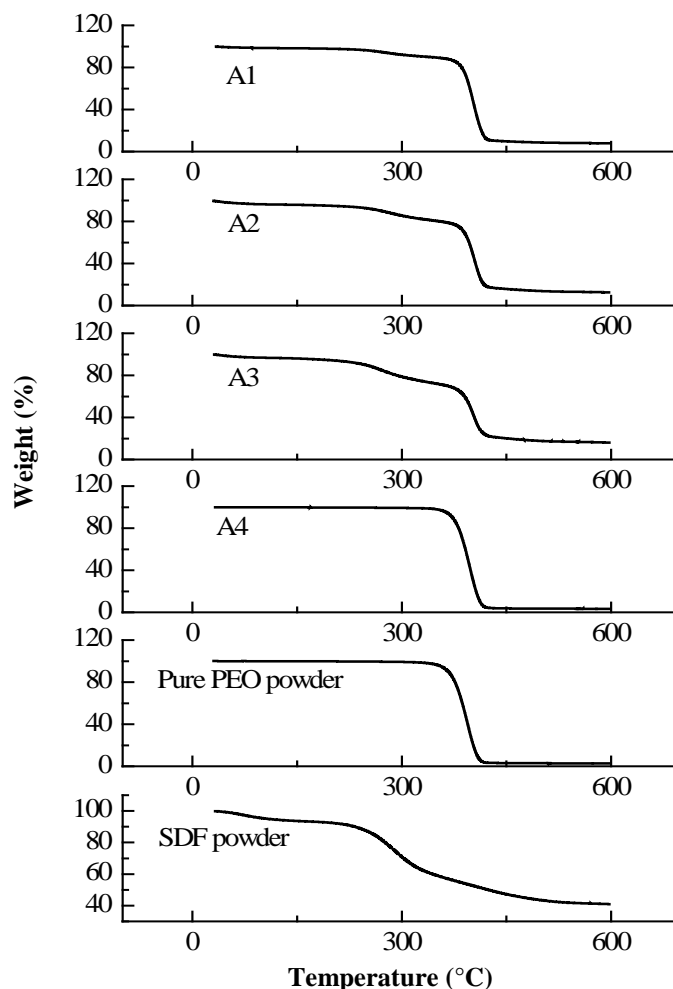
Figure 3.3 TGA curve of SDF based nanofibers

DSC scans of pure PEO powder, SDF powder, PEO nanofibers, and nanofibers containing SDF were shown in Figure 3.4. Pure PEO powder showed a melting peak at 72.6 °C with an enthalpy of 168.3 kJ/kg (Table 3.4). The A4 nanofibers had slightly lower melting peak at 71.9 °C with an enthalpy of 165.8 kJ/kg than that of pure PEO powder. The addition of SDF decreased melting peaks of nanofibers. However, A2 and A3 nanofibers had significantly hihger crystallinity than A1 and A4 nanofibers. These results were different from previous reports that low crystallinity was observed in nanofibers produced from polymer solutions (Xu et al. 2012, Deitzel et al. 2001), which indicated the addition of SDF increased the overall crystallinity in

39

nanofibers. Because of the increased crystallinity, more energy is needed to break down the

molecular order. Thus, SDF based nanofibers may be heat stable.
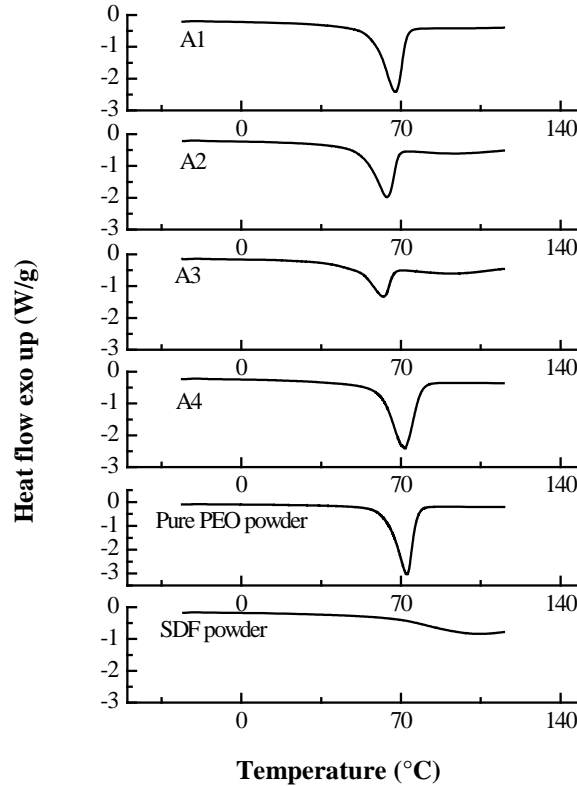
Figure 3.4 DSC thermograms of nanofibers and ingredients

Table 3.4 Summary of DSC curves of SDF based nanofibers

Sample	T_m (°C)	ΔH_m (kJ/kg)	χ_c
A1	67.5 ± 0.1^C	144.7 ± 6.8^B	0.59 ± 0.03^D
A2	63.9 ± 0.1^D	128.1 ± 0.7^C	1.01 ± 0.00^B
A3	62.2 ± 0.1^E	111.3 ± 1.4^D	1.10 ± 0.01^A
A4	71.9 ± 0.1^B	165.8 ± 0.9^A	0.81 ± 0.00^C
Pure PEO powder	72.6 ± 0.1^A	168.3 ± 1.0^A	0.82 ± 0.00^C
SDF powder	ND	ND	ND

Values are means ± SD of triplicate determinations. [ABCDE]means with the same letter in the columns are not significantly different (P>0.05).T_m (°C) is the melting peak; ΔH_m (kJ/kg) is the melting enthalpy; χ_c is the degree of crystallinity; $\chi_c =\Delta H_m/(\Delta H_m^{0}*w)$, ΔH_m^{0} is the melting heat of 100% crystalline PEO, which is reported as 203 kJ/kg (Fan et al. 2002); w is the weight fraction of PEO in nanofibers. ND means not detected in the test temperature region.

There was no melting peak appeared on SDF powder in the test temperature region, but an endothermic process was occurred around 105 °C. That may be caused by the evaporation of bound water, since polymer has a strong affinity with water (Luo, Teng and Wang 2012). It also may be the glass transition region of SDF powder.

3.3.4 FTIR

The intermolecular interaction of SDF based nanofibers was evaluated by ATR-FTIR. The spectra of each ingredient and nanofibers were shown in Figure 3.5.
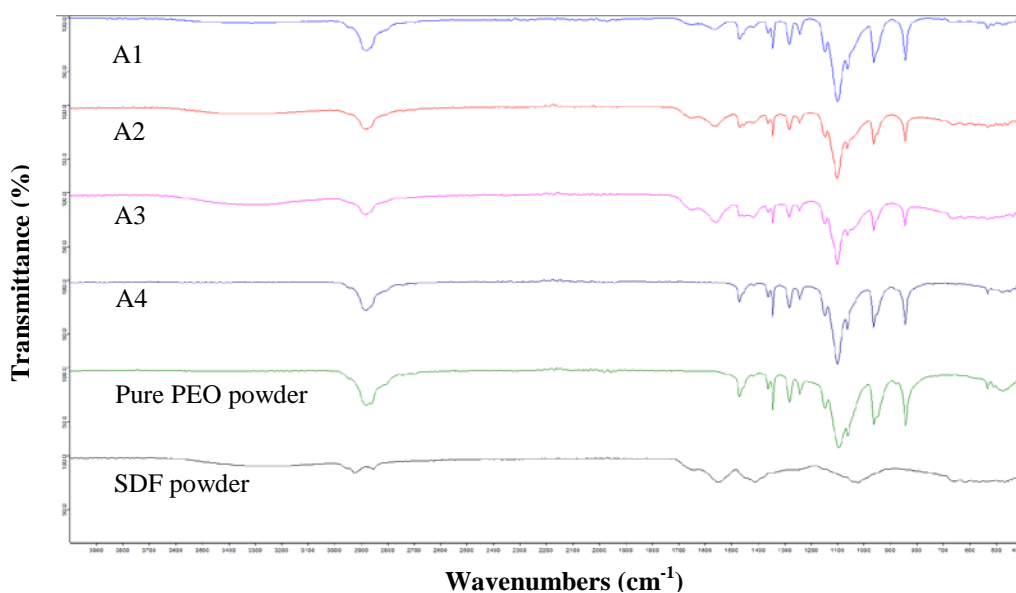
Figure 3.5 FTIR spectra of ingredients and nanofibers

There was a triplet peak at 1146 cm^{-1}, 1098 cm^{-1} and 1060 cm^{-1} in PEO powder with the highest absorption at 1098 cm^{-1}. This was because of the stretching vibrational mode of the C-O-C bond in PEO, an indication of a crystalline phase (Bianco et al. 2013, Li and Hsu 1984). The conformational structures will be modified if the intensity, shape and postion of the C-O-C peak change. The peak at 1235 cm^{-1} was assigned to the helical conformation and was observed in PEO powder, decreased in PEO nanofibers, which indicated the electrospinning process has promoted the planar conformation of PEO (Kim et al. 2005, Aluigi et al. 2007). The peak at 1060 cm^{-1}, which was attributed to the H structure of PEO, was weakened in nanofibers. This meant

the PEO chains were more aligned in the fiber direction due to the high extensional force caused by electrospinning, and T conformation structure was formed (Kim et al. 2005).

In SDF powder and SDF/PEO nanofibers, a broad band between 3000 and 3700 cm^{-1} may be assigned to O-H stretching from the polysaccharide molecules and intermolecular hydrogen bonds formed between SDF and PEO (Fung et al. 2011, Aliabadi et al. 2013). The peaks observed between 2850 and 2960 cm^{-1} were due to the C-H stretching from alkane groups. The peak at 1648 cm^{-1} in the SDF was usually associated with the absorbed water molecules in the fiber (Sain and Panthapulakkal 2006). Another peak at 1548 cm^{-1} were shown in the spectra of SDF powder and at 1557 cm^{-1} in the spectra of SDF/PEO nanofibers, which were attributed to the N-H bending from amine groups. The possible reason may because of the traces of protein that were contained in SDF. The peak at 1096 cm^{-1} indicated C-O stretching and O-H bending in PEO. In addition, peaks at 1466, 1342, 1279, and 1242 cm^{-1} represented C-H, O-H, or CH_2 bending (Himmelsbach, Khalili and Akin 2002).

3.4   Conclusions

SDF based nanofibers were successfully electrospun from the soluble dietary fiber extracted from purple rice bran. SDF based nanofibers (prepared by 3% SDF+5% PEO) had a uniform size distribution with an average diameter of 171.45 nm and no defects of either beads or junctions. It was selected for further study. DSC results showed that the melting point of SDF based nanofibers was slightly decreased compared to the control nanofibers. The crystallinity of SDF nanofibers increased with the increasing content of SDF. Compared to the control nanofibers, SDF based nanofibers had two weight losses during heat processing. The SDF showed good potential for fabrication of nanofibers, and it may interact with PEO by hydrogen bonds. Nanofibers produced by SDF are expected to have both characteristics of nanofibers and functional properties from SDF.

CHAPTER 4   ENCAPSULATION OF ALPHA-TOCOPHEROL IN SOLUBLE DIETARY FIBER BASED NANOFIBER DELIVERY SYSTEM

4.1   Introduction

Nanofibers are fine threads with cross sectional diameters ranging from a few nanometers to one micrometer, and the length is over several micrometers. Due to the specific properties of nanofibers, for example, a very high surface area to volume ratio and diverse structures, it has been widely used in biomedical fields like drug delivery, wound dressing, tissue enginnering and so on (Xie et al. 2008). The structure of nanofibers can be modified by adjusting the composition of the electrospinning solution, and changes in electrospinning conditions, such as voltage, flow rate and the distance between the tip of needle and collector, results in various diameters. Through controlling the structure and diameter of nanofibers, a controlled release of encapsulated components may be achieved. Also, the target delivery may be attained by modifying the surface properties of nanofibers. Nanofiber delivery systems for bioactive components are getting popular in recent years. Bioactive compounds, such as vitamins, probiotics, proteins and functional lipids, can be incorporated into nanofibers for required delivery purposes (Fernandez et al. 2009, Chen et al. 2010, Lopez-Rubio et al. 2009, Opanasopit et al. 2008). The functionality of incorporated materials in nanofibers can be potentially improved and enhanced due to the nano-scale effects (Shen et al. 2011).

Vitamin E is a hydrophobic antioxidant which has several important health benefits, for instance, it reduces the risk of cancer, cardiovascular disease, diabetes and aging (Herrera and Barbas 2001). Natural vitamin E includes four tocopherols (α, β, γ, and δ) and corresponding tocotrienols (α, β, γ, and δ) of which α-tocopherol (α-TOC) has the greatest biological activity (Herrera and Barbas 2001). It interacts with peroxy radicals in cell membranes to prevent the

propagation of free radical reactions. Therefore, vitamin E is commonly used as a dietary supplement. Vitamin E cannot dissolve in aqueous phase and has lower stability when exposed to extreme conditions such as heat, light, and oxygen during processing and storage (Miquel et al. 2004). Micro-/nano-emulsion systems have been developed for vitamin E to improve the stability and achieve controlled release (Feng et al. 2009, Laouini et al. 2012, Saberi et al. 2013, Li et al. 2011), as well as liposome systems (Xie and Ji 2008, Marsanasco et al. 2011a, Zhao et al. 2011, Laouini et al. 2013) and nanoparticle systems (Trombino et al. 2009, Luo et al. 2011, Khayata et al. 2012a, Khayata et al. 2012b). The application of nanofiber systems on vitamin E in the food field is few reported in the literature. Also, it was suggested that the bioavailability of vitamin E may be increased when it is delivered in nano-scale form rather than in bulk form (Feng et al. 2009).

Soluble dietary fiber (SDF) extracted from rice bran maintains its functional abilities, such as antioxidant activity (Zha et al. 2009a, Rivas et al. 2013), antitumor activity (Takeshita et al. 1992, Aoe et al. 1993b, Wang et al. 2009), and cholesterol lowering capacity (Anderson et al. 1994, Hu and Yu 2013, Aoe et al. 1993a). Due to the functional properties of soluble dietary fiber, the application in delivery systems for bioactive components has become popular recently. Wan et al. (2011) have incorporated soluble rice bran fiber into shell material and applied it in fish oil encapsulation, which protected fish oil from oxidation. Fung et al. (2010) fabricated nanofibers by using soluble dietary fiber from oil palm, and then applied those nanofibers as a carrier to encapsulate probiotics (Fung et al. 2011). However, less is known about the effect of SDF on α-TOC. In our previous study (Chapter 3), SDF extracted from defatted purple rice bran fiber was successfully fabricated into nanofibers by electrospinning. SDF based nanofibers not

only have the unique characteristics of nanofibers, but also have the combined healthy benefits of α-TOC and SDF.

The objective of this study was to encapsulate α-TOC into SDF based nanofibers for enhancing its stability and achieving controlled release. Due to the insolubility of α-TOC in water, two loading forms of α-TOC were used in this study for comparison: α-TOC O/W emulsion droplets and α-TOC entrapped zein particles. The characteristics include morphology, diameter, and encapsulation efficiency of α-TOC in nanofibers were evaluated. The molecular interactions and thermal properties of nanofibers were investigated by Fourier transform infrared spectroscopy (FTIR) and differential scanning calorimetry (DSC), respectively. The release profiles of α-TOC from SDF based nanofibers in vitro were studied as well.

4.2 Materials and Methods

4.2.1 Electrospinning Solutions Prepared with Emulsions

4.2.1.1 Preparation of α-TOC emulsion

Ten percent α-TOC oil/water (O/W) emulsion was prepared as described below. Two percent of surfactant solution was prepared by dissolving 2 g of Tween 80 in 98 g of deionized water. α-TOC emulsion was prepared by adding 1 g of α-TOC (Fluka, Sigma-Aldrich, St. Louis, MO, USA) to 9 g of surfactant solution and emulsifying with a homogenizer (Power Gen 500, Thermo Fisher Scientific Inc., Pittsburgh, PA) at 9500 rpm for 5 min. The emulsion was ultrasonicated in an ice bath at 500 W for 2 min with 50% amplitude (Ultrasonic Processor, Cole Parmer, Vernon Hills, IL). The concentration of α-TOC in emulsion was 10%.

4.2.1.2 Extraction of SDF from purple rice bran

SDF was extracted from purple rice bran using a modified method of Wan et al. (2011). Fifty grams of defatted purple rice bran was mixed with 500 mL of distilled water and 0.5 mL of heat stable α-amylase solution (13083 units/mL, Sigma-Aldrich, St Louis, MO, USA) was added

to the mixture. The pH of mixture was adjusted to 6.9 to digest starches at 90 °C for 15 min. Then the starch-free defatted purple rice bran was separated by centrifugation at 12,000 g and washed with distilled water four times. For soluble dietary fiber extraction, 3% of $Ca(OH)_2$ solution was added to starch-free defatted rice bran at a ratio of 30:1 (V/W) and was stirred for 1 h at 84 °C by a Talboys laboratory 134-1 stirrer (Troemner LLC, Thorofare, NJ). The extract was separated from the solid fraction by centrifugation (Beckman J2-HC centrifuge, GMI, Inc., Ramsey, MN, USA) at 12,000 g for 30 min at 4 °C, and then the soluble fraction was neutralized with concentrated acetic acid (99.85%). Furthermore, the neutralized soluble fraction was purified by a Millipore stirred ultrafiltration cell unit (Model 8400, Millipore Co., Bedford, MA) with 10 kDa molecular weight cut-off (MWCO) membrane (Millipore Corp, Bedford, USA) at 100 kPa Nitrogen gas pressure. The resulting purified SDF retained on the ultrafiltration cell unit was freeze dried and stored at 4 °C.

4.2.1.3 Electrospinning solutions preparation

Six spinning solutions containing α-TOC emulsion were prepared and the formulations were shown in Table 4.1. Poly (ethylene oxide) (PEO, 400,000MW; Sigma-Aldrich, St. Louis, MO, United States) was used as a cospinning polymer to help the fabrication of nanofibers. The nanofiber wall material polymer solution was prepared by dissolving SDF powder in distilled water, and then adding PEO powder to SDF solution and stirring overnight at room temperature. α-TOC emulsion was gradually added to the SDF/PEO polymer solution and stirred at room temperature for 2 h to obtain homogenous spinning solutions. Solution A1 without SDF adding was used as a control. The spinning solutions were characterized for flow properties. Flow property of spinning solutions was measured by a AR 2000 ex Rheometer (TA Instruments, New Castle, De, United State) with 40 mm diameter steel plate, where a gap of 200 μm was used and the shear rate was from 10 to 200 s^{-1} at 25 °C. The apparent viscosity at 200 s^{-1} was reported.

$$\sigma = K\dot{\gamma}^n \qquad\qquad (4.1)$$

where σ = shear stress (Pa), $\dot{\gamma}$ = shear rate (s^{-1}), K = consistency index (Pa•s^n), and n = flow

behavior index.

Table 4.1 Composition of spinning solutions containing α-TOC emulsion

Spinning solutions	α-TOC (wt%)	SDF (wt%)	PEO (wt%)	Surfactant (wt%)
A1	3	0	5	0.54
A2	1	3	5	0.18
A3	2	3	5	0.36
A4	3	3	5	0.54
A5	4	3	5	0.72
A6	5	3	5	0.9

A1: control sample (without SDF adding).

4.2.2 Electrospinning Solutions Prepared with Zein Particles

Electrospinning solutions containing zein encapsulated α-TOC particles were prepared

and the formulations for the electrospinning solution were shown in Table 4.2. Zein (Sigma

Aldrich, St. Louis, MO., USA) was used to encapsulate α-TOC first. A 30% zein stock solution

was prepared by dissolving zein power in 75% ethanol solution. Fifty percent of α-TOC stock

solution was prepared by dissolving α-TOC in pure ethanol. PEO and SDF were separately

prepared by dissolving them in deionized water. α-TOC entrapped zein nanoparticles were

prepared by gradually adding α-TOC solution into zein solution with stirring for 30 min. Then

the α-TOC entrapped zein solution was mixed with 0.5 g of 10% Tween 80 with 30 min stirring.

The final concentration of Tween 80 was 0.5%. PEO solution was added into the above mixture

with stirring for 1 h. Then SDF solution was added and stirred for another 30 min till

homogeneous. Flow properties of spinning solutions were measured as described section 4.2.1.3.

The apparent viscosity at 200 s^{-1} was reported.

Table 4.2 Composition of spinning solutions with zein encapsulated α-TOC

Spinning solutions	Zein (wt%)	α-TOC (wt%, relative to zein mass)	SDF (wt%)	PEO (wt%)
B1	8	30	3	5
B2	4	30	3	5
B3	6	30	3	5
B4	6	20	3	5
B5	6	50	3	5
B6	6	40	3	5
B7	6	30	0	5

B7: control sample (without SDF adding).

4.2.3 Electrospinning

The spinning solutions were separately electrospun in an electrospinning setup to produced nanofibers. The electrospinning setup included a high DC voltage power supply (Model: FC30R4, Glassman High Voltage, INC., High Bridge, NJ, USA), a KDS-100 syringe pump (KD Scientific, Hayward, CA, USA), and a 3 mL syringe with a 23 gauge (0.35 mm) needle. Aluminum foil was used as the collector. Electrospinning conditions were set as follows: flow rate was 0.2 mL/h, voltage was 20 kV, and the distance between the tip and collector was 15 cm. The electrospun nanofibers were dried in a vacuum oven at room temperature overnight and then stored at -20 ℃ for further analysis.

4.2.4 Morphology and Diameter of Nanofibers

The morphology of nanofiber was observed in a scanning electron microscopy (SEM). Nanofiber sample was placed on the SEM stub and coated with platinum for 4 min using EMS 550X sputter coating machine (Electron Microscopy Sciences, Hatfield, PA, United States). The morphology of sample was observed by a JSM-6610LV scanning electron microscope (SEM, JEOL, Peabody, MA, United States). The average size of nanofibers was calculated through measuring the diameter of 200 nanofibers from 10 images.

4.2.5 Chemical and Physical Properties of Nanofibers

The chemical interaction of nanofibers was measured by fourier transform infrared spectroscopy (FTIR) using ALPHA Platinum ATR QuickSnap (Bruker, Billerica, MA, United States) with a diamond ATR cell. The spectra were recorded at 600-4000 cm^{-1} with the resolution of 4 cm^{-1}, and 8 scans were used. The spectra data were collected and analyzed using OPUS 7.2 data collection program.

Differential scanning calorimetry (DSC) measurements of nanofibers were conducted using a DSC 2920 Modulated DSC (TA Instruments, New Castle, DE, United States). Five micrograms of nanofiber sample were accurately weighted, and then placed in a standard aluminum pan and sealed with the lid. Sample was heated from -30 °C to 120 °C at a heating rate of 10 °C/min under nitrogen, and then was cooled down to -30 °C at a rate of 5 °C/min. After 5 min maintenance, the sample was reheated from -30 °C to 120 °C at a rate of 10 °C/ min and the data was collected.

4.2.6 Encapsulation Efficiency of α-TOC in Nanofibers

Encapsulation efficiency of α-TOC was measured using a modified method of Liu et al. (2005). Ten milligrams of α-TOC entrapped nanofibers were washed with 1 mL of ethyl acetate for three times. The eluent containing free α-TOC was dried by N_2 and then extracted by hexane for α-TOC content measurement. The surface α-TOC content was measured by UV/vis spectrophotometer at 297 nm. Encapsulation efficiency (EE) of α-TOC in nanofibers was determined by following Equation 4.2.

$$\text{Encapsulation efficiency (\%)} = \frac{\text{total } \alpha - \text{TOC content} - \text{surface } \alpha - \text{TOC content}}{\text{total } \alpha - \text{TOC content}} * 100$$

(4.2)

where total α-TOC content was the added α-TOC in spinning solution.

4.2.7   In Vitro Release of α-TOC from Nanofibers

Nanofiber samples were cut into a 25×25 mm square shape with an average thickness of 0.30 mm and the mass of the nanofiber sample was about 35 mg. Each sample was separately suspended in 10 mL of PBS (phosphate buffer saline) medium which containing 0.5% of Tween 80 for increasing the solubility of α-TOC. The release study was performed in an incubator shaker (Model 3525, LAB-LINE Instruments Inc., Melrose Park, IL) at 37 ℃ with 100 rpm for 6 h. One milliliter of solution was removed for measuring α-TOC content and 1 mL of fresh PBS was replenished at each time interval (1, 2, 3, 4, 5 and 6 h). The supernatant containing released α-TOC was separated by centrifugation at 12,000 g for 10 min (Eppendorf centrifuge 5417c, Eppendorf North America, Hauppauge, NY, USA), and the solid fraction was transferred back to the release system. The supernatant was dried by nitrogen with a Zanntel Analytical Evaporator (Zip Vap, Glas-Col, LLC, Terre Haute, IN) at 30 ℃ and then α-TOC was extracted with hexane as described by Luo et al. (2011). α-TOC content was measured by UV/vis spectrophotometer (Genesys 2, Thermo Fisher Scientific Inc., Rochester, NY) at 297 nm and determined using a standard curve of α-TOC in hexane (R^2=0.9998).

The in vitro release profile of α-TOC from nanofibers under simulated gastric and intestinal environments was determined according to the method of Somchue et al. (2009) with some modification. Simulated gastric fluid (SGF, pH 1.2) was prepared by dissolving 2.0 g of NaCl and 3.2 g of pepsin (from porcine gastric mucosa, with an activity of 800 to 2500 units per mg of protein) (Sigma Chemical Co., St. Louis, MO, USA) in distilled water and 7.0 mL of HCl, and then the solution was diluted to 1 L with distilled water. Simulated intestinal fluid (SIF) was prepared by dissolving 6.8 g of monobasic potassium phosphate in 250 mL of distilled water, then mixed with 77 mL of 0.2 N NaOH solution and 500 mL of distilled water. Ten grams of pancreatin (sigma USP, Sigma Chemical Co., St. Louis, MO, USA) was mixed with the above

mentioned solution and the pH was adjusted with 0.2 N NaOH to 6.8. Distilled water was added to reach a final volume of 1 L. A square shape of nanofiber sample was cut from the whole mat and exactly weighed. Then it was incubated in 10 mL of SGF at 37 ºC with 100 rpm under an incubator shaker for 2 h. The supernatant was separated from the solid part by centrifugation at 12,000 g for 10 min. One milliliter of supernatant that containing released α-TOC was dried by nitrogen and then the released α-TOC was extracted by 2 mL of hexane solution and measured using UV/vis spectrophotometer at 297 nm. The solid portion was digested by 10 mL of SIF under an incubator shaker at 37 ºC with 100 rpm for 4 h. The released α-TOC in SIF was extracted with hexane solution and measured at 297 nm. The percentages of released α-TOC in SGF and SIF conditions were reported as $\%R_{SGF}$ and $\%R_{SIF}$, respectively.

4.2.8   Statistical Analysis

Mean values and standard deviation of triplicate determinations are reported. Analysis of variance (ANOVA) was conducted to test the significant differences ($P<0.05$) among the different treatments using SAS system (Version 9.3, SAS Inst. Inc., Cary, N.C., USA.).

4.3   Results and Discussion

4.3.1   Flow Properties of Electrospinning Solutions with Emulsions

The flow properties of spinning solutions containing α-TOC emulsion droplets were shown in Table 4.3. As α-TOC content increased from 1 to 5%, apparent viscosity of electrospinning solution significantly increased from 1.53 to 2.05 Pa.s, which might be due to the interactions of polymer - polymer and polymer - α-TOC droplets in the solution. A greater degree of the polymer chain entanglements within the solution results in higher viscosities, while lower apparent viscosity is related to the lower degree of polymer molecule chain entanglement (Kriegel et al. 2008). The addition of α-TOC to polymer solution increased the apparent viscosity. One reason was because of the high apparent viscosity that α-TOC had. It was reported

51

that 10% w/w VE-in-water emulsion has a viscosity of 0.3 Pa.s (Ziani et al. 2012). Also, the

addition of α-TOC droplets in a polymer solution could increase the polymer chain entanglement

with droplets. More droplets indicate a higher degree of chain entanglements, which results in a

higher apparent viscosity. Generally, high viscosity is required for the formation of nanofibers

without beads defects (Duan et al. 2004). The flow behavior index *n* value decreased with

increasing α-TOC concentration in spinning solution. Spinning solutions A1 (control, no α-TOC

adding) and A2 (containing 1% α-TOC) had significantly higher *n* value, and a lower *n* value

was observed in A4, A5 and A6, which containing 3%, 4% and 5% α-TOC, respectively. Due to

the shear-thinning liquid properties (*n*<1), spinning solutions appeared homogenous, and

emulsion droplets might orient themselves in the direction of spinning flow during

electrospinning process and thus be incorporated into nanofibers (Singh 2009). Different from *n*

value, a higher consistency index *K* value was shown in A5 and A6, while A1 and A2 had the

lower *K* values.

Table 4.3 Flow properties of α-TOC emulsion droplets loaded spinning solutions, diameter of
electrospun nanofibers, and encapsulation efficiency of α-TOC

Spinning solutions*	Apparent viscosity (Pa.s)	*n*	*K*	Average diameter (nm)	EE (%)
A1	1.47±0.00[e]	0.631±0.000[ab]	10.87±0.01[d]	199.0±26.1	41.53±0.29[e]
A2	1.53±0.00[d]	0.641±0.009[a]	10.79±0.45[d]	200.3±37.4	54.83±0.35[d]
A3	1.76±0.01[c]	0.625±0.002[b]	13.44±0.22[c]	228.7±29.4	60.22±0.05[c]
A4	1.83±0.03[b]	0.603±0.001[c]	15.69±0.30[b]	224.4±34.9	70.67±1.01[b]
A5	2.03±0.00[a]	0.617±0.001[bc]	16.10±0.10[ab]	249.0±22.4	87.75±0.66[a]
A6	2.05±0.00[a]	0.609±0.000[c]	16.95±0.07[a]	283.0±65.3	86.97±0.59[a]

* Refer to Table 4.1 for the abbreviation of each spinning solution. Values are expressed as mean
± standard error. [abcde]means with the same letter in the columns are not significantly different
(P>0.05). *n*=flow behavior index; *K*=consistency index.

4.3.2 Diameter and Morphology of Nanofibers with Emulsions

The addition of α-TOC droplets influenced the size of nanofibers. The average diameter

of nanofibers (cross section) was increased from 200.3 nm to 283 nm with α-TOC concentration

ranging from 1 to 5% (Table 4.3). A1 nanofibers had the lowest average diameter of 199 nm, and nanofibers produced from A5 and A6 had the highest average diameter of 249.0 nm and 283 nm, respectively. These results kept consistent with the results of apparent viscosities, since solutions A5 and A6 had the highest viscosities than other solutions. Apparent viscosity of spinning solutions was increased along with the increased concentration of α-TOC, which favored the formation of beads-free nanofibers. However, higher viscosity brought in increased diameters (Table 4.3).

α-TOC emulsion in polymer spinning solutions were observed under optical microscope (Figure 4.1A). The diameter of droplets ranged from 166.2 nm to 4 μm. Most droplets size was below 1 μm, while a very few were larger than 1 μm. α-TOC droplets separated from each other in spinning solution without coalescence. Since all spinning solutions were shearing-thinning flows ($n<1$), they appeared homogenous. The contained α-TOC emulsion droplets could be stretched along with the elongation of polymers and therefore be incorporated into fibers due to the repulsion during the electrospinning process. What's more, big size droplets can be broken up into small droplets and incorporated into fibers (Angeles, Cheng and Velankar 2008). Even though the droplets deformed during electrospinning, some droplets maintained their original round shape and size with a thin layer cover of polymers, and resulted in bead-like or dotted structures, as well as the increased nanofiber diameters (Choi et al. 2011, Arecchi et al. 2010). The morphology of α-TOC incorporated nanofibers was shown in Figure 4.1B-G. With increased of α-TOC concentration in spinning solutions, nanofibers were no longer uniform, and the bigger diameters were observed in nanofibers produced from A5 and A6 (Figure 4.1F, G). Also, small diameter nanofibers were generated from the big diameter nanofibers, which indicated the high concentration of spinning solutions (Table 4.3).
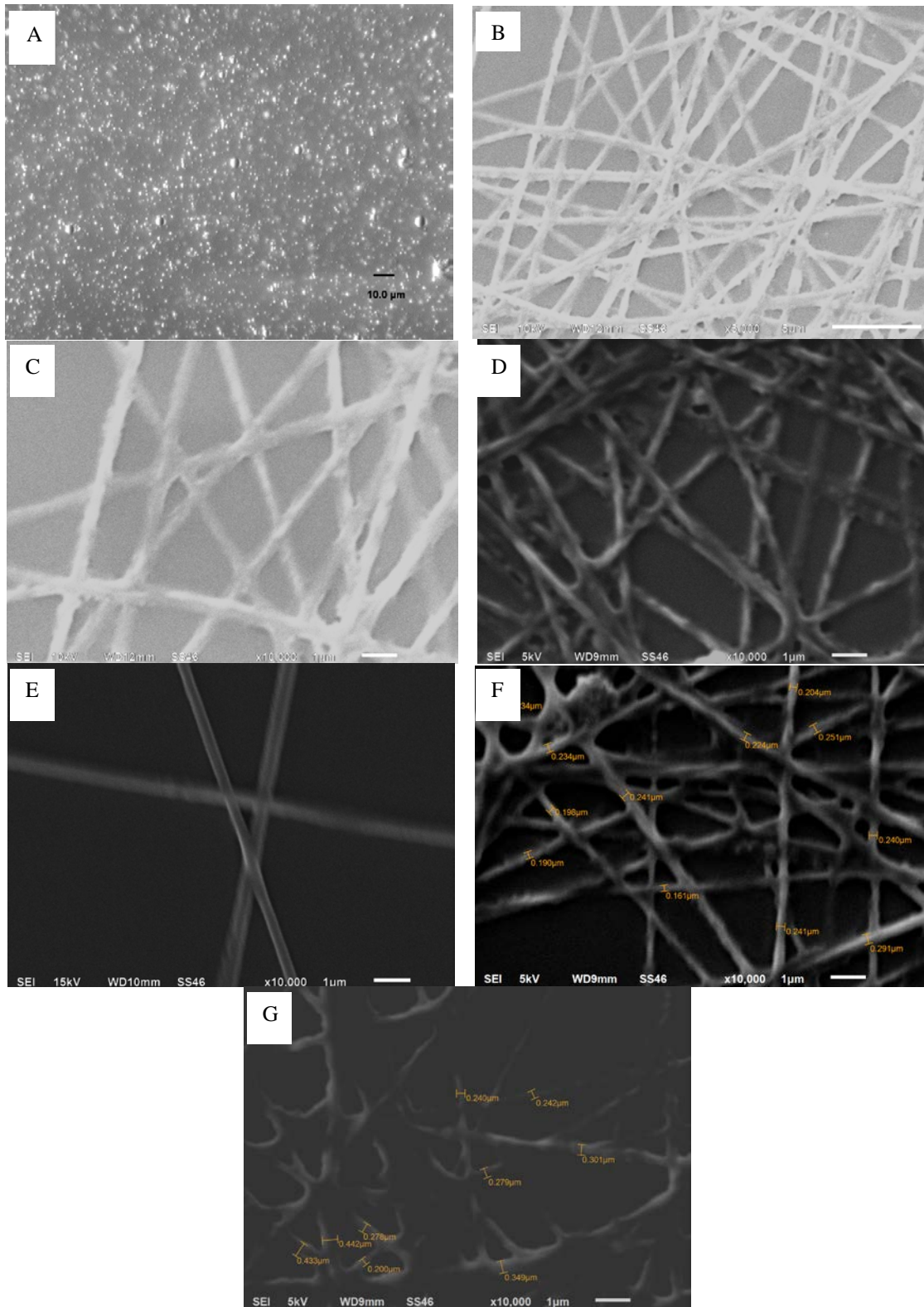
Figure 4.1 Optical microscope (OM) and scanning electron microscope (SEM) images (A) spinning solution containing α-TOC O/W emulsion, (B)-(G) nanofibers produced from spinning solutions A1-A6, respectively.

4.3.3 Encapsulation Efficiency of α-TOC in Nanofibers Containing α-TOC Droplets

The encapsulation efficiency of α-TOC in nanofibers varied from 41.53% to 86.97% with α-TOC concentration in spinning solutions ranging from 1 to 5% (Table 4.3). Nanofibers produced from spinning solutions A5 and A6 had encapsulation efficiencies of 87.75% and 86.97%, respectively, which were higher than that in nanofibers produced from spinning solutions A2 (54.83%), A3 (60.22%) and A4 (70.67%). These results were lower than the results reported by Zigoneanu et al. (2008), they found that the encapsulation efficiency was increased from 89.63 to 95.59% when initial α-TOC loading was increased from 8 to 16%. The increased encapsulation efficiency of α-TOC in nanofibers could be explained by the polymer chain entanglement. At the lower concentration in spinning solutions, α-TOC droplets attached to the polymer surface with less polymer chain entanglement. By increasing the concentration of α-TOC in spinning solutions, more chain entanglement occurred and SDF/PEO polymers were over α-TOC, and more α-TOC was incorporated deep into the polymer matrix. Thus more α-TOC was entrapped into the center of nanofibers during the electrospinning process. The lowest encapsulation efficiency of α-TOC was observed in A1 nanofiber, which was electrospun from 5% PEO spinning solution containing 3% α-TOC. The possible reason was due to the overloaded α-TOC and low content of polymers. α-TOC was incompletely encapsulated by polymers, and resulted in low encapsulation efficiency.

4.3.4 In Vitro Release Profile of α-TOC from Nanofibers with Emulsions

4.3.4.1 Release profile of α-TOC in PBS medium

The release profiles of α-TOC from the SDF/PEO nanofibers were investigated in PBS medium. The release profile showed an initial burst during the first hour, followed by a slow release of α-TOC in all samples (Figure 4.2). The burst effect was higher for nanofibers produced from spinning solutions A2, A3, A4, and A5, where 83.69, 75.65, 73.47, and 62.85%

of α-TOC was released in the first hour, respectively. Nanofibers produced from A6 had a lower burst effect compared with other samples, which was 42.51% in the first hour followed by a constant release. This value was significantly lower than the reported release rate of α-TOC by Zigoneanu et al. (2008), which 86% was released from nanoparticles in first hour with 8% α-TOC loading. These results indicated that the higher the α-TOC content, the lower the initial release.
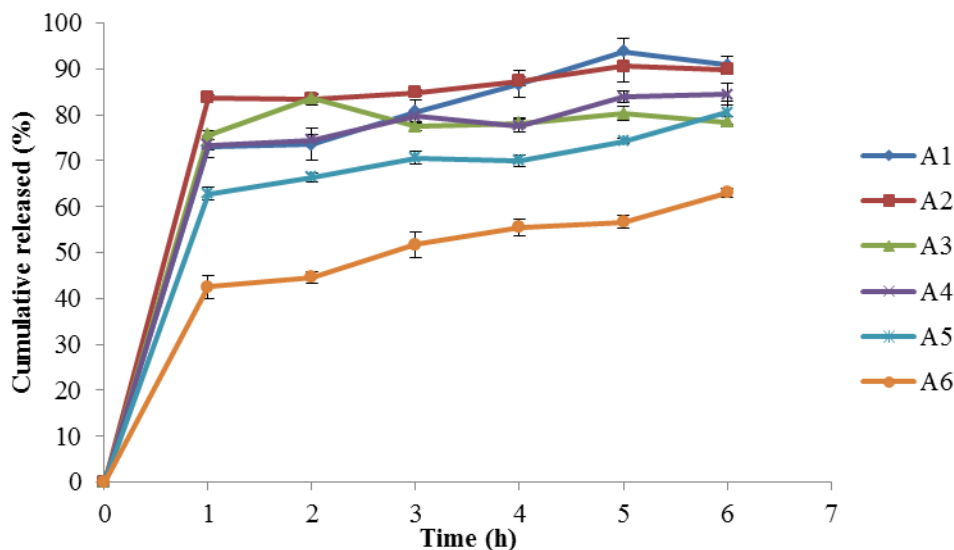
Figure 4.2 Release profile of α-TOC from SDF based nanofibers in PBS media
A1: control nanofibers without α-TOC; A2: nanofibers produced from 1% α-TOC spinning solution; A3: nanofibers produced from 2% α-TOC spinning solution; A4: nanofibers produced from 3% α-TOC spinning solution; A5: nanofibers produced from 4% α-TOC spinning solution; A6: nanofibers produced from 5% α-TOC spinning solution.

This phenomenon was attributed to the higher encapsulation efficiency of α-TOC in nanofibers. Un-entrapped α-TOC or free α-TOC that attached on the surface of nanofibers released rapidly and formed a burst release effect. While encapsulated α-TOC in nanofiber matrix diffused slowly from nanofiber inside to outside and resulted in a constant release profile. Other factors, including penetration of the release medium and polymer matrix degradation, as well as molecule diffusion mentioned above, are three mechanisms of release profile (Sansdrap

and Moës 1997). There was no difference in release profile between nanofibers produced from A1 and A4, which indicated that SDF/PEO nanofiber had a similar characteristic to PEO as a delivery system for α-TOC.

4.3.4.2 In simulated gastric and intestinal environments

The release profiles of α-TOC from nanofibers under SGF and SIF were shown in Figure 4.3. After treatment in SGF for 2 h, the released α-TOC in A1 (21.27%), A2 (20.69%), and A3 (21.12%) nanofibers was significantly lower than that in A5 (32.23%) and A6 (33.83%) nanofibers. There was no significant difference in released α-TOC percentage among A1, A2 and A3 nanofibers. A5 and A6 nanofibers had the highest released α-TOC percentages, which indicated that higher α-TOC concentration resulted in higher release in SGF. The release of α-TOC in SGF was mainly due to the diffusion of α-TOC from nanofibers to the medium. Since there were no solubilizing agents present in SGF, for instance, Tween 80, the release of α-TOC was very slow until enough α-TOC was released and formed transport vehicles by associating with each other (Murugeshu et al. 2011). After 4 h of treatment in SIF, only 6.48% of α-TOC was released from A6 nanofiber. Nanofiber produced from A1 (17.59%) had the highest released percentage of α-TOC in SIF (Figure 4.3) due to its highest surface area to volume ratio. Thus the shortest time was needed for α-TOC to diffuse from the inside to the outside of the nanofibers. The release of α-TOC in SIF was slower than that in SGF. This might be due to the emulsion droplets form of α-TOC in SIF. The surfactant coated on α-TOC droplets served as a barrier and increased the resistance of digestion in SIF. Also, the environment pH may be another reason. Low pH value (1.2) in SGF may cause the degradation of nanofibers, thus more α-TOC are released compared with that in neutral SIF (pH 6.8).
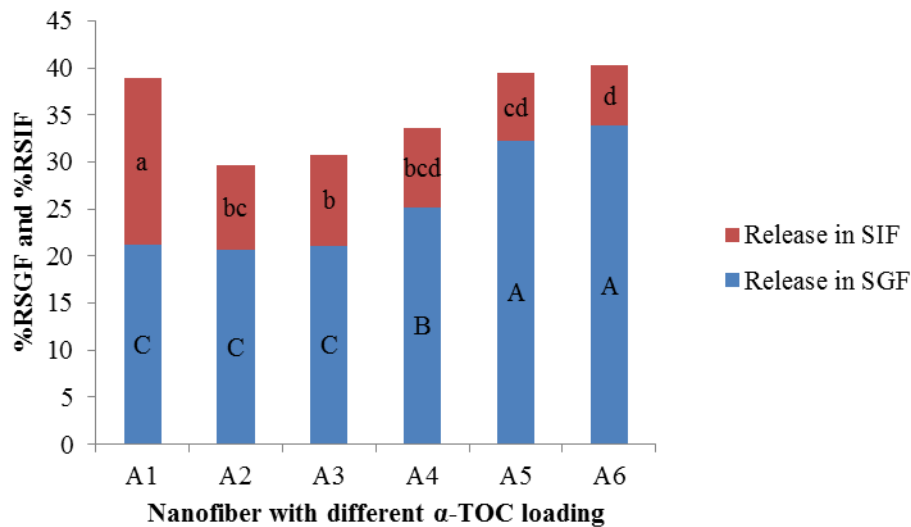
Figure 4.3 Gastrointestinal release of α-TOC from SDF/PEO nanofibers
A1: control nanofibers without α-TOC; A2: nanofibers produced from 1% α-TOC spinning solution; A3: nanofibers produced from 2% α-TOC spinning solution; A4: nanofibers produced from 3% α-TOC spinning solution; A5: nanofibers produced from 4% α-TOC spinning solution; A6: nanofibers produced from 5% α-TOC spinning solution. ABC: same letter means there was no significant difference in the release of α-TOC in SGF between different samples (P>0.05); abcd: same letter means there was no significant difference in the release of α-TOC in SIF between different samples (P>0.05).

4.3.5 Nanofiber Containing Zein Encapsulated α-TOC Particles

4.3.5.1 Flow properties

The apparent viscosity of electrospinning solution containing zein encapsulated α-TOC particles was shown in Table 4.4. The viscosity of spinning solutions (from B1 to B3) was significantly increased with increased concentration of zein, where B1 containing 8% of zein had the highest viscosity of 3.63 Pa.s and B2 with 4% of zein had the lowest viscosity of 2.63 Pa.s. That was because of the increased amount of polymer in the spinning solution. The concentration of α-TOC also affected the viscosity of spinning solutions. With consistent zein concentration at 6%, B4 had the lowest viscosity due to the lowest α-TOC content of 20% (relative to zein mass). Interestingly, the highest viscosity was observed in B3 and B6, which contained 30% and 40% α-TOC, respectively. B5 had the highest α-TOC concentration (50%, relative to zein mass), but the

viscosity was 2.88 Pa.s. That may be because α-TOC molecules attach on the surfaces of zein particles when the concentration of α-TOC is low (Luo et al. 2011). Thus the polymer chain entanglement with both zein and α-TOC increased and resulted in high viscosity. With increased α-TOC concentration, α-TOC may migrate to zein particles and reduce the polymer chain entanglement, therefore gave the spinning solution a low viscosity. There was no significant difference in viscosity between control solution B7 and B3, which had the same content of α-TOC and zein.

Table 4.4 Flow properties of electrospinning solutions containing zein encapsulated α-TOC, and diameter and encapsulation efficiency of corresponded nanofibers

Spinning solutions*	Apparent viscosity (Pa.s)	n	K	Diameter (nm)	Encapsulation efficiency (%)
B1	3.63±0.08[a]	0.495±0.003[c]	55.55±0.09[a]	324.6±10.0	68.28±0.10[c]
B2	2.63±0.02[d]	0.539±0.003[a]	31.59±0.25[e]	283.1±23.2	74.50±0.41[a]
B3	3.04±0.00[b]	0.523±0.002[b]	39.83±0.55[b]	307.4±33.3	70.61±0.37[b]
B4	2.64±0.01[d]	0.538±0.004[a]	32.09±0.76[e]	279.3±23.9	63.48±0.33[d]
B5	2.88±0.02[c]	0.532±0.002[ab]	36.03±0.30[d]	291.3±36.6	74.51±0.18[a]
B6	2.95±0.02[b]	0.532±0.001[ab]	36.38±0.50[cd]	290.2±46.9	56.94±0.22[e]
B7	2.97±0.03[b]	0.535±0.006[ab]	37.74±0.01[c]	294.5±36.1	63.16±0.24[d]

* Refer to Table 4.2 for the abbreviation of each spinning solution. Values are expressed as mean ± standard error. [abcde]means with the same letter in the columns are not significantly different (P>0.05). n=flow behavior index; K=consistency index.

The flow behavior index n values for all spinning solutions were less than 1.0, which indicated the shear thinning properties of spinning solutions. Because of the shear thinning flow properties, spinning solutions were homogenous, and zein particles could be incorporated into nanofibers by deforming and elongating during electrospinning. The significantly high K value was shown in B1 spinning solution, which containing 8% of zein with 30% of α-TOC. And the low K values were observed in B2 and B4 spinning solutions, which containing 4% of zein with 30% α-TOC and 6% zein with 20% α-TOC, respectively.

4.3.5.2 Morphology and naofiber size

α-TOC loaded zein particles were observed under optical microscope and were shown in Figure 4.4A. The zein particles separated from each other and exhibited spherical structures with a smooth surface, and the diameter was less than 1 μm. α-TOC was incorporated into self-assembled zein particles by both ionic and hydrophobic interactions between α-TOC and zein molecules (Luo et al. 2011). When SDF/PEO polymer solution was added to α-TOC/zein solution, polymer chains entangled with α-TOC/zein particles and coated the surface. Therefore α-TOC/zein particles were incorporated into nanofibers during the electrospinning process. The morphology of nanofibers was shown in Figure 4.4B-H. Bead-free nanofibers containing α-TOC/zein particles were produced with a cross-section average diameter ranging from 279.3 to 324.6 nm (Table 4.4). With same α-TOC loading percentage (30% relative to zein mass) in spinning solutions, B1 (324.6 nm) nanofiber had higher average diameter than B2 (283.1 nm) and B3 (307.4 nm) nanofibers. With the same zein concentration (6%) in spinning solutions, B4 nanofiber had the lower average diameter of 279.3 nm compared with B3 (307.4 nm), B5 (291.3 nm), B6 (290.2 nm) and B7 (294.5 nm) nanofibers. The results of the average diameter of nanofibers were consistent with the results of the viscosities of spinning solutions. Even though the spinning solutions had high zein and α-TOC concentration, there was no significant branching of nanofibers observed in each nanofiber sample, and the diameter distribution was narrow (Table 4.4). This indicated that the charge was uniformly distributed on the jet, and the spinning solution was homogeneous.
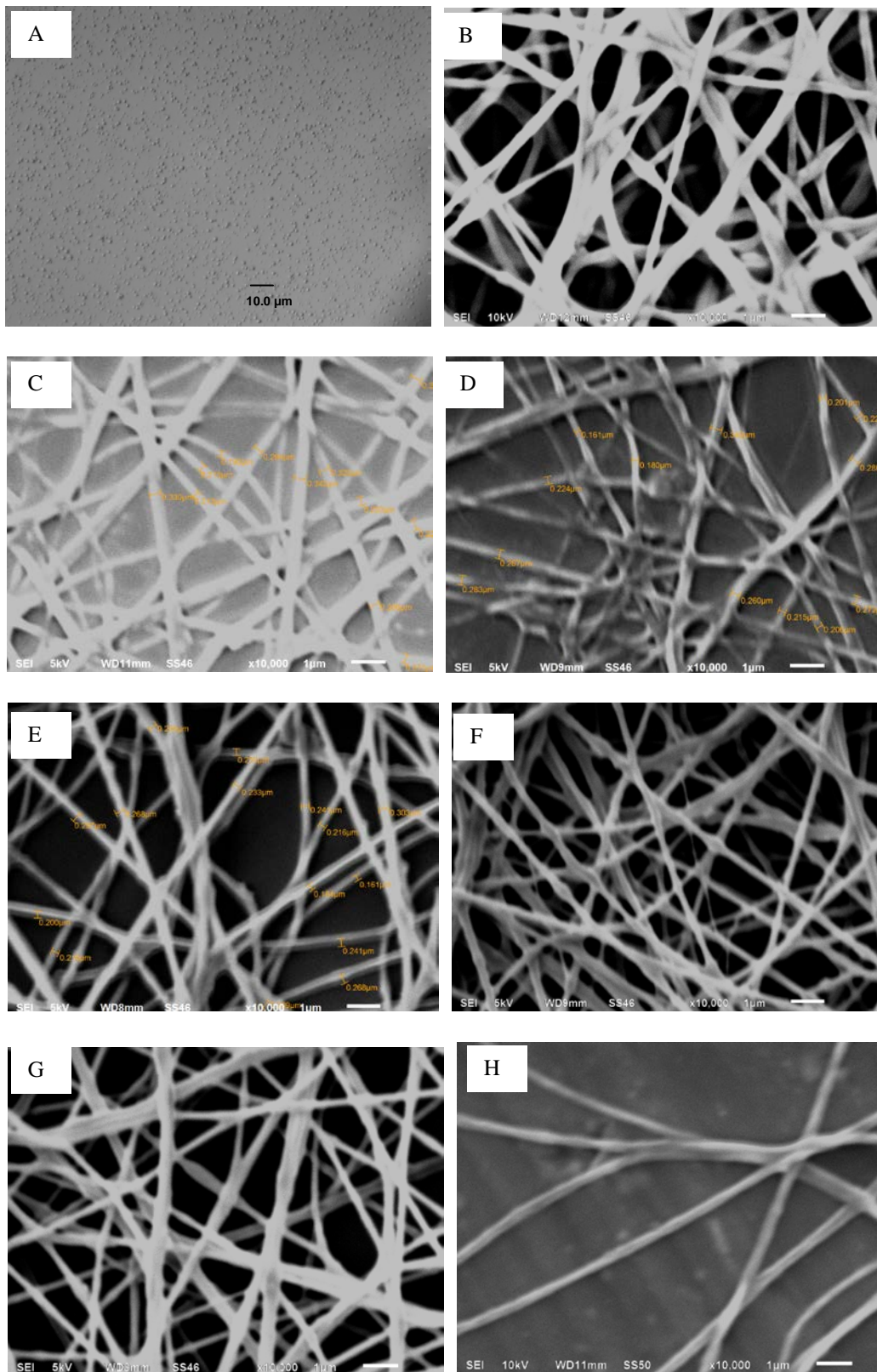
Figure 4.4 Optical microscope (OM) and scanning electron microscope (SEM)
(A) α-TOC loaded zein particles; (B)-(H) nanofibers produced from spinning solutions B1-B7,
respectively.

4.3.5.3 Encapsulation efficiency

Encapsulation efficiency of α-TOC in nanofibers was demonstrated in Table 4.4. Encapsulation efficiency of α-TOC decreased from 74.50 to 68.28% when zein concentration increased from 4 to 8%. That may because of overloaded zein particles in a certain amount of SDF/PEO polymer solution, thus α-TOC/zein particles were incompletely incorporated into SDF/PEO nanofibers. With different concentrations of α-TOC in spinning solutions, the encapsulation efficiency also varied. The high EE of α-TOC was observed in B5 nanofiber, and the low EE was in B6 nanofiber, which were 74.51 and 56.94%, respectively. The possible reason was that the high α-TOC content resulted in the migration of α-TOC from zein particle surface to the internal part, and therefore the encapsulation efficiency was increased. Nanofiber produced from B7 had a encapsulation efficiency of 63.16%, which might be due to the overloaded α-TOC/zein particles.

4.3.5.4 In vitro release

Figure 4.5 shows the release profile of zein entrapped α-TOC from nanofibers in PBS medium. B2 (containing 4% zein) nanofiber had the highest initial burst, 85.48% of α-TOC was released in the first hour, followed by a constant release. With increased zein concentration, the burst effect decreased dramatically. B1 nanofiber with 8% of zein had the lowest initial burst, where 45.35% of α-TOC was released in the first hour and 61.73% was released after 6 h treatment. High zein concentration resulted in bigger nanofiber diameters (Table 4.4), thus the diffusion rate of α-TOC was slow, and more time was needed for entrapped α-TOC to diffuse from the inside to the outside. The initial α-TOC loading (relative to zein mass) influenced the release profile of α-TOC from nanofibers. With the highest loading of 50%, the burst effect was 61.52% in the first hour (B5 nanofiber). B4 nanofiber with 20% α-TOC had released 79.82% and 90.14% of α-TOC at 1 h and 6 h, respectively. The initial release percentage of α-TOC was

higher than the reported value (30%) by Luo et al. (2011). However, the loaded α-TOC was

higher (30%) than this study (20%). Luo et al. (2011) also reported that the release percentage of

α-TOC is increased with lower α-TOC loading percentage.
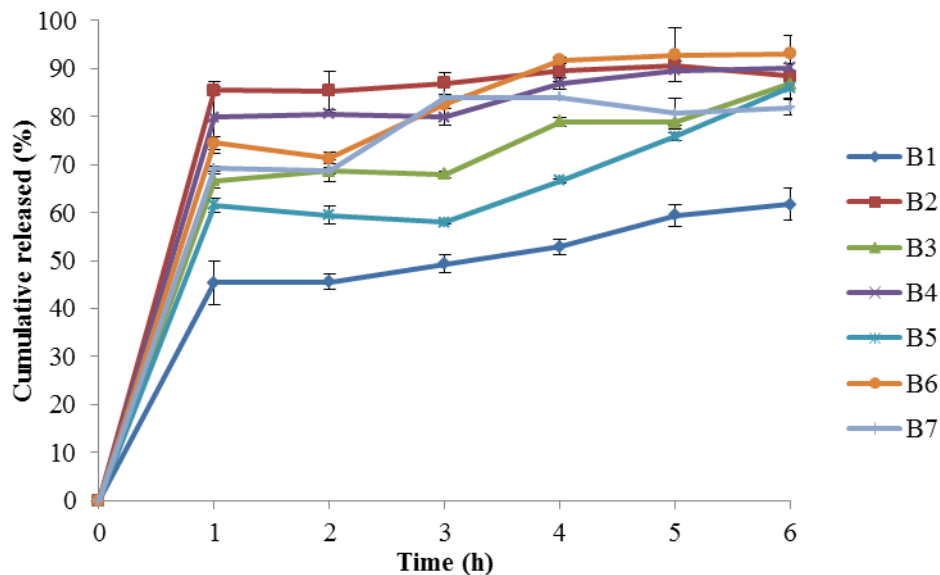
Figure 4.5 Release profile of zein encapsulated α-TOC from SDF based nanofibers in PBS media Nanofibers produced from B1: spinning solution containing 8% of zein with 30% of α-TOC; B2: spinning solution containing 4% of zein with 30% of α-TOC; B3: spinning solution containing 6% of zein with 30% of α-TOC; B4: spinning solution containing 6% of zein with 20% of α-TOC; B5: spinning solution containing 6% of zein with 50% of α-TOC; B6: spinning solution containing 6% of zein with 40% of α-TOC; B7: control.

The in vitro release profile of α-TOC in SGI conditions were shown in Figure 4.6. The

released α-TOC in SGF was decreased with increased zein amount in the nanofibers. Only

22.29% of α-TOC was released in SGF from B1 nanofiber with 8% zein, while 48.15% of α-

TOC was released from B2 nanofiber with 4% zein loading. Due to the addition of zein,

degradation of polymer was the main factor for the release profile. With enzymatic hydrolysis of

zein, entrapped α-TOC was released into SGF. However, nanofibers with higher zein

concentration had a bigger diameter (Table 4.4), a longer time was taken for pepsin to diffuse

into the nanofiber and hydrolyze zein, and therefore the diffusion rate for α-TOC was slower.

Similar to the release profile of α-TOC in PBS, the cumulative released α-TOC in SGF was

decreased with increased α-TOC loading.
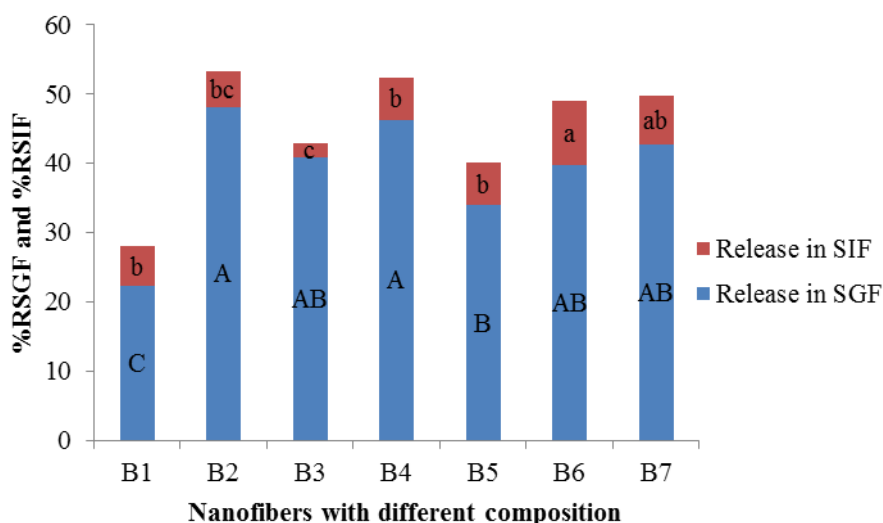
Figure 4.6 Gastrointestinal release of zein encapsulated α-TOC from SDF/PEO nanofibers Nanofibers produced from B1: spinning solution containing 8% of zein with 30% of α-TOC; B2: spinning solution containing 4% of zein with 30% of α-TOC; B3: spinning solution containing 6% of zein with 30% of α-TOC; B4: spinning solution containing 6% of zein with 20% of α-TOC; B5: spinning solution containing 6% of zein with 50% of α-TOC; B6: spinning solution containing 6% of zein with 40% of α-TOC; B7: control. ABC: same letter means there was no significant difference in the release of α-TOC in SGF between different samples (P>0.05); abc: same letter means there was no significant difference in the release of α-TOC in SIF between different samples (P>0.05).

The released α-TOC in SIF was lower than that in SGF after 4 h treatment. The reason

could be due to the hydrolyzed zein (Liang et al. 2010, Luo et al. 2011). Zein that hydrolyzed in

SGF by pepsin might serve as an emulsifier and coating on α-TOC droplets. Thus the digestion

resistance was increased in SIF and slow release occurred.

4.3.6   Physicochemical Characterization

4.3.6.1 DSC thermal properties of α-TOC encorporated nanofibers

The differential scanning calorimetry (DSC) curves of zein, α-TOC emulsion droplets

loaded nanofibers, and zein encapsulated α-TOC loaded nanofibers were compared in Figure 4.7.

The melting points of α-TOC-PEO and α-TOC-SDF/PEO nanofibers were at 65.3 and 60.7 °C,

respectively. This was due to the melting of the crystalline PEO phase (Kim et al. 2005). The

melting point of zein was observed at 92.8 °C. That may be due to the evaporation of bound

water since polymer has a strong affinity with water (Luo et al. 2011). In α-TOC/zein-PEO and

α-TOC/zein-SDF/PEO nanofibers, only one melting peak was observed at 63.9 and 64.4 °C,

respectively. No melting peak of zein was detected in those nanofibers. This indicated that α-

TOC entrapped zein particles were dispersed and encapsulated into nanofibers. Previous studies

have reported that the absence of melting point indicated the encapsulation (Lai and Guo 2011,

Luo et al. 2012).
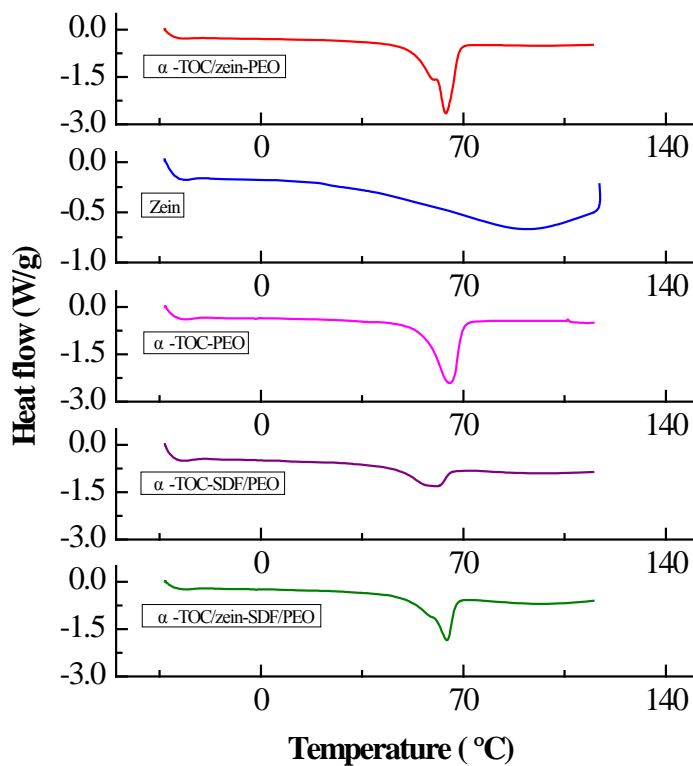
Figure 4.7 DSC thermograms of α-TOC incorporated nanofibers

4.3.6.2 FTIR

The intermolecular interactions of α-TOC incorporated nanofibers were evaluated by

FTIR and the results were shown in Figure 4.8. In α-TOCdroplets loaded nanofibers, the triplet

peak at 2924, 2867, and 2961 cm^{-1} in α-TOC decreased to 2885 cm^{-1} in α-TOC-PEO nanofiber

and 2878 cm^{-1} in α-TOC-SDF/PEO nanofibers. That indicated the conformational structures of

C-H stretching from alkanes were changed. The triplet peak at 1146 cm^{-1}, 1098 cm^{-1} and 1060

cm^{-1} is assigned to the C-O-C stretching from PEO. α-TOC-PEO nanofibers had more intensive

C-O-C bond than α-TOC-SDF/PEO, which indicated α-TOC-PEO nanofifbers had more

crystallinity.
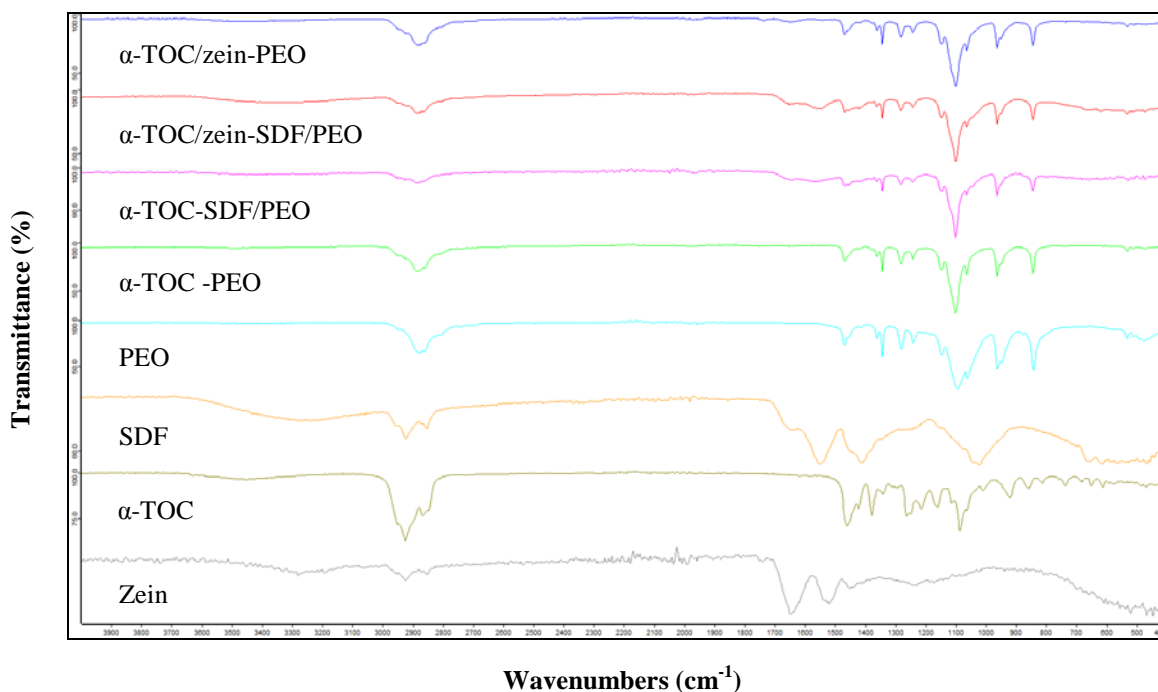
Figure 4.8 FTIR spectra of α-TOC incorporated nanofibers and the individual components

The broad bands of hydrogen bonds in VE shifted from 3459 cm^{-1} to 3315 cm^{-1} in the

spectra of α-TOC/zein-SDF/PEO nanofibers. This shift may be due to the formation of hydrogen

bonds (Luo et al. 2011). α-TOC contains hydroxyl groups, which can form hydrogen bonds with

amide groups in zein. Also, PEO contains hydroxyl groups, and SDF contains both amide and

hydroxyl groups. The hydrogen bonds could be easily formed between SDF/PEO and zein,

SDF/PEO and α-TOC. The hydrogen bond was at 3456 cm^{-1} in α-TOC-PEO nanofibers, at 3441

cm^{-1} in α-TOC/zein-PEO nanofibers, and at 3421 cm^{-1} in α-TOC-SDF/PEO nanofibers. In addition, the hydrophobic attraction may be another force between α-TOC and Zein.

Two peaks at 1532 and 1650 cm^{-1} in the spectra of zein powder. Peaks at 1643 and 1559 cm^{-1} were shown in α-TOC-SDF/PEO nanofibers. Also, two peaks at 1645 and 1548 cm^{-1} in α-TOC/zein-SDF/PEO nanofibers. No peak was observed between 1500 and 1700 cm^{-1} in α-TOC-PEO nanofibers. Those peaks were contributed by amide I and amide II groups. Electrostatic interactions may be another intermolecular force between α-TOC and zein, α-TOC and SDF, zein and SDF (Luo et al. 2011).

4.4   Conclusions

In this study, SDF/PEO nanofibers were produced as a carrier for α-TOC delivery. α-TOC was loaded into nanofibers either by emulsion form or by zein encapsulated particles. The molecular interactions in α-TOC-SDF/PEO and α-TOC/zein-SDF/PEO may be hydrogen bonds. α-TOC had lower initial release in PBS medium from A6 and B1 nanofibers in the first hour compared with that from other nanofibers, and the slow release profile was observed in both PBS and SGI conditions. The results indicated that SDF based nanofibers can be used as delivery system for α-TOC. This delivery system may not only improve the stability of α-TOC but also enhance the bioavailability and controlled release property of α-TOC.

CHAPTER 5   STABILITY STUDY OF ALPHA-TOCOPHEROL ENTRAPPED IN SOLUBLE DIETARY FIBER BASED NANOFIBER

5.1   Introduction

Because of its antioxidant activities, vitamin E as an essential micronutrient plays a very important role in maintaining body health. It can capture free radicals in cell membranes and break lipid peroxidation chain reactions, therefore it protects membrane lipids against oxidation (Khayata et al. 2012b). It is claimed that vitamin E can inhibit the effects of oxidative stress, reduce the risk of cancer, cardiovascular disease, diabetes and aging (Herrera and Barbas 2001). Vitamin E can be found in many natural sources and is widely used as functional ingredients in food, pharmaceutical, and cosmetic preparations (Yang and McClements 2013b). α-Tocopherol is the most biologically active form of vitamin E. One molecule of α-tocopherol can capture two peroxyl radicals, and it has been used in fortifying food products and supplements (McClements et al. 2009, Yang and Huffman 2011). However, there are also many concerns related to the addition of vitamin E in commercial products since it is chemically instable, has poor water solubility, as well as the variable bioavailability.

α-Tocopherol is highly prone to oxidation when is exposed to heat, oxygen and light, thus led to lose its bioactivity (Gawrysiak-Witulska, Siger and Nogala-Kalucka 2009, Yoon and Choe 2009). Oxygen is the main factor that related to the degradation of α-tocopherol. It was reported that α-tocopherol is stable at high temperature with the absence of oxygen, while the oxidation rate increases under atmospheric conditions with the presence of oxygen, which increases its degradation (Shin et al. 1997). High temperature accelerates the degradation of α-tocopherol. About 70-80% of vitamin E was lost when heating white flour over 150 °C for 15 min (Hakansson and Jagerstad 1990). Another study showed that more α-tocopherol was lost under 100 °C than under 60 °C with atmospheric pressure, and only 100 h was needed to degrade all α-

tocopherol in olive oil (Nissiotis and Tasioula-Margari 2002). Besides aforementioned studies, in which α-tocopherol as a component existed in a food matrix, some studies tested the stability of free form α-tocopherol. It was reported that the free form of α-tocopherol had the highest degradation rate when heated at 180 °C, in which about 55% was degraded after 2 h of heating.

Photooxidation is another reason that causes the α-tocopherol degradation. Under artificial light (λ > 290 nm), α-tocopherol degraded 50% after 500 min, and only 17% remained in olive oil after exposure to artificial light for 2500 min (Pirisi et al. 1998). In addition, due to the highly lipophilic property, α-tocopherol cannot be directly used in aqueous media (Sagalowicz et al. 2006, Velikov and Pelan 2008). Therefore, it is very import to develop a system to overcome these deficiencies. The ideal system should protect α-tocopherol from chemical degradation and maintain its bioavailability during processing and storage.

Encapsulation incorporates core materials into wall materials to achieve both protection and bioavailability enhancement. Several systems have been developed for encapsulating lipophilic nutraceuticals, such as micro/nano-emulsions, nanoparticles, liposomes, and polymer particles (Matalanis, Jones and McClements 2011, McClements 2011, Velikov and Pelan 2008, Yang and McClements 2013b). After encapsulating into shell materials, the stability and high retention of α-tocopherol were maintained after being exposed to high temperatures and UV light during storage (Marsanasco et al. 2011a, Zhao et al. 2011, Laouini et al. 2013, Khayata et al. 2012b).

However, encapsulation is not enough to prevent the degradation of encapsulated bioactive compounds, oxidation happens on core materials during processing and storage if there is no antioxidant presence (Wan et al. 2011, Zhao et al. 2011). Especially in nanoencapsulation system, oxygen can penetrate through the wall and react with α-tocopherol due to the high

surface area to volume ratio, thus cause the loss of bioactivity. Thus, it is necessary to find a system that can protect α-tocopherol from degradation and maintain its bioactivity when is exposed to severe conditions. In our previous studies, a soluble dietary fiber (SDF) based nanofiber delivery system had been successfully developed for α-tocopherol (α-TOC). This study focused on investigating the effect of SDF based nanofiber on the stability of entrapped α-TOC. Both temperature and UV light were examined for effect on the degradation of encapsulated α-TOC. Also, the stability of α-TOC was evaluated during storage at room temperature.

5.2 Materials and Methods

5.2.1 Production of Nanofiber with α-TOC

Two samples were prepared for α-TOC stability test and the formulations were shown in Table 5.1. Sample A was SDF based nanofibers loaded with α-TOC. Based on the previous study (Chapter 4), electrospinning solution with composition of 3% soluble dietary fiber (SDF), 5% polyethylene oxide (PEO), 6% zein and 50% of α-tocopherol (α-TOC, relative to zein mass) was selected in this study because of its high encapsulation efficiency and its slow release profile of α-TOC. Electrospinning solution A was prepared as described below. Thirty percent zein (Sigma Aldrich, St. Louis, MO., USA) stock solution and 50% α-TOC stock solution were prepared by dissolving zein power in 75% ethanol solution and dissolving pure α-TOC (Fluka, Sigma-Aldrich, St. Louis, MO, USA) in pure ethanol solution, respectively. SDF and PEO solutions were separately prepared by dissolving them in deionized water. α-TOC solution was gradually added into zein solution with mild stirring for 30 min to obtain α-TOC loaded zein particles. Then 0.5 g of 10% Tween 80 solution was added into α-TOC loaded zein particles solution with stirring for 30 min. The final concentration of Tween 80 was 0.5%. PEO solution was added into the solution and the solution was vigorous stirred for 1 h. Then SDF solution was added into the solution and stirred for another 30 min to obtain homogenous α-TOC loaded spinning solution.

Table 5.1 Composition of solutions

Solutions	SDF (wt%)	PEO (wt%)	Zein (wt%)	α-TOC (wt%)	Tween 80 (wt%)	Nanofiber/Film
A	3	5	6	50 (relative to zein mass)	0.5	Nanofiber A
B	0	5	6	50 (relative to zein mass)	0.5	Nanofiber B
C	3	5	6	50 (relative to zein mass)	0.5	Film C
D	0	5	0	1	0	Film D

Electrospinning solution B was prepared as described in preparation of solution A but without SDF. The spinning solutions A and B were separately electrospun into nanofibers. The laboratory scale electrospinning setup consisted of a high DC voltage power supply (Model: FC30R4, Glassman High Voltage, INC., High Bridge, NJ, USA), a KDS-100 syringe pump (KD Scientific, Hayward, CA, USA), and a 3 mL syringe with a 23 gauge (0.35 mm) needle. Aluminum foil was used as the collector. Electrospinning conditions were set as follows: flow rate was 0.2 mL/h, voltage was 20 kV, and the distance between tip and collector was 15 cm. The collected electrospun nanofibers A and B with α-TOC were dried in a vacuum oven at room temperature overnight and were stored at -20 ℃. The thickness of nanofiber mats was controlled at 0.30 mm by controlling the spinning time.

5.2.2 Production of Film with α-TOC

Two films containing α-TOC were prepared to compare with the electrospun nanofibers. Film solution C was prepared as similar to the electrospinning solution A composition (Table 5.1). The second film solution D was PEO containing α-TOC. Solution D was prepared by mixing 1 g of 10% α-TOC solution (dissolved in 100% ethanol) with 5 g of 10% PEO solution and 4 g of deionized water to form α-TOC/PEO blend that containing 1% α-TOC and 5% PEO. Both solutions C and D were cast onto clean aluminum plates with a diameter of 70 mm and

dried at room temperature to obtain cast films with a thickness of 0.30 mm. Resulted two films α-TOC/zein-SDF/PEO films and α-TOC-PEO films were dried in a vacuum oven at room temperature overnight and were stored at -20 ℃.

5.2.3 Effect of Temperature on Nanofibers and Films Containing α-TOC

The stability of α-TOC was measured at a temperature of 40 °C under atmospheric pressure. Nanofibers and films that containing α-TOC were cut into 25×25 mm square samples with a thickness of 0.30 mm. The weight of each piece was about 35 mg. Each sample was transferred to the sealed amber bottles which were placed in a preheated incubator (model 3525, LAB-LINE Instruments Inc., Melrose Park, IL). The temperature was maintained at 40 °C. Samples were removed after certain times (0, 12, 24, 36, 48, and 72 h) and were analyzed for α-TOC content.

The α-TOC content in each sample was determined by a modified method reported by Wang, Tian and Chen (2011). Ten microgram of nanofibers was mixed with 2 mL of distilled water. The mixture was stirred on a magnetic stirrer (IKA® C-MAG HS7, Wilmington, NC, USA) for 5 min to completely dissolve wall materials of nanofibers. Then, 6 ml of pure ethanol was added to reach the ethanol final concentration of 75%. The mixture was vigorously shaken on a vortex mixer (Mini vortexer MV1, VWR Scientific, IKA® Works, INC., Wilmington, NC, USA) for 5 min to dissolve zein particles. Then 5 mL of hexane was added and vigorously shaken for 30 min at 1000 rpm. The mixture was centrifuged at 800 g at 4 °C for 5 min (Beckman J2-HC centrifuge, GMI, Inc., Ramsey, MN, USA). The absorbance of the top layer (hexane layer) that contained α-TOC was measured by a UV/vis spectrophotometer (Genesys 2, Thermo Fisher Scientific Inc., Rochester, NY) at 297 nm. Concentrations of α-TOC were determined from a standard curve prepared with pure α-TOC in hexane (R^2=0.9998).

The retention of α-TOC was calculated by as follows:

$$\text{Retention} (\%) = m/m_0 * 100 \qquad (5.1)$$

where, m is the α-TOC content in each sample after time t treatment (µg/mg of sample), m_0 is the initial α-TOC content in each sample (µg/mg of sample).

5.2.4 Effect of UV Irradiation on Nanofibers and Films Containing α-TOC

The photochemical stability of α-TOC was conducted on α-TOC entrapped in nanofibers (A and B) and films (C and D). Both nanofibers and films were transferred to uncovered petri dishes placed in a light proof cabinet (SG 403A, Baker, Sanford, Maine, USA), and exposed to UV light (253.7 nm, 40 W) for up to 8 hours at room temperature. Samples were withdrawn after exposure times of 0, 0.5, 1.0, 2.0, 4.0, 6.0 and 8.0 h for α-TOC content measurement as described in section 5.2.3.

5.2.5 Effect of Storage on Nanofibers and Films Containing α-TOC

The stability of α-TOC during storage was investigated. Samples were separately transferred into sealed amber bottles and the bottled samples were placed at room temperature for up to 15 d storage. The changes of α-TOC content in each sample were measured at day 0, 1, 3, 5, 7, 9, 11, 13 and 15 as described in section 5.2.3.

5.2.6 Statistical Analysis

All experiments were conducted in triplicate, and the results were reported as mean values and their standard deviations. Analysis of variance (ANOVA) was conducted by SAS software (Version 9.3, SAS Inst. Inc., Cary, NC, USA.) to test the difference of α-TOC retention in each matrix and the difference between treatment time.

5.3 Results and Discussion

5.3.1 Effect of Temperature on Nanofibers and Films Containing α-TOC

α-TOC contents in both nanofibers and films were varied after exposed to treatment at 40 °C (Figure 5.1).
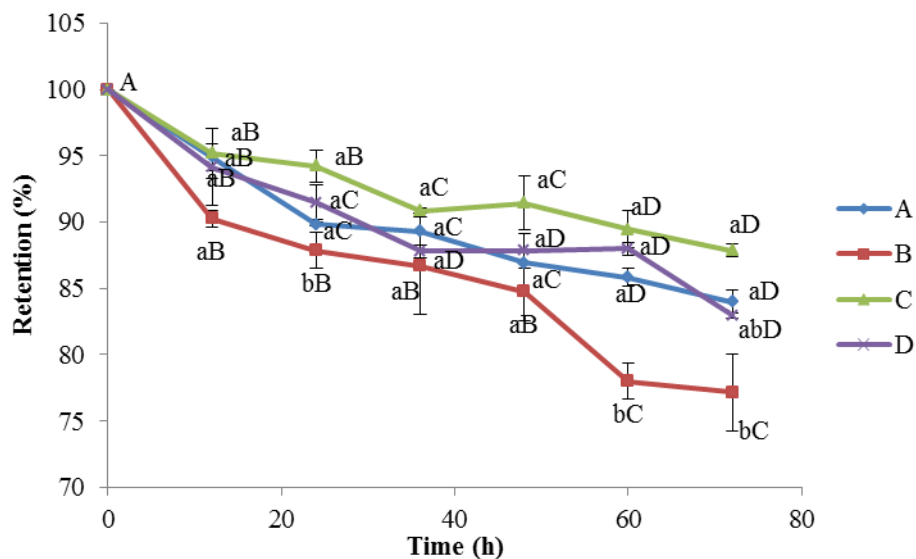
Figure 5.1 Retention of α-TOC under heat treatment

A: α-TOC entrapped SDF based nanofibers; B: α-TOC entrapped nanofibers without SDF; C: α-TOC entrapped cast film with SDF adding; D: α-TOC/PEO blend cast films without SDF adding. Values are expressed as mean ± standard error. ab: Same letter means there was no significant difference in the retention of α-TOC between samples A, B, C and D after a certain period of heat treatment (P>0.05); ABCD: same letter means there was no significant difference in the retention of α-TOC between different heat treatment times in the same sample (P>0.05).

After exposure to 40 °C for 12 h, the retention of α-TOC significantly decreased to 94.89%, 90.26%, 95.21% and 94.15% in nanofiber A, nanofiber B, film C, and film D, respectively. All the nanofibers and films had similar α-TOC retention after 36 h at 40 °C. Both nanofiber A (84.01%) and film C (87.85%) had significantly higher α-TOC retention than nanofiber B (77.16%) and film D (82.95%) after 72 h at 40 °C. The results indicated that SDF minimized α-TOC degradation in nanofiber A and film C. SDF extracted from rice bran is known to be have antioxidant activity, and it scavenges superoxide radical, hydroxyl free radical and reduces lipid peroxidation propagation (Zha et al. 2009b, Rivas et al. 2013). The addition of SDF into wall materials is believed to protect lipids from oxidation. Wan et al. (2011) have reported that SDF reduces the lipid oxidation in encapsulated fish oils.

Nanofiber A and film C had similar α-TOC retention after 72 h at 40 °C, which indicated that there was no significant difference between nanofiber and film forms in the protection on α-

TOC degradation with the presence of SDF. However, film D had higher α-TOC retention than nanofiber B after 72 h at 40 °C, which were 82.95% and 77.16%, respectively. This indicated that film had better effect on the protection of α-TOC than nanofiber at 40 °C without the presence of SDF. In nanofiber B, α-TOC had high surface area to volume and was more accessible to oxygen compared with its bulk size. In flim D, α-TOC existed as the free form with bulk size, thus its interaction with oxygen was less compared to that in nanofiber B, and more α-TOC was retained.

Nanofiber A and film C had α-TOC retention of 84.01% and 87.85%, respectively after 72 h at 40 °C, which were higher than the reported results by Zhao et al. (2011) that the retention percentage of VE in liposome carrier was lower than 70% after 3 days of storage at 40 °C. This indicated that SDF nanofiber and SDF film had better effect on protection of α-TOC degradation at 40 °C than liposome system.

5.3.2   Effect of UV Irradiation on Nanofibers and Films Containing α-TOC

The stability of α-TOC in both nanofibers and films under UV irradiation was evaluated and the results were shown in Figure 5.2. After exposure to UV light for 0.5 h, the retention of α-TOC in nanofiber A, nanofiber B and film D was significantly decreased compared with the initial α-TOC content in each sample, while the α-TOC in film C was not significantly degraded. Film C had significantly higher retention of α-TOC when exposure to UV light over 2 h than that of nanofiber A, nanofiber B and film D. Both nanofiber A and film C had similar α-TOC retention after 8 h of UV exposure, while nanofiber B and film D had significantly lower α-TOC retention.
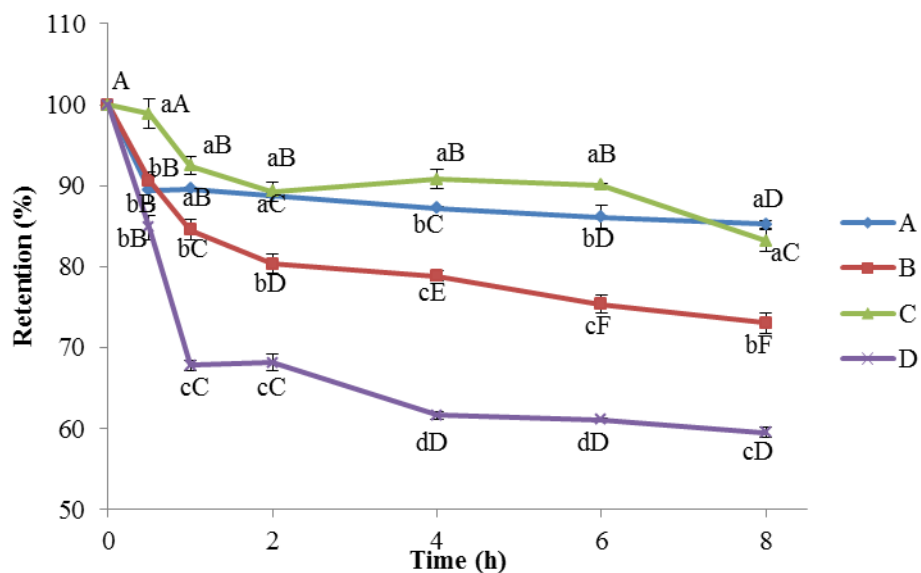
Figure 5.2 Retention of α-TOC with UV irradiation

A: α-TOC entrapped SDF based nanofibers; B: α-TOC entrapped nanofibers without SDF; C: α-TOC entrapped cast film with SDF adding; D: α-TOC/PEO blend cast films without SDF adding. Values are expressed as mean ± standard error. abcd: Same letter means there was no significant difference in the retention of α-TOC between Samples A, B, C and D after a certain period of UV irradiation (P>0.05); ABCDEF: same letter means there was no significant difference in the retention of α-TOC between different UV irradiation times in the same sample (P>0.05).

Film C (90.04%) had significantly higher α-TOC retention than nanofiber A (86.11%) when exposed to UV light for 6 h. This indicated that the film had better protection on α-TOC degradation during the UV exposure. That may be due to the α-TOC form presented in samples. α-TOC in nanofiber A had the smallest size with the highest surface area, thus light could access α-TOC molecules rapidly and interact with them, thereby resulting in α-TOC degradation. In film C, α-TOC had a low surface area with a bulk size, which might reduce the penetration of UV light and delay the photo-oxidation of α-TOC. However, there was no significant difference in α-TOC retention between nanofiber A (85.21%) and film C (83.20%) after 8 h of UV irradiation. That might be due to the initial lipid oxidation. SDF interacted with free radicals that produced during initial lipid oxidation and inhibited the propagation of lipid oxidation.

Nanofiber A had significantly higher α-TOC retention than nanofiber B, about 85.21% of α-TOC was retained in nanofiber A, while 27% of α-TOC was degraded in nanofiber B after 8 h of UV irradiation (Figure 5.2). These results indicated that SDF prevented the degradation of α-TOC during UV treatment. Also, there only 59.53% of α-TOC was retained in film D after UV irradiation for 8 h. That may because of the free bulk form of α-TOC in film D. Due to the immiscibility of α-TOC and PEO, a part of α-TOC might distribute on the surface of cast films. This portion was exposed to UV light directly without any block, thus it degraded very quick.

The retention of α-TOC in nanofiber A (85.21%) and film C (83.20%) after 8 h of UV irradiation was higher than that of previous reported result of 62.05% (Zhao et al. 2011). This indicated that α-TOC degradation from UV irradiation can be inhibited by adding SDF in nanofiber and film.

5.3.3 Effect of Storage on Nanofibers and Films Containing α-TOC

The stability of α-TOC during storage was examined under room temperature. Figure 5.3 shows the retention of α-TOC in nanofiber A, nanofiber B, film C, and film D during storage. Film D had significantly higher α-TOC retention after 1 d of storage at room temperature than nanofiber A, nanofiber B and film C, which were 100.35%, 91.31%, 65.90% and 95.19%, respectively. There was no significant degradation of α-TOC in film D after 1 d storage at room temperature. That might be due to the bulk form of α-TOC existed in film D. α-TOC agglomerated in solution D and formed big oil droplets due to the immiscibility with PEO solution. After casting on aluminum plates, a bumpy surface structure formed on the surface of the film D during drying (Taepaiboon et al. 2007). This bulk α-TOC was less available for oxygen, and exhibited no degradation during short storage period (1 d) at room temperature. Nanofiber B had the lowest retention of α-TOC after storage at room temperature for 1 d compared with other samples. This may be due to the oxidation of surface α-TOC in nanofiber

B. α-TOC had a higher surface area to volume ratio in nanofiber B, thus the interaction between surface α-TOC and oxygen was higher than that in film C and film D. Without the presence of SDF, oxidation happened on the surface α-TOC in nanofiber B at room temperature rapidly and caused degradation of α-TOC.
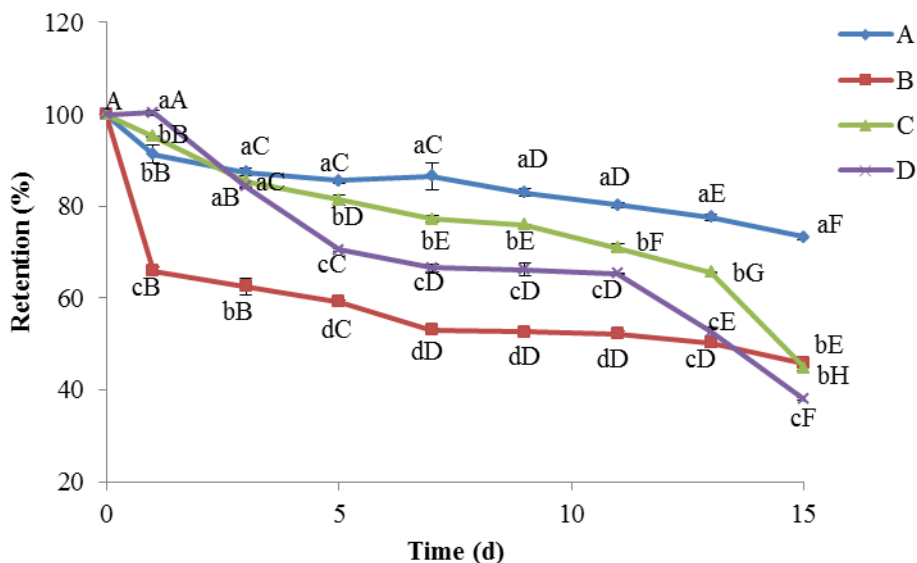
Figure 5.3 Retention of α-TOC during storage
A: α-TOC entrapped SDF based nanofibers; B: α-TOC entrapped nanofibers without SDF; C: α-TOC entrapped cast film with SDF adding; D: α-TOC/PEO blend cast films without SDF adding. Values are expressed as mean ± standard error. abcd: Same letter means there was no significant difference in the retention of α-TOC between sample A, B, C and D after a certain time of storage ($P>0.05$); ABCDEFGH: same letter means there was no significant difference in the retention of α-TOC between different storage times in the same sample ($P>0.05$).

The similar and significantly higher α-TOC retention was observed in nanofiber A, film C and film D after 3 d storage at room temperature than nanofiber B, which were 87.46%, 85.40%, 84.28%, and 62.49%, respectively. These results indicated that SDF inhibited α-TOC degradation in nanofber A and film C during room temperature storage, and bulk form α-TOC in film D had slower degradation than nano form α-TOC in nanofiber B without the presence of SDF.

After storage at room temperature for 13 d, the losses of α-TOC were 22.43%, 49.7%, 34.43% and 47.39% for nanofiber A, nanofiber B, film C and film D, respectively. Nanofiber A had significantly higher α-TOC retention than film C, film D and nanofiber B. The reason may be due to SDF contained in nanofiber A. α-TOC was incorporated in SDF based nanofibers, thus SDF served as an antioxidant and provide protection of encapsulated α-TOC from oxidation. Film C had significantly higher α-TOC retention than nanofiber B and film D, but the retention was lower than that in nanofiber A. This indicated that SDF contained in film C reduced the oxidation of α-TOC and resulted in significantly higher retention of α-TOC than that in nanofiber B and film D. However, SDF was not uniformly coated on α-TOC in film C, the protection that provided by SDF was insufficient to against α-TOC oxidation. Hence higher degradation of α-TOC was occurred in film C than that in nanofiber A.

After 15 d of storage, the retention of α-TOC in nanofiber A achieved 73.29%. This value was higher than that in other systems, in which was reported that 65% of VE was retained in a liposome delivery carrier after storage at 25°C for 15 d (Zhao et al. 2011). Nanofiber B (45.86%) and film C (44.86%) had similar α-TOC retention after 15 d storage at room temperature, and film D (37.99%) had significantly low α-TOC retention.

5.4 Conclusions

In this study, the stability of α-TOC in SDF based nanofiber and film was evaluated by measuring the retention of α-TOC after exposure to heat, light and during storage. Heat degradation of α-TOC was lower in SDF based nanofiber and film than that in nanofiber and film without the addition of SDF. In UV irradiation test, α-TOC had significantly higher retention in SDF based nanofiber and film than that in nanofiber and film without the addition of SDF. These studies indicated SDF reduced the degradation of α-TOC at 40 °C and in the UV irradiation. SDF based nanofiber and film matrix was effective in protecting α-TOC from heat

79

degradation and photooxidation. In storage test, the high retention of α-TOC was observed in SDF based nanofiber and film after stored at room temperature for 13 d, while the lowest retention of α-TOC was found in film and nanofiber without SDF. Therefore, SDF could effectively inhibit the degradation of α-TOC in nanofiber and film. The bioactivity of α-TOC could be maintained in nanofiber and film by adding SDF.

CHAPTER 6   EFFECT OF ALPHA-TOCOPHEROL DELIVERED BY SOLUBLE DIETARY FIBER BASED NANOFIBER ON THE LIFESPAN OF *C. ELEGANS*

6.1   Introduction

Vitamin E as a major lipophilic antioxidant contains eight substances with a chromanol ring and a saturated (tocopherols) or unsaturated (tocotrienols) carbon side chain. These compounds are classified as α, β, γ and δ-tocopherols and α, β, γ and δ-tocotrienols according to the number and the position of methyl groups attached on the chromanol groups (KamalEldin and Appelqvist 1996). α-Tocopherol (α-TOC) has the highest antioxidant ability in lipid oxidation in both foods and biological systems, and it is widely used for supplementation. In biological systems, α-TOC reacts with fatty acid peroxides through electron transfer and protects the membranes from oxidative damage (Traber and Atkinson 2007). In addition, it may regulate gene expression (Rimbach et al. 2010).

Aging is related to the free radicals produced by aerobic metabolism, which causes the accumulation of oxidative damage in cell membrane and thus accelerates the aging process (Harman 1956). The supplementation of antioxidant is regarded as a potential approach to delay aging. Vitamin E has been tested for the influence on lifespan in animal models, including rotifers, nematodes , flies, mice and rats (Ernst et al. 2013). Ernst et al. (2013) have reported that vitamin E can increase the lifespan in certain organisms but not all the organisms. The relationship between vitamin E and lifespan is still unclear. In aforementioned studies, vitamin E was fed to organisms in a free form. It is known that vitamin E is sensitive to oxygen, heat and light. Its bioactive ability may be lost due to degradation when exposed to these factors. Also, it suggests that the bioavailability of vitamin E can increase when it is delivered in nano scale form rather than in bulk form (Feng et al. 2009).

The nematode *Caenorhabditis elegans* (*C. elegans*) is widely used in aging studies. It has a short lifespan of a few weeks and uncomplicated morphology with well-differentiated cell systems. Meanwhile, it is biologically and genetically well-characterized, as well as easy to maintain in the lab (Harrington and Harley 1988, Aan et al. 2013). Also, this organism model is inexpensive. Different from the larger and more complicated mammalian and cell culture models, no expensive or huge facilities are needed for the culture and maintenance of worms, thousands of worms can grow on an agar Petri dish with feeding *Escherichia coli* (Dexter, Caldwell and Caldwell 2012). *C. elegans* intakes and transports food through the pharyngeal movement and relaxation in the terminal bulb of the pharynx (Finley et al. 2013). The aging of *C. elegans* relates with the decreased pharyngeal pumping rate because of sarcopenia (Huang, Xiong and Kornfeld 2004). Therefore, the lifespan can be predicted and premature aging can be detected through measuring the pharyngeal pumping rate.

It was reported that environmental stimuli, e.g., hyperthermia, UV light and chemotherapeutic agents, can cause disorder in the normal redox balance and make the cells shift to a state of oxidative stress, which results in a shorter lifespan (Finkel and Holbrook 2000). Increased resistance to oxidative stress relates with increased lifespan of *C. elegans* (Butov et al. 2001). Hence, the supplementation of antioxidant could delay aging and extend the lifespan.

In our previous study (Chapters 4 and 5), α-TOC delivered by soluble dietary fiber (SDF) based nanofibers had gradually release profiles in vitro and was more stable when exposed to heat, light and oxygen compared with the free form α-TOC. It may have the increased bioavailability and may increase the lifespan of *C. elegans* due to the nano scale, gradually release and higher stability compared with free from α-TOC. In this study, the effect of α-TOC delivered by SDF based nanofiber on the lifespan of nematode *C. elegans* was evaluated by

counting the live *C. elegans*. Meanwhile, heat shock was applied to induce an oxidative stress. It was assumed that the heat shock group of *C. elegans* had more oxidative stress, and thus had a shorter lifespan compared to the group without heat shock. The effect of encapsulated α-TOC on the lifespan of *C. elegans* with/without heat shock was compared. Also, the pharyngeal pumping rate of *C. elegans* was measured to examine the relationship with lifespan.

6.2 Materials and Methods

6.2.1 Nematode Strain and Solutions Preparation

The wild type *C. elegans* N2 strain and TK22 strain (*mev-1* genetic mutant strain) used in this study were generously provided by Pennington Biomedical Research Center at Louisiana State University. Potassium phosphate buffer was prepared by dissolving 136 g of KH_2PO_4 in 900 mL deionized water, and the pH was adjusted to 6.0 with 5 M KOH. Then deionized water was added to the final volume of 1 L and autoclaved (Brinkman, Riverview, FL, USA). Trace metal solution was prepared by dissolving 1.86 g of Na_2EDTA, 0.69 g of $FeSO_4.7H_2O$, 0.20 g of $MnCl_2.4H_2O$, 0.29 g of $ZnSO_4.7H_2O$ and 0.016 g of $CuSO_4$ in 1000 mL deionized water and then autoclaved. S-basal medium was prepared by mixing 5.9 g of NaCl with 50 mL of 1 M potassium phosphate (pH 6.0), then diluted to 1 L with deionized water and autoclaved. One milliliter of 5 mg/mL cholesterol ethanol solution was added after the solution was cooled to room temperature. Liquid culture medium S-complete was prepared by mixing 977 mL of S-basal, 10 mL of 1 M potassium citrate pH 6, 10 mL of trace metals solution, 3 mL 1 M $CaCl_2$ (sterile) and 3 mL of 1M $MgSO_4$ (sterile).

6.2.2 Preparation of α-TOC Incorporated Soluble Dietary Fiber Based Nanofibers

α-TOC loaded soluble dietary fiber based nanofibers were prepared by electrospinning. α-TOC was mixed with 2% Tween 80 solution and homogenized to form 10% O/W emulsions. Then 5 g of 10% α-TOC O/W emulsion was gradually added to 5 g of SDF/PEO polymer

solution (containing 6% SDF and 10% PEO) and stirred at room temperature for 2 h to obtain a homogenous spinning solution. The spinning solution was electrospun into nanofibers under an electrospinning setup, which contained a high DC voltage power supply (Model: FC30R4, Glassman High Voltage, INC., High Bridge, NJ, USA), a KDS-100 syringe pump (KD Scientific, Hayward, CA, USA), and a 3 mL syringe with a 23 gauge (0.35 mm) needle. Aluminum foil was used as the collector. Electrospinning conditions were set as follows: flow rate was 0.2 mL/h, voltage was 20 kV, and the distance between tip and collector was 15 cm. α-TOC loaded SDF based nanofibers were dried in vacuum oven at room temperature overnight and then stored at -20 ℃. The α-TOC content in SDF based nanofiber was 359.7 µg/mg. SDF/PEO nanofibers without the loading of α-TOC were prepared as control sample.

6.2.3 Preparation of Stock Solutions

Twelve stock solutions were prepared as described in Table 6.1. SDF nanofiber stock solutions were prepared from SDF nanofiber without α-TOC. The concentrations of nanofiber were 356 µg/mL (S1-a), 712.01 µg/mL (S1-b) and 1424.08 µg/mL (S1-c). Three concentrations of α-TOC stock solutions were prepared by dissolving 10.0, 20.0 and 40.0 mg of pure α-TOC (Fluka, Sigma-Aldrich, St. Louis, MO, USA) in 100% purity ethanol to a total volume of 0.5 mL, respectively. Then 20 µL of each of above α-TOC solutions was integrated into S-complete solution for a total volume of 2 mL (containing 0.5mg/mL Tween 80). The concentration of α-TOC in these stock solutions were 200, 400 and 800 µg/mL, and they were named as S2-a, S2-b and S2-c, respectively. α-TOC loaded SDF nanofiber containing 359.7 µg/mg of α-TOC were accurately weighed and dissolved in S-complete to obtain the stock solutions containing 200 µg/mL (S3-a), 400 µg/mL (S3-b) and 800 µg/mL (S3-c) of encapsulated α-TOC. In these stock solutions, the wall material concentration (SDF/PEO) was 356 µg/mL, 712.01 µg/mL and 1424.08 µg/mL, respectively. Ethanol stock solution S4 was prepared as a solvent control. It was

84

prepared by adding pure ethanol into S-complete solution to obtain concentrations of 9.8 mg/mL

(S4-a), 9.6 mg/mL (S4-b) and 9.2 mg/mL (S4-c) (containing 0.5% Tween 80).

Table 6.1 Composition of stock solutions

Stock solutions	Description	α-TOC content (μg/mL)	nanofiber content (μg/mL)	Ethanol /Tween 80 content (mg/mL)
S1-a	Nanofiber (without α-TOC)	0	356.00	0/0
S1-b	Nanofiber (without α-TOC)	0	712.01	0/0
S1-c	Nanofiber (without α-TOC)	0	1424.08	0/0
S2-a	Pure α-TOC	200	0	9.8/0.5
S2-b	Pure α-TOC	400	0	9.6/0.5
S2-c	Pure α-TOC	800	0	9.2/0.5
S3-a	α-TOC loaded SDF based nanofibers	200	356.00	0
S3-b	α-TOC loaded SDF based nanofibers	400	712.01	0
S3-c	α-TOC loaded SDF based nanofibers	800	1424.08	0
S4-a	Ethanol control	0	0	9.8/0.5
S4-b	Ethanol control	0	0	9.6/0.5
S4-c	Ethanol control	0	0	9.2/0.5

6.2.4 Preparation of Synchronized *C. elegans*

Less than 1 week old chunk dishes with good condition (having a large number of gravid

adults) were chosen to prepare synchronized *C. elegans*. Worms were washed off plates with 5

mL of distilled water into a 15 mL conical tube. Then worms were separated from supernatant

after centrifuging for 2 min in an IEC clinical centrifuge (International Equipment Company,

Needham Heights, MA, USA). A lysis solution that was prepared by mixing 5 mL of 1 M NaOH

with 2 mL of fresh bleach was added into worms and vortexed for 3 times in a Roto (miniRoto

S56, Fisher Scientific, Waltham, MA, USA) to lyse worms (3-4 min). Slow movement of worms

in lysis solution was observed under microscope (Nikon SMZ1500, Tokyo, Japan), and worms

were broken and eggs were released after vortexing (a clear solution appeared). Lysis solution

was centrifuged and the supernatant was removed. Then 5 mL of S-complete was immediately

added to deactivate the lysis buffer with vortexing for 30 seconds. The eggs were separated from supernatant after centrifugation, and then were washed by S-complete for another 2 times. After three washings, 5 mL of S-complete buffer was added into eggs. The conical tube was placed in the rocker (VWR Signature ^{TM} 3-D Rotator Waver, VWR International Co., Radnor, Pennsylvania, USA) overnight and laid on its side to maximize the air exchange.

6.2.5 Preparation of Feeding Bacteria

First, feeding bacteria *E. coli* OP50 was washed from media by 5 mL of distilled water. Then OP50 was separated from the supernatant after centrifugation (Servall Legend X1R centrifuge, Thermo Scientific, Waltham, MA, USA) at 2200 rpm for 10 min. Then OP50 was washed three times using S-complete. The S-complete was added to OP50 to get OP50 solution after wash.

6.2.6 Seed Worms into Plates

Worms were hatched after 24 hours of synchronization. The concentration of worms was determined by counting the number of worms in 10×10 µl drops under microscope (Nikon SMZ1500, Tokyo, Japan). S-complete containing feeding bacteria *E. coli* OP50 was added into worms to obtain a final concentration of 100 worms per milliliter. Then 120 µL of worm/OP50 solution was transferred to each well in a 96-well plate. The plate was sealed using a tape sealer to avoid contamination and evaporation. Then it was incubated in a 20 °C incubator (Isotemp®, Fisher Scientific, Waltham, MA, USA) for 2 days until worms reach the L4 stage.

6.2.7 Sterilization Worms Using Fluorodeoxyuridine (FUDR)

A 30 µL aliquot of a 0.8 mM 5-Fluoro-2'-deoxyuridine (Sigma-Aldrich, St. Louis, MO, USA) FUDR stock solution was added into each well for L4 stage worms after 2 days incubation. A final volume of 150 µL in each well was reached after this process. Then the plates were put back in the 20 °C incubator.

6.2.8   Heat Shock Treatment

After 1 day of incubation at 20 °C with FUDR, the worms with three days of age were divided into two groups with N2 and TK22 contained in both groups. Group 1 was maintained at 20 °C as a non-heat treatment. Worms in Group 2 were exposed to a heat shock at 35 °C under an incubator (VWR 1530, Sheldon Manufacturing Inc., Cornelius, OR, USA) for 4 h and then maintained at 20 °C for the remainder of their lives. Four hours heating was selected because the preliminary test results showed that over 90% of worms (N2 strain) survived after 4 h heating at 35 °C, and over 50% of worms were dead if heating longer. After the heat shock, the worms in each group was divided into 13 subsidiary groups (each subsidiary group contained 6 wells for replicates, n=6). Then 50 µL stock solutions (S1, S2, S3 and S4) were added into each well to obtain a final volume of 200 µL (Table 6.2). Thus, the concentration for α-TOC was 50, 100 and 200 µg/mL. Worms with 50 mL S-complete were used as the blank control.

Table 6.2 Sample treatments in each group

Subsidiary group	Treatments
1	S1-a
2	S1-b
3	S1-c
4	S2-a
5	S2-b
6	S2-c
7	S3-a
8	S3-b
9	S3-c
10	S4-a
11	S4-b
12	S4-c
13	Blank control, S-complete

6.2.9 Lifespan of Worms

The number of live and dead nematodes was counted under microscope (Nikon, SMZ-U, Kanagawa, Japan). Movement was used to determine whether worms live or not. Starting at day three, the numbers of live worms were counted three times per week for each group.

6.2.10 Pharyngeal Pumping Rate of Worms

For pharyngeal pumping rate of *C. elegans* during the lifespan study, worms were synchronized under the above described method (6.2.4) with slight modification. Distilled water (0.5 mL) was used to wash worms off plates into a 1.5 mL eppendorf tube. Then the mixture was centrifuged and the supernatant was removed. A lysis solution consisting of 500 µL of 1 M NaOH and 200 µL of fresh bleach was added to the eppendorf and immediately vortexed Ptill the solution became clear (the worms were straight and dead under microscope, and eggs were released). Then worms/lysis mixture was centrifuged and the lysis solution was removed after centrifugation. The eggs were washed by 1 mL of S-complete for three times. Then 1 mL S-complete was added into washed eggs and the eppendorf was placed in a rocker overnight and laid on its side to maximize the air exchange. The hatched worms were mixed with 1.2 mL of OP50 solution, and 100 µL of the mixture transferred into each agar plate. The worms in agar plates were placed in 20 °C incubator for 3 days, and separated into two groups, non-heat and heat groups. Heat group was placed in a 35 °C incubator for 4 h, and non-heat group was placed in a 25 °C incubator. The pharyngeal pumping of worms in each group (n=5) was observed 3 times a week under microscope (Nikon, SMZ-U, Kanagawa, Japan). The pharyngeal pumping (oscillating movement of the terminal bulb) times were recorded in a 20 second period, and the pumping rate was calculated in times/min. The first generation of worms (at least 30 worms at the beginning) were transferred to new agar plates after measurement and fed with 50 µL of samples with 10 µL of OP 50. Stock solutions S1-b, S2-b, S3-b and S4-b were used in this test

due to their effects on the lifespan of worms. The blank control was the group that fed with 50 µL S-complete and 10 µL of OP 50.

6.2.11 Statistical Analysis

One-way analysis of variance (ANOVA) was conducted to test the significant differences (p<0.05) among the different treatments using SAS system (Version 9.3, SAS Inst. Inc., Cary, N.C., USA.).

6.3 Results and Discussion

6.3.1 Lifespan of Worms

6.3.1.1 Non-heat shock treatment

The lifespans for worms N2 without heat shock treatment were shown in Figure 6.1. Lifespans of worms N2 treated with S3-a, S3-b increased (survival curves are shifted to the right of the control group) (P>0.05). The death rate for worms with treatments of S1-c and S3-c at early ages sharply increased (survival curves shifted to the left of the control group). For treatment with S1-a and S2-a, the survival rate of worms before day 18 was increasing (survival curves shifted to the right of the control group with short distance), and there was no much difference in survival rate between worms treated with S1-b and the control worms. Groups fed with S2-b, S2-c had slightly increased survival rate. This could be due to the antioxidant ability of α-TOC and SDF, both of them can serve as antioxidant to reduce the lipid oxidation happened on the cell membrane. Figure 6.1 showed that with higher concentration of α-TOC, the survival rate of worms was also slightly higher. For free form α-TOC, it showed that 50 µg/mL α-TOC was the optimum concentration to extent the mean lifespan of N2. This concentration was lower than that obtained in previous studies, in which 200 µg/mL of α-TOC was used to increase the mean lifespan of C. elegans (Harrington and Harley 1988, Zuckerman and Geist 1983). The possible reason could be attributed to the differences in the C. elegans strain. A higher

concentration of α-TOC may result in a weaker cytotoxic effect, because α-TOC can be converted into the pro-oxidants α-TOC semiquinone radical and α-TOC quinone (Minogue and Thomas 2004).

Figure 6.1 Survival curves of N2 without heat shock treatment
Worms treated with S1: SDF nanofiber only, no α-TOC contained; S2: α-TOC only; S3: α-TOC entrapped SDF based nanofibers; S4: solvent control. abc: three concentrations of stock solutions.

The survival rate of N2 decreased when worms were fed with a high concentration of SDF (356.02 μg/mL). That might be due to the Ca^{2+} in the SDF material. The SDF extracted from calcium hydroxide was purified by ultrafiltration in our previous study (3.2.1). However, a few Ca^{2+} ions were left in the SDF (containing 6.85% of calcium) and were involved in

nanofibers. The entry of excess Ca^{2+} into cells can trigger apoptosis due to the stress response (Orrenius, Zhivotovsky and Nicotera 2003). Importantly, the survival rate of N2 increased when worms were fed with α-TOC entrapped in SDF based nanofibers (S3-a and S3-b). The reason could be the synergistic effect of α-TOC and SDF. Another possible reason could be the increased bioavailability of α-TOC when it was encapsulated in nanofiber carriers. Entrapped α-TOC was released gradually, which resulted in the decrease of the accumulation of α-TOC in worms and the reduced cytotoxic effect of α-TOC. On day 51, N2 had a survival rate of 0.12 on groups treated with S3-b, 0.01 on the S2-a treated group, and there were no live worms in other groups. This indicated that SDF nanofiber encapsulated α-TOC treatment with a concentration of 100 µg/mL increased lifespan of N2.

TK22 exhibited a shorter mean lifespan in all treatment groups than N2 (Figure 6.2). This was due to the shorter lifespan of *mev-1* strain than the wild type *C. elegans* (Kondo et al. 2005, Ishii et al. 1998). The survival rate of TK22 was decreased in the early age in all treatment groups (survival curves are shifted to the left of the control group before the age of 11 days). That might be because TK22 is more sensitive than N2 wild type, the addition of sample treatment served as a stimuli which caused oxidative stress and resulted in death (Finkel and Holbrook 2000). The survival rate in each treatment group was increased in the later age of worms (survival curves are shifted to the right of the control group after age of 11 days). At day 34, a few worms were still alive in groups treated with SDF (S1), pure α-TOC (S2) and nanofiber encapsulated α-TOC (S3), but no worms were alive in the blank control group and solvent control groups. This result supported the hypothesis that free radical caused oxidative damage is linked to aging (Harman 1956), and the presence of antioxidant can protect cells against oxidative stress .
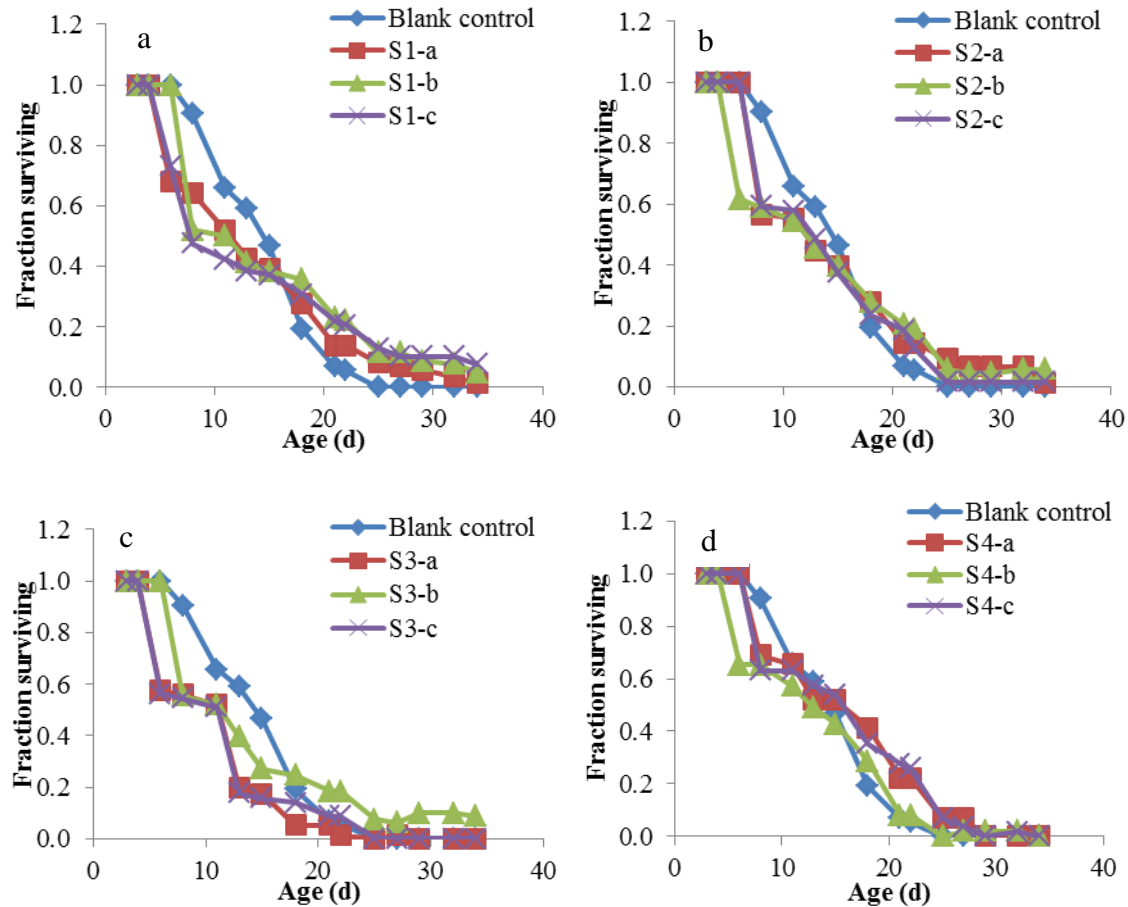
Figure 6.2 Survival curves of TK22 without heat shock treatment
Worms treated with S1: SDF nanofiber only, no α-TOC contained; S2: α-TOC entrapped SDF based nanofibers; S4: solvent control. abc: three concentrations of stock solutions.

TK22 treated with S3-b had the highest survival rate at day 34 when compared to the control group and other treatment groups. This result was consistent with the results in N2. Therefore, α-TOC encapsulated in SDF based nanofibers showed enhanced bioavailability in both wild type and mev-1 mutant.

There was no difference in survival rate between N2 solvent control groups (fed with S4) and the blank control group, while TK22 solvent control groups had lower survival rate compared to the blank control groups. Ethanol had minor effect on the activity of worms, as well as Tween 80, DMSO, methanol and acetone, while Tween 20 had huge toxicity for them (Katiki

et al. 2011). The concentration of ethanol in solvent control groups was less than 3 mg/mL and Tween 80 concentration was less than 0.2 mg/mL, which had no effect on the lifespan of N2. However, TK22 is more sensitive than N2, thus even the lowest concentration could result in the death of worms.

6.3.1.2 Heat shock treatment

Heat shock increased the death rate of N2 (Figure 6.3). Similar to the result for N2 group without heat shock, high SDF concentration (356.02 µg/mL) increased the death rate of worms at the early age. At the later age of worms, higher survival rate was observed in groups treated with S1-a, S1-b, S3-b and S3-c. There was no significant difference in survival rate between free α-TOC treated groups (S2) and the control group, which was different from the result of S2 treated N2 strain non-heat shock groups. This might be due to the degradation of α-TOC in S2 treatment groups. In contrast, less oxidation might occur in nanofiber encapsulated α-TOC. Due to the protective effect of wall materials, entrapped α-TOC maintained its antioxidant ability without degradation when exposed to the severe environment. A few worms survived in S3-c treatment group at the age of 49 days. This result was different from the result of N2 non-heat shock group. The potential reason was more oxidative stress was generated in heat-shock treated worms than in no heat shock treatment *C. elegans*. Hence more antioxidant was required to balance the redox in cells. S3-c contained 200 µg/mL of α-TOC and 356.02 µg/mL of SDF, α-TOC together with SDF could provide enough antioxidant to prevent the oxidative damage in cells and therefore reduce the death rate. In a previous study, the optimized concentration of 400 µg/mL α-TOC was reported to increase the lifespan of wild type *C. elegans* under induced oxidative damage treatment (Ishii et al. 2004).
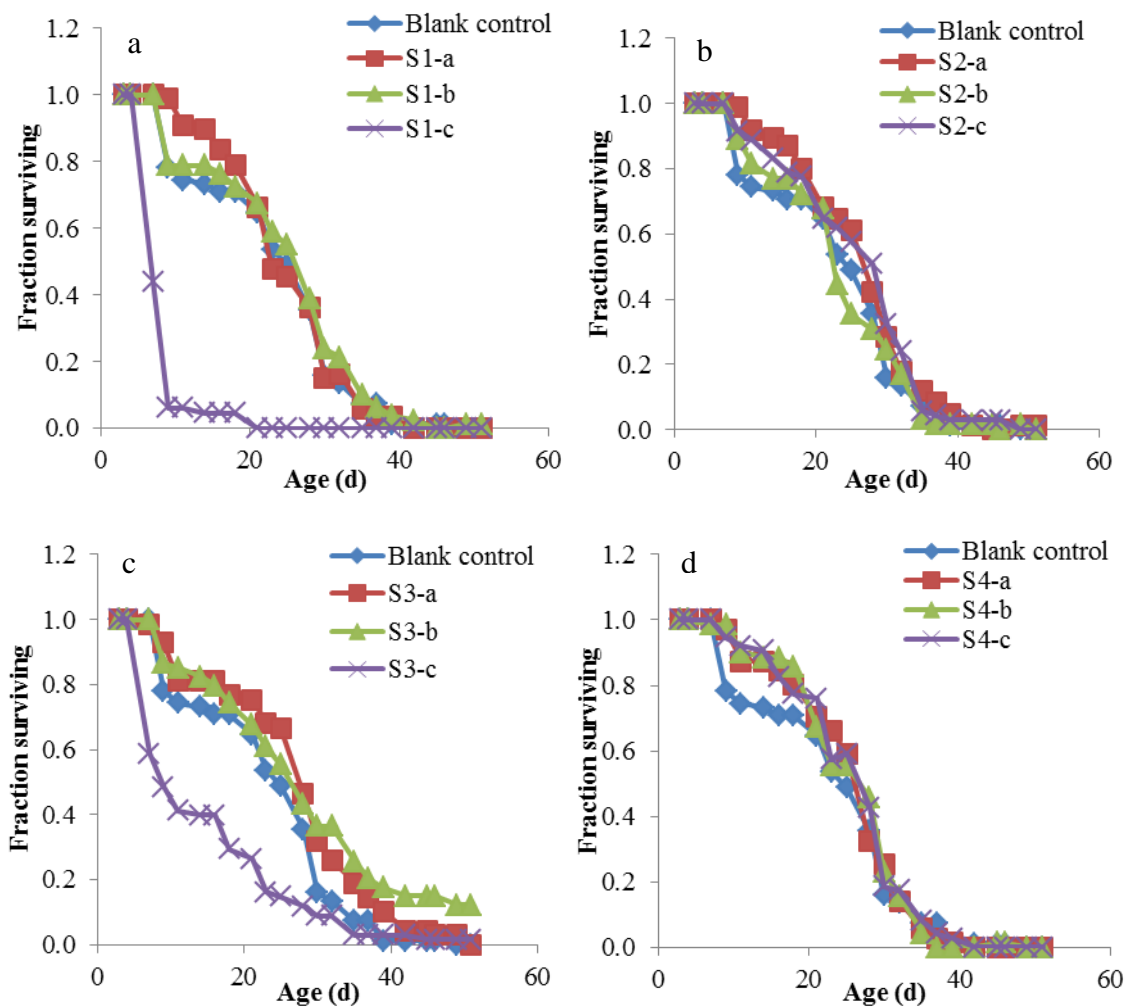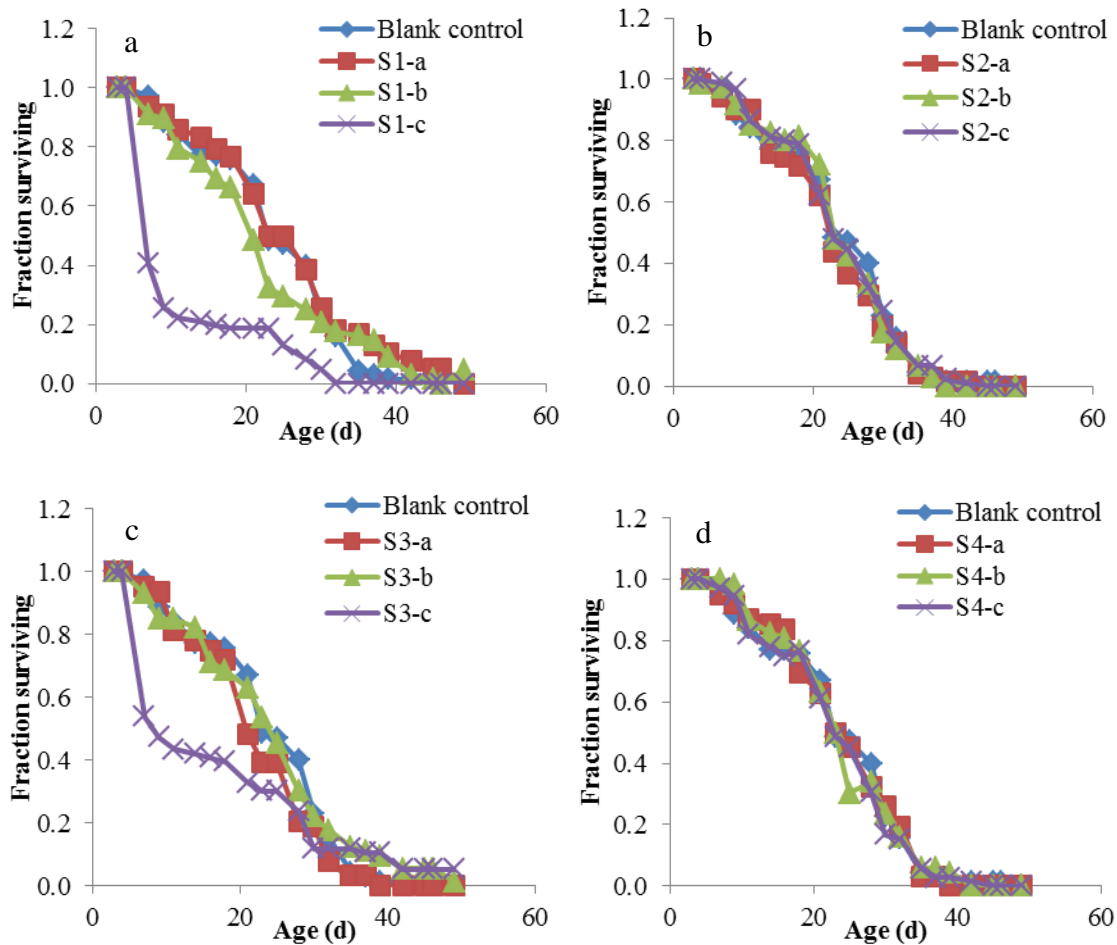
Figure 6.3 Survival curves of N2 with heat shock treatment
Worms treated with S1: SDF nanofiber only, no α-TOC contained; S2: α-TOC only; S3: α-TOC entrapped SDF based nanofibers; S4: solvent control. abc: three concentrations of stock solutions.

No difference was observed in survival rate between the solvent control groups and the blank control group. This result was consistent with the survival rate of N2 no heat shock solvent control groups, and reconfirmed that ethanol and Tween 80 had minor effect on *C. elegans*.

Interestingly, S1-c treated heat shock group of N2 had a higher survival rate in the early age than that in S1-c treated non-heat shock group, which were 0.26 and 0.06 at the age of 9 days, respectively. Also, the increased lifespan was observed in heat shock group with S1-c treatment compared to that in N2 non-heat shock group, which was 30 d and 18 d, respectively. The reason was still not clear, it might be because of the activation and modulation effect of Ca^{2+}

overload and Ca^{2+} dependent processes on the execution of a non-apoptotic death program in *C. elegans* (Xu, Tavernarakis and Driscoll 2001).

There were no worms that survived after heating at 35 °C for 4 h in all treatment groups of TK22. The reason may be because stressor heat accelerated the oxidative stress in *mev-1* mutant, and subsequently induced oxidative damage caused quick death of worms.

6.3.2   Pharyngeal Pumping Rate of Worms

6.3.2.1 Non-heat shock treatment

The pharyngeal pumping rate for each treatment was shown in Figure 6.4. In N2 non-heat shock groups, there was no significant difference in pumping rate between each treatment at the early age of 6 days, which displayed 304.8±4.1 pharyngeal pumps per minute (Figure 6.4a). However, an increased pharyngeal pumping rate was observed in all treatment groups when compared with the blank control group in day 6. S2-b and S3-b treatment groups had pumping rates of 310.2±8.1 and 309±13.9, respectively, while the blank control group had a pumping rate of 300±8 in day 6. At the age of 8 days, a significantly higher pumping rate was observed in all treatment groups than that in the blank control group. At the age of 10 d, significantly increased pumping rate was shown in S2-b and S4-b treatment groups compared to the blank control group, which were 265.4±13.5 and 259.5±3.9, respectively. No significant difference in pumping rate was observed in S1-b, S3-b and the blank control group, which were 238.8±14.1, 231±16.6 and 257.4±18.2, respectively. This result was inconsistent with the lifespan result for N2 no heat shock group, which showed S3-b treatment subgroup worms had the highest survival rate at the age of 51 days and suggested an increased lifespan. This inconsistency may be due to the short observation period of pumping rate, it may not represent the whole lifespan.

In TK22 non-heat shock groups, the mean pumping rate in day 6 was around 292.6±6.0 (Figure 6.4c). The pumping rate in S1-b, S2-b and S3-b treatment groups in day 6 were 295±1.7,

297±6 and 300±3, respectively. A lower pumping rate was observed in the blank control group when compared with other groups in day 6, which was 280±17.1. A significantly increased pumping rate was observed in S2-b, S3-b and S4-b treatment groups in day 8 compared to the blank control group. In contrast to other treatment groups, S3-b treatment group had the significantly highest pumping rate during the observation period, which was 203±21.1 in day 17. For blank control group, the pumping times were 64±22.1 per minute in day 17. There was no significant difference in pumping rate between the solvent control group and the blank control group in the later age of worms. This result suggested that nanofiber encapsulated α-TOC effectively protected C. elegans against natural accumulated oxidative damage produced by other factors.

6.3.2.2 Heat shock treatment

For heat shock treatment groups, the observation of pharyngeal pumping rate was started in day 6, 2 days recovery time were provided to worms after heat shock in day 3.

No significant difference was observed in pumping rate between all treatment groups and the blank control group in day 6 for N2 strain (Figure 6.4b), which was 284.3±3.7. This value was lower than that in N2 non-heat shock treatment groups in day 6. That meant heat shock produced oxidative stress impacted aging in N2 strain. In day 8, S2-b, S3-b and S4-b treatment groups had significantly higher pumping rate than the blank control group. S1-b treatment group had a higher pumping rate than the blank control group during the whole observation period, which indicated SDF could serve as an antioxidant to protect N2 against heat shock induced oxidative stress. It was shown that S2-b treatment group containing 100 µg/mL of free form α-TOC had lower pumping rate than the blank control group in day 13 and 15. This could because the degradation of free form α-TOC during heating process thus resulted in the loss of its antioxidant ability.
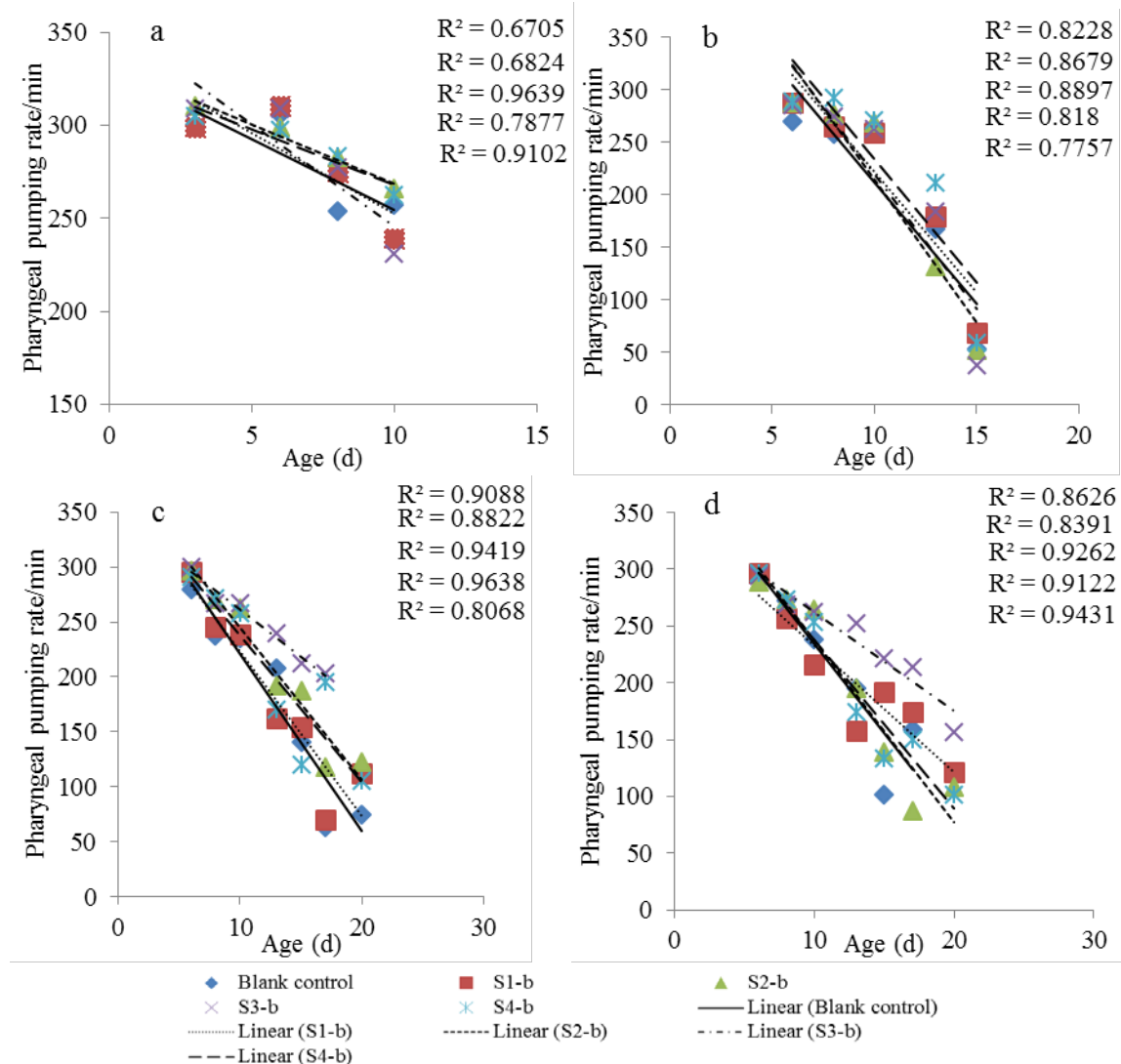
Figure 6.4 Age-related change of pharyngeal pumping rate of C. elegans
a, N2, without heat shock; b, N2, with heat shock; c, TK22, without heat shock; d, TK22, with heat shock. Worms treated with S1: SDF nanofiber only, no α-TOC contained; S2: α-TOC only; S3: α-TOC entrapped SDF based nanofibers; S4: solvent control. b: concentration of α-TOC with 100 μg/mL.

Different from the results of TK22 in liquid media, no death was observed in TK22 after heat shock in agar media. The possible reason may because solid media served as a heat insulator and provided protection for worms during heating.

In TK22 heat shock treatment groups, the average pumping rate in day 6 was 294.2 ±3.0 (Figure 6.4d). There was no significant difference in pumping rate between all the treatment groups and the blank control group in day 6. S3-b treatment group had a significantly increased

97

pumping rate during the whole observation period compared to the blank control group. S2-b treatment group containing 100 µg/mL of free form α-TOC did not exhibit significant increase in the pumping rate of TK22. The pumping rate of S1-b treatment group was increased compared to the blank control group ($P > 0.05$). The results demonstrated that nanofiber can protect incorporated α-TOC from degradation in severe environments. The α-TOC encapsulated in SDF based nanofiber showed increased bioavailability in TK22 heat shock group compared to the blank control group.

6.4   Conclusions

In this study, SDF nanofibers, free form α-TOC and nanofiber encapsulated α-TOC treatments increased the lifespan and pharyngeal pumping rates of both wild type N2 and *mev-1* mutant TK22 ($p > 0.05$). Nanofiber encapsulated α-TOC exhibited enhanced bioavailability in protecting *C. elegans* from oxidative stress and thus increased the lifespan of worms. TK22 was heat sensitive, and a higher concentration of nanofiber encapsulated α-TOC was required than that for N2 strain. In pharyngeal pumping rate test, S3-b treatment showed significant increases in TK22 strain groups with/without heat shock treatment than that in N2 groups. This study suggested that α-TOC and SDF nanofibers could increase the lifespan and pumping rate of *C. elegans*, and the enhanced bioavailability could be obtained in encapsulated α-TOC in SDF based nanofibers.

CHAPTER 7   CONCLUSION

In this study, soluble dietary fiber (SDF) based nanofiber delivery system was successfully developed for α-TOC. First, SDF based nanofibers were electrospun from electrospinning solutions that contained 3% SDF and 5% PEO. Nanofibers had an average diameter of 171.45 nm with uniform size distribution and smooth surface morphology without defects of beads and junctions. The DSC and FTIR results confirmed the presence of SDF and PEO in nanofibers. Then, α-TOC was loaded into SDF based nanofiber by electrospun spinning solutions containing α-TOC O/W emulsions or α-TOC entrapped zein particles. The results showed that spinning solution containing 5% of α-TOC emulsion droplets, and nanofiber wall materials of 3% SDF and 5% PEO resulted in α-TOC loaded nanofibers with average cross section diameter of 283 nm and encapsulation efficiency of α-TOC was 86.97%. Spinning solution containing 3% SDF and 5% PEO of wall materials and 6% of zein particles loaded with 50% of α-TOC (relative to zein mass) resulted in α-TOC incorporated nanofibers with average cross section diameter of 291.3 nm, and the encapsulation efficiency of α-TOC was 74.51%. These two ways of adding α-TOC to SDF based nanofibers resulted in slow release of α-TOC from nanofibers. The DSC and FTIR results indicated that α-TOC was incorporated in nanofibers and may interact with wall materials by hydrogen bonds. In the third part of this study, the stability of entrapped α-TOC in SDF based nanofiber and film was evaluated under heat, UV irradiation and storage. SDF based nanofiber and film protected α-TOC against degradation, and the higher retention of encapsulated α-TOC was obtained compared with that in nanofiber and film without the addition of SDF. In the last part of this study, the bioavailability of α-TOC delivered by SDF based nanofiber was investigated. *C. elegans* was selected as animal model, and two strains, wild type N2 and mutant TK22, were used for the test. The results

showed that 100 µg/mL of α-TOC that was contained in SDF based nanofiber increased the survival rate of worms, which indicated the increased lifespan of worms. Also, significantly increased pharyngeal pumping rate was observed in TK22, and the effect of nanofiber entrapped α-TOC on the pumping rate of N2 was not significant.

In summary, SDF based nanofibers can be used for α-TOC delivery. This delivery system can protect α-TOC from severe conditions during processing and storage. Also, the slow release of α-TOC can be obtained. The bioavailability of carried α-TOC can be enhanced as well. The SDF based nanofiber delivery system can not only be applied to α-TOC, but also can be applied to other hydrophobic nutrients.

REFERENCES

AACC (2001) The definition of dietary fiber. *Cereal Foods World,* 46**,** 112-126.

Aan, G. J., M. S. A. Zainudin, N. A. Karim & W. Z. W. Ngah (2013) Effect of the tocotrienol-rich fraction on the lifespan and oxidative biomarkers in Caenorhabditis elegans under oxidative stress. *Clinics,* 68**,** 599-604.

Abdul-Hamid, A. & Y. S. Luan (2000) Functional properties of dietary fibre prepared from defatted rice bran. *Food Chemistry,* 68**,** 15-19.

Aghdam, R. M., S. Najarian, S. Shakhesi, S. Khanlari, K. Shaabani & S. Sharifi (2012) Investigating the effect of PGA on physical and mechanical properties of electrospun PCL/PGA blend nanofibers. *Journal of Applied Polymer Science,* 124**,** 123-131.

Aliabadi, M., M. Irani, J. Ismaeili, H. Piri & M. J. Parnian (2013) Electrospun nanofiber membrane of PEO/Chitosan for the adsorption of nickel, cadmium, lead and copper ions from aqueous solution. *Chemical Engineering Journal,* 220**,** 237-243.

Aluigi, A., A. Varesano, A. Montarsolo, C. Vineis, F. Ferrero, G. Mazzuchetti & C. Tonin (2007) Electrospinning of keratin/poly(ethylene oxide)blend nanofibers. *Journal of Applied Polymer Science,* 104**,** 863-870.

Anderson, J. W., A. E. Jones & S. Riddellmason (1994) 10 different dietrary-fibers have significantly different effects on serum and liver lipids of cholesterol-fed rats. *Journal of Nutrition,* 124**,** 78-83.

Angeles, M., H. L. Cheng & S. S. Velankar (2008) Emulsion electrospinning: composite fibers from drop breakup during electrospinning. *Polymers for Advanced Technologies,* 19**,** 728-733.

Aoe, S., T. Oda, K. Tatsumi, M. Yamauchi & Y. Ayano (1993a) Extraction of soluble dieraty-fibers from defatted rice bran. *Cereal Chemistry,* 70**,** 423-425.

Aoe, S., T. Oda, T. Tojima, M. Tanaka, K. Tatsumi & T. Mizutani (1993b) Effects of rice bran hemicellulose on 1,2-dimethylhydrazine-induced intestinal carcinogenesis in Fischer 344 rats. *Nutrition and Cancer-an International Journal,* 20**,** 41-49.

Arecchi, A., S. Mannino & J. Weiss (2010) Electrospinning of poly(vinyl alcohol) nanofibers loaded with hexadecane nanodroplets. *Journal of Food Science,* 75**,** N80-N88.

Baba, R., C. J. Angammana, S. H. Jayaram & L. Loong-Tak (2013) An IGBT-based pulsed power supply for fabricating noncontinuous nanofibers using electrospinning. *Industry Applications, IEEE Transactions on,* 49**,** 1801-1807.

Barakat, N. A. M., M. A. Kanjwal, F. A. Sheikh & H. Y. Kim (2009) Spider-net within the N6, PVA and PU electrospun nanofiber mats using salt addition: Novel strategy in the electrospinning process. *Polymer,* 50**,** 4389-4396.

Bianco, A., M. Calderone & I. Cacciotti (2013) Electrospun PHBV/PEO co-solution blends: Microstructure, thermal and mechanical properties. *Materials Science & Engineering C-Materials for Biological Applications,* 33**,** 1067-1077.

Bonino, C. A., K. Efimenko, S. I. Jeong, M. D. Krebs, E. Alsberg & S. A. Khan (2012) Three-dimensional electrospun alginate nanofiber mats via tailored charge repulsions. *Small,* 8**,** 1928-1936.

Brahatheeswaran, D., A. Mathew, R. G. Aswathy, Y. Nagaoka, K. Venugopal, Y. Yoshida, T. Maekawa & D. Sakthikumar (2012) Hybrid fluorescent curcumin loaded zein electrospun nanofibrous scaffold for biomedical applications. *Biomedical Materials,* 7.

Branca, C., L. Auditore, D. Loria, M. Trimarchi & U. Wanderlingh (2013) Radiation synthesis and characterization of poly(ethylene oxide)/chitosan hydrogels. *Journal of Applied Polymer Science,* 127**,** 217-223.

Brennan, C. S., C. M. Tudorica & V. Kuri (2002) Soluble and insoluble dietary fibres (non-starch polysaccharides) and their effects on food structure and nutrition. *Food Industry Journal,* 5**,** 261-272.

Butov, A., T. Johnson, J. Cypser, I. Sannikov, M. Volkov, M. Sehl & A. Yashin (2001) Hormesis and debilitation effects in stress experiments using the nematode worm Caenorhabditis elegans: the model of balance between cell damage and HSP levels. *Experimental Gerontology,* 37**,** 57-66.

Chakraborty, S., I. C. Liao, A. Adler & K. W. Leong (2009) Electrohydrodynamics: A facile technique to fabricate drug delivery systems. *Advanced Drug Delivery Reviews,* 61**,** 1043-1054.

Chang, W. K., F. J. Xu, X. Y. Mu, L. L. Ji, G. P. Ma & J. Nie (2013) Fabrication of nanostructured hollow TiO2 nanofibers with enhanced photocatalytic activity by coaxial electrospinning. *Materials Research Bulletin,* 48**,** 2661-2668.

Chen, H. D., J. C. Weiss & F. Shahidi (2006) Nanotechnology in nutraceuticals and functional foods. *Food Technology,* 60**,** 30-36.

Chen, P., Y. J. Sun, Z. C. Zhu, R. X. Wang, X. D. Shi, C. Lin & Y. T. Ye (2010) A controlled release system of superoxide dismutase by electrospun fiber and its antioxidant activity in vitro. *Journal of Materials Science-Materials in Medicine,* 21**,** 609-614.

Cheng, H. H., H. Y. Huang, Y. Y. Chen, C. L. Huang, C. J. Chang, H. L. Chen & M. H. Lai (2010) Ameliorative effects of stabilized rice bran on type 2 diabetes patients. *Annals of Nutrition and Metabolism,* 56**,** 45-51.

Cho, S. S., L. Qi, G. C. Fahey & D. M. Klurfeld (2013) Consumption of cereal fiber, mixtures of whole grains and bran, and whole grains and risk reduction in type 2 diabetes, obesity, and cardiovascular disease. *American Journal of Clinical Nutrition,* 98**,** 594-619.

Choi, S.-H., D.-Y. Youn, S. M. Jo, S.-G. Oh & I.-D. Kim (2011) Micelle-mediated synthesis of single-crystalline beta(3C)-SiC fibers via emulsion electrospinning. *Acs Applied Materials & Interfaces,* 3**,** 1385-1389.

Chuysinuan, P., N. Chimnoi, S. Techasakul & P. Supaphol (2009) Gallic acid-loaded electrospun poly(L-cactic acid) fiber mats and their release characteristic. *Macromolecular Chemistry and Physics,* 210**,** 814-822.

Crespy, D., K. Friedemann & A. M. Popa (2012) Colloid-electrospinning: fabrication of multicompartment nanofibers by the electrospinning of organic or/and Inorganic dispersions and emulsions. *Macromolecular Rapid Communications,* 33**,** 1978-1995.

Cui, W. G., Y. Zhou & J. Chang (2010) Electrospun nanofibrous materials for tissue engineering and drug delivery. *Science and Technology of Advanced Materials,* 11.

Cummings, J. H., S. A. Bingham, K. W. Heaton & M. A. Eastwood (1992) Fecal weight, colon cancer rish, and dieraty-intake of nonstarch polysaccharides (dietray fiber). *Gastroenterology,* 103**,** 1783-1789.

Deitzel, J. M., J. Kleinmeyer, D. Harris & N. C. B. Tan (2001) The effect of processing variables on the morphology of electrospun nanofibers and textiles. *Polymer,* 42**,** 261-272.

Dexter, P. M., K. A. Caldwell & G. A. Caldwell (2012) A predictable worm: application of caenorhabditis elegans for mechanistic investigation of movement disorders. *Neurotherapeutics,* 9**,** 393-404.

Dogan, G., F. Ozyildiz, G. Basal & A. Uzel (2013) Fabrication of electrospun chitosan and chitosan/poly(ethylene oxide) nanofiber webs and assessment of their antimicrobial activity. *International Polymer Processing,* 28**,** 143-150.

Doleyres, Y., I. Fliss & C. Lacroix (2002) Quantitative determination of the spatial distribution of pure- and mixed-strain immobilized cells in gel beads by immunofluorescence. *Applied Microbiology and Biotechnology,* 59**,** 297-302.

Doshi, J. & D. H. Reneker (1995) Electrospinning process and applications of electrospun fibers. *Journal of Electrostatics,* 35**,** 151-160.

Duan, B., C. H. Dong, X. Y. Yuan & K. D. Yao (2004) Electrospinning of chitosan solutions in acetic acid with poly(ethylene oxide). *Journal of Biomaterials Science-Polymer Edition,* 15**,** 797-811.

Ernst, I. M. A., K. Pallauf, J. K. Bendall, L. Paulsen, S. Nikolai, P. Huebbe, T. Roeder & G. Rimbach (2013) Vitamin E supplementation and lifespan in model organisms. *Ageing Research Reviews,* 12**,** 365-375.

Eussen, S., C. J. M. Rompelberg, K. E. Andersson, O. H. Klungel, P. Hellstrand, R. Oste, H. van Kranen & J. Garssen (2011) Simultaneous intake of oat bran and atorvastatin reduces their efficacy to lower lipid levels and atherosclerosis in LDLr-/- mice. *Pharmacological Research,* 64**,** 36-43.

Fan, L. Z., Z. M. Dang, C. W. Nan & M. Li (2002) Thermal, electrical and mechanical properties of plasticized polymer electrolytes based on PEO/P(VDF-HFP) blends. *Electrochimica Acta,* 48**,** 205-209.

Fang, J., Wang, Xungai, Lin, Tong 2011. Functional applications of electrospun nanofibers. In *Nanofibers - production, properties and functional applications,* ed. T. Lin, 287-326. Rijeka, Croatia: InTech – Open Access Publisher.

FDA. 2012. CFR-code of federal regulations title 21. U.S. Food and Drug Administration.

Fechner, A., K. Fenske & G. Jahreis (2013) Effects of legume kernel fibres and citrus fibre on putative risk factors for colorectal cancer: a randomised, double-blind, crossover human intervention trial. *Nutrition Journal,* 12.

Feng, J. L., Z. W. Wang, J. Zhang, Z. N. Wang & F. Liu (2009) Study on food-grade vitamin E microemulsions based on nonionic emulsifiers. *Colloids and Surfaces a-Physicochemical and Engineering Aspects,* 339**,** 1-6.

Fernandez, A., S. Torres-Giner & J. M. Lagaron (2009) Novel route to stabilization of bioactive antioxidants by encapsulation in electrospun fibers of zein prolamine. *Food Hydrocolloids,* 23**,** 1427-1432.

Finkel, T. & N. J. Holbrook (2000) Oxidants, oxidative stress and the biology of ageing. *Nature,* 408**,** 239-247.

Finley, J. W., C. Sandlin, D. L. Holliday, M. J. Keenan, W. Prinyawiwatkul & J. Zheng (2013) Legumes reduced intestinal fat deposition in the Caenorhabditis elegans model system. *Journal of Functional Foods,* 5**,** 1487-1493.

Fong, H., I. Chun & D. H. Reneker (1999) Beaded nanofibers formed during electrospinning. *Polymer,* 40**,** 4585-4592.

Fung, W. Y., K. H. Yuen & M. T. Liong (2010) Characterization of Fibrous Residues from Agrowastes and the Production of Nanofibers. *Journal of Agricultural and Food Chemistry,* 58**,** 8077-8084.

--- (2011) Agrowaste-Based Nanofibers as a Probiotic Encapsulant: Fabrication and Characterization. *Journal of Agricultural and Food Chemistry,* 59**,** 8140-8147.

Gawrysiak-Witulska, M., A. Siger & M. Nogala-Kalucka (2009) Degradation of tocopherols during near-ambient rapeseed drying. *Journal of Food Lipids,* 16**,** 524-539.

Gerhardt, A. L. & N. B. Gallo (1998) Full-fat rice bran and oat bran similarly reduce hypercholesterolemia in humans. *Journal of Nutrition,* 128**,** 865-869.

Goh, Y.-F., I. Shakir & R. Hussain (2013) Electrospun fibers for tissue engineering, drug delivery, and wound dressing. *Journal of Materials Science,* 48**,** 3027-3054.

Gunness, P. & M. J. Gidley (2010) Mechanisms underlying the cholesterol-lowering properties of soluble dietary fibre polysaccharides. *Food & Function,* 1**,** 149-155.

Hakansson, B. & M. Jagerstad (1990) The effect of thermal inactivation of lipoxygenase on the stability of vitamin E in wheat. *Journal of Cereal Science,* 12**,** 177-185.

Harman, D. (1956) Aging: a theory based on free radical and radiation chemistry. *Journals of Gerontology,* 11**,** 298-300.

Harrington, L. A. & C. B. Harley (1988) Effect of vitamin E on lifespan and reproduction in Caenorhabditis elegans. *Mechanisms of Ageing and Development,* 43**,** 71-78.

Havrlentova, M., Z. Petrulakova, A. Burgarova, F. Gago, A. Hlinkova & E. Sturdik (2011) Cereal beta-glucans and their significance for the preparation of functional foods - a review. *Czech Journal of Food Sciences,* 29**,** 1-14.

He, W., T. Yong, W. E. Teo, Z. W. Ma & S. Ramakrishna (2005) Fabrication and endothelialization of collagen-blended biodegradable polymer nanofibers: Potential vascular graft for blood vessel tissue engineering. *Tissue Engineering,* 11**,** 1574-1588.

Herrera, E. & C. Barbas (2001) Vitamin E: action, metabolism and perspectives. *Journal of Physiology and Biochemistry,* 57**,** 43-56.

Himmelsbach, D. S., S. Khalili & D. E. Akin (2002) The use of FT-IR microspectroscopic mapping to study the effects of enzymatic retting of flax (Linum usitatissimum L) stems. *Journal of the Science of Food and Agriculture,* 82**,** 685-696.

Hu, G. H. & W. J. Yu (2013) Binding of cholesterol and bile acid to hemicelluloses from rice bran. *International Journal of Food Sciences and Nutrition,* 64**,** 461-466.

Hu, H. T., S. Y. Lee, C. C. Chen, Y. C. Yang & J. C. Yang (2013a) Processing and properties of hydrophilic electrospun polylactic acid/beta-tricalcium phosphate membrane for dental applications. *Polymer Engineering and Science,* 53**,** 833-842.

Hu, J., J. C. Wei, W. Y. Liu & Y. W. Chen (2013b) Preparation and characterization of electrospun PLGA/gelatin nanofibers as a drug delivery system by emulsion electrospinning. *Journal of Biomaterials Science-Polymer Edition,* 24**,** 972-985.

Huang, C., C. J. Xiong & K. Kornfeld (2004) Measurements of age-related changes of physiological processes that predict lifespan of Caenorhabditis elegans. *Proceedings of the National Academy of Sciences of the United States of America,* 101**,** 8084-8089.

Huang, W. D., T. Zou, S. F. Li, J. Q. Jing, X. Y. Xia & X. L. Liu (2013) Drug-loaded Zein nanofibers prepared using a modified coaxial electrospinning process. *Aaps Pharmscitech,* 14**,** 675-681.

Huang, Z. M., Y. Z. Zhang, M. Kotaki & S. Ramakrishna (2003) A review on polymer nanofibers by electrospinning and their applications in nanocomposites. *Composites Science and Technology,* 63**,** 2223-2253.

Ishii, N., M. Fujii, P. S. Hartman, M. Tsuda, K. Yasuda, N. Senoo-Matsuda, S. Yanase, D. Ayusawa & K. Suzuki (1998) A mutation in succinate dehydrogenase cytochrome b causes oxidative stress and ageing in nematodes. *Nature,* 394**,** 694-697.

Ishii, N., N. Senoo-Matsuda, K. Miyake, K. Yasuda, T. Ishii, P. S. Hartman & S. Furukawa (2004) Coenzyme Q(10) can prolong C-elegans lifespan by lowering oxidative stress. *Mechanisms of Ageing and Development,* 125**,** 41-46.

Jacobs, V., A. Patanaik & R. D. Anandjiwala (2011) Optimization of Process and Solution Parameters in Electrospinning Polyethylene Oxide. *Advanced Science Letters,* 4**,** 3590-3595.

Ji, X. Y., W. J. Yang, T. Wang, C. Mao, L. L. Guo, J. Q. Xiao & N. Y. He (2013) Coaxially Electrospun Core/Shell Structured Poly(L-Lactide) Acid/Chitosan Nanofibers for Potential Drug Carrier in Tissue Engineering. *Journal of Biomedical Nanotechnology,* 9**,** 1672-1678.

Kahlon, T. S., F. I. Chow, B. E. Knuckles & M. M. Chiu (1993) Cholesterol-lowering effects in hamsters of beta-Glucan-enriehed barley fraction, dehulled whole barley, rice bran, and oat bran and their combinations. *Cereal Chemistry,* 70**,** 435-440.

Kahlon, T. S., R. M. Saunders, R. N. Sayre, F. I. Chow, M. M. Chiu & A. A. Betschart (1992) Cholesterol-lowering effects of rice bran and rice bran oil fractions in hypercholesterolemic hamsters. *Cereal Chemistry,* 69**,** 485-489.

Kahlon, T. S. & C. L. Woodruff (2003) In vitro binding of bile acids by rice bran, oat bran, barley and beta-glucan enriched barley. *Cereal Chemistry,* 80**,** 260-263.

KamalEldin, A. & L. A. Appelqvist (1996) The chemistry and antioxidant properties of tocopherols and tocotrienols. *Lipids,* 31**,** 671-701.

Katiki, L. M., J. F. S. Ferreira, A. M. Zajac, C. Masler, D. S. Lindsay, A. C. S. Chagas & A. F. T. Amarante (2011) Caenorhabditis elegans as a model to screen plant extracts and compounds as natural anthelmintics for veterinary use. *Veterinary Parasitology,* 182**,** 264-268.

Khayata, N., W. Abdelwahed, M. F. Chehna, C. Charcosset & H. Fessi (2012a) Preparation of vitamin E loaded nanocapsules by the nanoprecipitation method: From laboratory scale to large scale using a membrane contactor. *International Journal of Pharmaceutics,* 423**,** 419-427.

--- (2012b) Stability study and lyophilization of vitamin E-loaded nanocapsules prepared by membrane contactor. *International Journal of Pharmaceutics,* 439**,** 254-259.

Kim, G. M., A. Wutzler, H. J. Radusch, G. H. Michler, P. Simon, R. A. Sperling & W. J. Parak (2005) One-dimensional arrangement of gold nanoparticles by electrospinning. *Chemistry of Materials,* 17**,** 4949-4957.

Kim, H. J. & H. D. Paik (2012) Functionality and application of dietary fiber in meat products. *Korean Journal for Food Science of Animal Resources,* 32**,** 695-705.

Kobayashi, H., D. Terada, Y. Yokoyama, D. W. Moon, Y. Yasuda, H. Koyama & T. Takato (2013) Vascular-inducing poly(glycolic acid)-collagen nanocomposite-fiber scaffold. *Journal of Biomedical Nanotechnology,* 9**,** 1318-1326.

Kondo, M., N. Senoo-Matsuda, S. Yanase, T. Ishii, P. S. Hartman & N. Ishii (2005) Effect of oxidative stress on translocation of DAF-16 in oxygen-sensitive mutants, mev-1 and gas-1 of Caenorhabditis elegans. *Mechanisms of Ageing and Development,* 126**,** 637-641.

Konwarh, R., N. Karak & M. Misra (2013) Electrospun cellulose acetate nanofibers: the present status and gamut of biotechnological applications. *Biotechnology Advances,* 31**,** 421-437.

Kriegel, C., A. Arrechi, K. Kit, D. J. McClements & J. Weiss (2008) Fabrication, functionalization, and application of electrospun biopolymer nanofibers. *Critical Reviews in Food Science and Nutrition,* 48**,** 775-797.

Kriegel, C., K. A. Kit, D. J. McClements & J. Weiss (2009) Nanofibers as carrier systems for antimicrobial microemulsions. part I: fabrication and characterization. *Langmuir,* 25**,** 1154-1161.

Kriel, H., R. D. Sanderson & E. Smit (2012) Coaxial electrospinning of miscible PLLA-core and PDLLA-shell solutions and indirect visualisation of the core-shell fibres obtained. *Fibres & Textiles in Eastern Europe,* 20**,** 28-33.

Lai, L. F. & H. X. Guo (2011) Preparation of new 5-fluorouracil-loaded zein nanoparticles for liver targeting. *International Journal of Pharmaceutics,* 404**,** 317-323.

Lambo, A. M., R. Oste & M. Nyman (2005) Dietary fibre in fermented oat and barley beta-glucan rich concentrates. *Food Chemistry,* 89**,** 283-293.

Laouini, A., C. Charcosset, H. Fessi, R. G. Holdich & G. T. Vladisavljevic (2013) Preparation of liposomes: a novel application of microengineered membranes - investigation of the process parameters and application to the encapsulation of vitamin E. *Rsc Advances,* 3**,** 4985-4994.

Laouini, A., H. Fessi & C. Charcosset (2012) Membrane emulsification: A promising alternative for vitamin E encapsulation within nano-emulsion. *Journal of Membrane Science,* 423**,** 85-96.

Leung, V. & F. Ko (2011) Biomedical applications of nanofibers. *Polymers for Advanced Technologies,* 22**,** 350-365.

Li, B., Y. F. Jiang, F. Liu, Z. Chai, Y. X. Li, Y. Y. Li & X. J. Leng (2012) Synergistic effects of whey protein-polysaccharide complexes on the controlled release of lipid-soluble and water-soluble vitamins in W1/O/W2 double emulsion systems. *International Journal of Food Science and Technology,* 47**,** 248-254.

Li, B., Y. F. Jiang, F. Liu, Z. Chai, Y. Y. Li & X. J. Leng (2011) Study of the encapsulation efficiency and controlled release property of whey protein Isolate-polysaccharide complexes in W-1/O/W-2 double emulsions. *International Journal of Food Engineering,* 7.

Li, Q., T. R. Holford, Y. W. Zhang, P. Boyle, S. T. Mayne, M. Dai & T. Z. Zheng (2013) Dietary fiber intake and risk of breast cancer by menopausal and estrogen receptor status. *European Journal of Nutrition,* 52**,** 217-223.

Li, W. J., R. L. Mauck & R. S. Tuan (2005) Electrospun nanofibrous scaffolds: production, characterization, and applications for tissue engineering and drug delivery. *Journal of Biomedical Nanotechnology,* 1**,** 259-275.

Li, X. & S. L. Hsu (1984) An analysis of the crystallization behavior of poly(ethylene oxide)/poly(methyl methacrylate) blends by spectroscopic and calorimetric techniques. *Journal of Polymer Science: Polymer Physics Edition,* 22**,** 1331-1342.

Li, Y., L. T. Lim & Y. Kakuda (2009) Electrospun Zein fibers as carriers to stabilize (-)-epigallocatechin gallate. *Journal of Food Science,* 74**,** C233-C240.

Liang, L., V. L. S. Line, G. E. Remondetto & M. Subirade (2010) In vitro release of alpha-tocopherol from emulsion-loaded beta-lactoglobulin gels. *International Dairy Journal,* 20**,** 176-181.

Liu, X., Q. Sun, H. Wang, L. Zhang & J.-Y. Wang (2005) Microspheres of corn protein, zein, for an ivermectin drug delivery system. *Biomaterials,* 26**,** 109-115.

Liu, Z. H., Y. P. Jiao, Y. F. Wang, C. R. Zhou & Z. Y. Zhang (2008) Polysaccharides-based nanoparticles as drug delivery systems. *Advanced Drug Delivery Reviews,* 60**,** 1650-1662.

Lopez-Rubio, A., E. Sanchez, Y. Sanz & J. M. Lagaron (2009) Encapsulation of living bifidobacteria in ultrathin PVOH electrospun fibers. *Biomacromolecules,* 10**,** 2823-2829.

Luo, Y., Z. Teng & Q. Wang (2012) Development of Zein nanoparticles coated with carboxymethyl chitosn for encapsulation and controlled release of vitamin D3. *Journal of Agricultural and Food Chemistry,* 60**,** 836-843.

Luo, Y. C., B. C. Zhang, M. Whent, L. L. Yu & Q. Wang (2011) Preparation and characterization of zein/chitosan complex for encapsulation of alpha-tocopherol, and its in vitro controlled release study. *Colloids and Surfaces B-Biointerfaces,* 85**,** 145-152.

Maleki, M., M. Latifi, M. Amani-Tehran & S. Mathur (2013) Electrospun core-shell nanofibers for drug encapsulation and sustained release. *Polymer Engineering and Science,* 53**,** 1770-1779.

Marsanasco, M., A. L. Marquez, J. R. Wagner, S. D. Alonso & N. S. Chiaramoni (2011a) Liposomes as vehicles for vitamins E and C: An alternative to fortify orange juice and offer vitamin C protection after heat treatment. *Food Research International,* 44**,** 3039-3046.

Marsanasco, M., A. L. Márquez, J. R. Wagner, S. del V. Alonso & N. S. Chiaramoni (2011b) Liposomes as vehicles for vitamins E and C: An alternative to fortify orange juice and offer vitamin C protection after heat treatment. *Food Research International,* 44**,** 3039-3046.

Matalanis, A., O. G. Jones & D. J. McClements (2011) Structured biopolymer-based delivery systems for encapsulation, protection, and release of lipophilic compounds. *Food Hydrocolloids,* 25**,** 1865-1880.

McClements, D. J. (2011) Edible nanoemulsions: fabrication, properties, and functional performance. *Soft Matter,* 7**,** 2297-2316.

McClements, D. J., E. A. Decker, Y. Park & J. Weiss (2009) Structural design principles for delivery of bioactive components in nutraceuticals and functional foods. *Critical Reviews in Food Science and Nutrition,* 49**,** 577-606.

Minogue, P. J. & J. N. Thomas (2004) An alpha-tocopherol dose response study in Paramecium tetraurelia. *Mechanisms of Ageing and Development,* 125**,** 21-30.

Miquel, E., A. Alegria, R. Barbera, R. Farre & G. Clemente (2004) Stability of tocopherols in adapted milk-based infant formulas during storage. *International Dairy Journal,* 14**,** 1003-1011.

Moore, M. A., C. B. Park & H. Tsuda (1998) Soluble and insoluble fiber influences on cancer development. *Critical Reviews in Oncology Hematology,* 27**,** 229-242.

Mozafari, M. R., C. Johnson, S. Hatziantoniou & C. Demetzos (2008) Nanoliposomes and Their Applications in Food Nanotechnology. *Journal of Liposome Research,* 18**,** 309-327.

Murugeshu, A., C. Astete, C. Leonardi, T. Morgan & C. M. Sabliov (2011) Chitosan/PLGA particles for controlled release of alpha-tocopherol in the GI tract via oral administration. *Nanomedicine,* 6**,** 1513-1528.

Neo, Y. P., S. Ray, J. Jin, M. Gizdavic-Nikolaidis, M. K. Nieuwoudt, D. Y. Liu & S. Y. Quek (2013) Encapsulation of food grade antioxidant in natural biopolymer by electrospinning technique: A physicochemical study based on zein-gallic acid system. *Food Chemistry,* 136**,** 1013-1021.

Newman, R. K., A. A. Betschart, C. W. Newman & P. J. Hofer (1992) Effect of full-fat defatted rice bran on serum-cholesterol. *Plant Foods for Human Nutrition,* 42**,** 37-43.

Nissiotis, M. & M. Tasioula-Margari (2002) Changes in antioxidant concentration of virgin olive oil during thermal oxidation. *Food Chemistry,* 77**,** 371-376.

O'Shea, N., E. K. Arendt & E. Gallagher (2012) Dietary fibre and phytochemical characteristics of fruit and vegetable by-products and their recent applications as novel ingredients in food products. *Innovative Food Science & Emerging Technologies,* 16**,** 1-10.

Opanasopit, P., U. Ruktanonchai, O. Suwantong, S. Panomsuk, T. Ngawhirunpat, C. Sittisombut, T. Suksamran & P. Supaphol (2008) Electrospun poly(vinyl alcohol) fiber mats as carriers for extracts from the fruit hull of mangosteen. *Journal of Cosmetic Science,* 59**,** 233-242.

Orrenius, S., B. Zhivotovsky & P. Nicotera (2003) Regulation of cell death: The calcium-apoptosis link. *Nature Reviews Molecular Cell Biology,* 4**,** 552-565.

Pakravan, M., M. C. Heuzey & A. Ajji (2012) Core-shell structured PEO-chitosan nanofibers by coaxial electrospinning. *Biomacromolecules,* 13**,** 412-421.

Park, J. Y., I. H. Lee & G. N. Bea (2008) Optimization of the electrospinning conditions for preparation of nanofibers from polyvinylacetate (PVAc) in ethanol solvent. *Journal of Industrial and Engineering Chemistry,* 14**,** 707-713.

Pillay, V., C. Dott, Y. E. Choonara, C. Tyagi, L. Tomar, P. Kumar, L. C. du Toit & V. M. K. Ndesendo (2013) A review of the effect of processing variables on the fabrication of electrospun nanofibers for drug delivery applications. *Journal of Nanomaterials*.

Pirisi, F. M., A. Angioni, G. Bandino, P. Cabras, C. Guillou, E. Maccioni & F. Reniero (1998) Photolysis of alpha-tocopherol in olive oils and model systems. *Journal of Agricultural and Food Chemistry,* 46**,** 4529-4533.

Qi, R. L., R. Guo, M. W. Shen, X. Y. Cao, L. Q. Zhang, J. J. Xu, J. Y. Yu & X. Y. Shi (2010) Electrospun poly(lactic-co-glycolicacid)/halloysite nanotube composite nanofibers for drug encapsulation and sustained release. *Journal of Materials Chemistry,* 20**,** 10622-10629.

Randall, J. M., R. N. Sayre, W. G. Schultz, R. Y. Fong, A. P. Mossman, R. E. Tribelhorn & R. M. Saunders (1985) Rice bran stabilization by extrusion cokking for extraction of edible oil. *Journal of Food Science,* 50**,** 361-364.

Rathna, G. V. N., J. P. Jog & A. B. Gaikwad (2011) Development of non-woven nanofibers of egg albumen-poly (vinyl alcohol) blends: influence of solution properties on morphology of nanofibers. *Polymer Journal,* 43**,** 654-661.

Rimbach, G., J. Moehring, P. Huebbe & J. K. Lodge (2010) Gene-regulatory activity of alpha-tocopherol. *Molecules,* 15**,** 1746-1761.

Rivas, S., E. Conde, A. Moure, H. Dominguez & J. C. Parajo (2013) Characterization, refining and antioxidant activity of saccharides derived from hemicelluloses of wood and rice husks. *Food Chemistry,* 141**,** 495-502.

Rouanet, J. M., C. Laurent & P. Besancon (1993) Rice bran and wheat bran: selective effect on plasma and liver cholesterol in high-cholesterol fed rats. *Food Chemistry,* 47**,** 67-71.

Saberi, A. H., Y. Fang & D. J. McClements (2013) Fabrication of vitamin E-enriched nanoemulsions: Factors affecting particle size using spontaneous emulsification. *Journal of Colloid and Interface Science,* 391**,** 95-102.

Sabliov, C. M., C. Fronczek, C. E. Astete, M. Khachaturyan, L. Khachatryan & C. Leonardi (2009) Effects of temperature and UV light on degradation of alpha-tocopherol in free and dissolved form. *Journal of the American Oil Chemists Society,* 86**,** 895-902.

Sadri, M., A. Maleki, F. Agend & H. Hosseini (2012) Fast and efficient electrospinning of chitosan-poly(ethylene oxide) nanofibers as potential wound dressing agents for tissue engineering. *Journal of Applied Polymer Science,* 126.

Sagalowicz, L., M. E. Leser, H. J. Watzke & M. Michel (2006) Monoglyceride self-assembly structures as delivery vehicles. *Trends in Food Science & Technology,* 17**,** 204-214.

Sain, M. & S. Panthapulakkal (2006) Bioprocess preparation of wheat straw fibers and their characterization. *Industrial Crops and Products,* 23**,** 1-8.

Sansdrap, P. & A. J. Moës (1997) In vitro evaluation of the hydrolytic degradation of dispersed and aggregated poly(dl-lactide-co-glycolide) microspheres. *Journal of Controlled Release,* 43**,** 47-58.

Saunders, R. M. (1990) The properties of rice bran as a foodstuff. *Cereal Foods World,* 35**,** 632-636.

Scheller, H. V. & P. Ulvskov. 2010. Hemicelluloses. In *Annual Review of Plant Biology, Vol 61,* eds. S. Merchant, W. R. Briggs & D. Ort, 263-289.

Shen, X. X., D. G. Yu, L. M. Zhu, C. Branford-White, K. White & N. P. Chatterton (2011) Electrospun diclofenac sodium loaded Eudragit (R) L 100-55 nanofibers for colon-targeted drug delivery. *International Journal of Pharmaceutics,* 408**,** 200-207.

Sheng, X. Y., L. P. Fan, C. L. He, K. H. Zhang, X. M. Mo & H. S. Wang (2013) Vitamin E-loaded silk fibroin nanofibrous mats fabricated by green process for skin care application. *International Journal of Biological Macromolecules,* 56**,** 49-56.

Shin, T. S., J. S. Godber, D. E. Martin & J. H. Wells (1997) Hydrolytic stability and changes in E vitamers and oryzanol of extruded rice bran during storage. *Journal of Food Science,* 62**,** 704-&.

Shukat, R., C. Bourgaux & P. Relkin (2012) Crystallisation behaviour of palm oil nanoemulsions carrying vitamin E. *Journal of Thermal Analysis and Calorimetry,* 108**,** 153-161.

Singh, R. P. H., Dennis R. . 2009. *Introduction to Food Engineering, 4th ed*. Burlington, MA: Elsevier.

Somchue, W., W. Sermsri, J. Shiowatana & A. Siripinyanond (2009) Encapsulation of alpha-tocopherol in protein-based delivery particles. *Food Research International,* 42**,** 909-914.

Song, W., X. W. Yu, D. C. Markel, T. Shi & W. P. Ren (2013) Coaxial PCL/PVA electrospun nanofibers: osseointegration enhancer and controlled drug release device. *Biofabrication,* 5.

Sridhar, R., S. Sundarrajan, J. R. Venugopal, R. Ravichandran & S. Ramakrishna (2013) Electrospun inorganic and polymer composite nanofibers for biomedical applications. *Journal of Biomaterials Science-Polymer Edition,* 24**,** 365-385.

Sudha, M. L., R. Vetrimani & K. Leelavathi (2007) Influence of fibre from different cereals on the rheological characteristics of wheat flour dough and on biscuit quality. *Food Chemistry,* 100**,** 1365-1370.

Suwantong, O., P. Opanasopit, U. Ruktanonchai & P. Supaphol (2007) Electrospun cellulose acetate fiber mats containing curcumin and release characteristic of the herbal substance. *Polymer,* 48**,** 7546-7557.

Suwantong, O., U. Ruktanonchai & P. Supaphol (2010) In vitro biological evaluation of electrospun cellulose acetate fiber mats containing asiaticoside or curcumin. *Journal of Biomedical Materials Research Part A,* 94A**,** 1216-1225.

Taepaiboon, P., U. Rungsardthong & P. Supaphol (2007) Vitamin-loaded electrospun cellulose acetate nanofiber mats as transdermal and dermal therapeutic agents. of vitamin A acid and vitamin E. *European Journal of Pharmaceutics and Biopharmaceutics,* 67**,** 387-397.

Takeshita, M., S. Nakamura, F. Makita, S. Ohwada, Y. Miyamoto & Y. Morishita (1992) Antitumor effect of RBS (rice bran saccharide) on ENNG-induced carcinogenesis. *Biotherapy,* 4**,** 139-145.

Thuy, T. T. N., C. Ghosh, S. G. Hwang, N. Chanunpanich & J. S. Park (2012) Porous core/sheath composite nanofibers fabricated by coaxial electrospinning as a potential mat for drug release system. *International Journal of Pharmaceutics,* 439**,** 296-306.

Tong, H. W., X. Zhang & M. Wang (2012) A new nanofiber fabrication technique based on coaxial electrospinning. *Materials Letters,* 66**,** 257-260.

Torres-Giner, S., E. Gimenez & J. M. Lagarona (2008) Characterization of the morphology and thermal properties of zein prolamine nanostructures obtained by electrospinning. *Food Hydrocolloids,* 22**,** 601-614.

Traber, M. G. & J. Atkinson (2007) Vitamin E, antioxidant and nothing more. *Free Radical Biology and Medicine,* 43**,** 4-15.

Trombino, S., R. Cassano, R. Muzzalupo, A. Pingitore, E. Cione & N. Picci (2009) Stearyl ferulate-based solid lipid nanoparticles for the encapsulation and stabilization of beta-carotene and alpha-tocopherol. *Colloids and Surfaces B-Biointerfaces,* 72**,** 181-187.

Unnithan, A. R., N. A. M. Barakat, P. B. T. Pichiah, G. Gnanasekaran, R. Nirmala, Y. S. Cha, C. H. Jung, M. El-Newehy & H. Y. Kim (2012) Wound-dressing materials with antibacterial activity from electrospun polyurethane-dextran nanofiber mats containing ciprofloxacin HCl. *Carbohydrate Polymers,* 90**,** 1786-1793.

Veenashri, B. R. & G. Muralikrishna (2011) In vitro anti-oxidant activity of xylo-oligosaccharides derived from cereal and millet brans - A comparative study. *Food Chemistry,* 126**,** 1475-1481.

Velikov, K. P. & E. Pelan (2008) Colloidal delivery systems for micronutrients and nutraceuticals. *Soft Matter,* 4**,** 1964-1980.

Viuda-Martos, M., M. C. Lopez-Marcos, J. Fernandez-Lopez, E. Sendra, J. H. Lopez-Vargas & J. A. Perez-Alvarez (2010) Role of Fiber in Cardiovascular Diseases: A Review. *Comprehensive Reviews in Food Science and Food Safety,* 9**,** 240-258.

Wan, Y. T., J. D. Bankston, P. J. Bechtel & S. Sathivel (2011) Microencapsulation of menhaden fish oil containing soluble rice bran fiber using spray drying technology. *Journal of Food Science,* 76**,** E348-E356.

Wan, Y. T., A. Prudente & S. Sathivel (2012) Purification of soluble rice bran fiber using ultrafiltration technology. *Lwt-Food Science and Technology,* 46**,** 574-579.

Wang, L., X. X. Li & Z. X. Chen (2009) Sulfated modification of the polysaccharides obtained from defatted rice bran and their antitumor activities. *International Journal of Biological Macromolecules,* 44**,** 211-214.

Wang, L., H. B. Zhang, X. Y. Zhang & Z. X. Chen (2008) Purification and identification of a novel heteropolysaccharide RBPS2a with anti-complementary activity from defatted rice bran. *Food Chemistry,* 110**,** 150-155.

Wang, R., Z. Tian & L. Chen (2011) Nano-encapsulations liberated from barley protein microparticles for oral delivery of bioactive compounds. *International Journal of Pharmaceutics,* 406**,** 153-162.

Wang, S., M. F. Marcone, S. Barbut & L.-T. Lim (2013) Electrospun soy protein isolate-based fiber fortified with anthocyanin-rich red raspberry (Rubus strigosus) extracts. *Food Research International,* 52**,** 467-472.

Woerdeman, D. L., P. Ye, S. Shenoy, R. S. Parnas, G. E. Wnek & O. Trofimova (2005) Electrospun fibers from wheat protein: Investigation of the interplay between molecular structure and the fluid dynamics of the electrospinning process. *Biomacromolecules,* 6**,** 707-712.

Wu, X. M., C. J. Branford-White, D. G. Yu, N. P. Chatterton & L. M. Zhu (2011) Preparation of core-shell PAN nanofibers encapsulated alpha-tocopherol acetate and ascorbic acid 2-phosphate for photoprotection. *Colloids and Surfaces B-Biointerfaces,* 82**,** 247-252.

Xiang, T., Z. L. Zhang, H. Q. Liu, Z. Z. Yin, L. Li & X. M. Liu (2013) Characterization of cellulose-based electrospun nanofiber membrane and its adsorptive behaviours using Cu(II), Cd(II), Pb(II) as models. *Science China-Chemistry,* 56**,** 567-575.

Xie, J. B. & Y. L. Hsieh (2003) Ultra-high surface fibrous membranes from electrospinning of natural proteins: casein and lipase enzyme. *Journal of Materials Science,* 38**,** 2125-2133.

Xie, J. W., X. R. Li & Y. N. Xia (2008) Putting Electrospun Nanofibers to Work for Biomedical Research. *Macromolecular Rapid Communications,* 29**,** 1775-1792.

Xie, W. L. & J. M. Ji (2008) Antioxidant activities of vitamins E and C in a novel liposome system. *Journal of Food Biochemistry,* 32**,** 766-781.

Xiong, X., Q. Li, J. W. Lu, Z. X. Guo, Z. H. Sun & J. Yu (2012) Fibrous scaffolds made by co-electrospinning soluble eggshell membrane protein with biodegradable synthetic polymers. *Journal of Biomaterials Science-Polymer Edition,* 23**,** 1217-1230.

Xu, K. L., N. Tavernarakis & M. Driscoll (2001) Necrotic cell death in C-elegans requires the function of calreticulin and regulators of Ca2+ release from the endoplasmic reticulum. *Neuron,* 31**,** 957-971.

Xu, X. L., X. L. Zhuang, X. S. Chen, X. R. Wang, L. X. Yang & X. B. Jing (2006) Preparation of core-sheath composite nanofibers by emulsion electrospinning. *Macromolecular Rapid Communications,* 27**,** 1637-1642.

Xu, X. Z., L. Jiang, Z. P. Zhou, X. F. Wu & Y. C. Wang (2012) Preparation and properties of electrospun soy protein Isolate/polyethylene oxide nanofiber membranes. *Acs Applied Materials & Interfaces,* 4**,** 4331-4337.

Yang, J. M., L. S. Zha, D. G. Yu & J. Y. Liu (2013) Coaxial electrospinning with acetic acid for preparing ferulic acid/zein composite fibers with improved drug release profiles. *Colloids and Surfaces B-Biointerfaces,* 102**,** 737-743.

Yang, Y. & D. J. McClements (2013a) Encapsulation of vitamin E in edible emulsions fabricated using a natural surfactant. *Food Hydrocolloids,* 30**,** 712-720.

Yang, Y. & D. J. McClements (2013b) Vitamin E bioaccessibility: Influence of carrier oil type on digestion and release of emulsified α-tocopherol acetate. *Food Chemistry,* 141**,** 473-481.

Yang, Z. Y. & S. L. Huffman (2011) Review of fortified food and beverage products for pregnant and lactating women and their impact on nutritional status. *Maternal and Child Nutrition,* 7**,** 19-43.

Yao, C., X. S. Li & T. Y. Song (2009) Preparation and characterization of Zein and Zein/Poly-L-lactide nanofiber yarns. *Journal of Applied Polymer Science,* 114**,** 2079-2086.

Yoo, H. S., T. G. Kim & T. G. Park (2009) Surface-functionalized electrospun nanofibers for tissue engineering and drug delivery. *Advanced Drug Delivery Reviews,* 61**,** 1033-1042.

Yoon, Y. & E. Choe (2009) Lipid oxidation and stability of tocopherols and phospholipids in soy-added fried products during storage in the dark. *Food Science and Biotechnology,* 18**,** 356-361.

You, Y., B. M. Min, S. J. Lee, T. S. Lee & W. H. Park (2005) In vitro degradation behavior of electrospun polyglycolide, polylactide, and poly(lactide-co-glycolide). *Journal of Applied Polymer Science,* 95**,** 193-200.

Yu, D.-G., Zhu, Li-Min, White, Kenneth, Branford-White, Chris (2009) Electrospun nanofiber-based drug delivery systems. *Health,* 01**,** 67-75.

Zha, X. Q., J. P. Luo, L. Zhang & J. Hao (2009a) Antioxidant properties of different polysaccharides extracted with water and sodium hydroxide from rice bran. *Food Science and Biotechnology,* 18**,** 449-455.

Zha, X. Q., J. H. Wang, X. F. Yang, H. Liang, L. L. Zhao, S. H. Bao, J. P. Luo, Y. Y. Xu & B. B. Zhou (2009b) Antioxidant properties of polysaccharide fractions with different molecular mass extracted with hot-water from rice bran. *Carbohydrate Polymers,* 78**,** 570-575.

Zhang, X. W., R. Nakagawa, K. H. K. Chan & M. Kotaki (2012) Mechanical property enhancement of polylactide nanofibers through optimization of molecular weight, electrospinning conditions, and stereocomplexation. *Macromolecules,* 45**,** 5494-5500.

Zhang, Y. Z., X. Wang, Y. Feng, J. Li, C. T. Lim & S. Ramakrishna (2006) Coaxial electrospinning of (fluorescein isothiocyanate-conjugated bovine serum albumin)-encapsulated poly(epsilon-caprolactone) nanofibers for sustained release. *Biomacromolecules,* 7**,** 1049-1057.

Zhao, L. P., H. Xiong, H. L. Peng, Q. Wang, D. Han, C. Q. Bai, Y. Z. Liu, S. H. Shi & B. Deng (2011) PEG-coated lyophilized proliposomes: preparation, characterizations and in vitro release evaluation of vitamin E. *European Food Research and Technology,* 232**,** 647-654.

Zhu, K. X., S. Huang, W. Peng, H. F. Qian & H. M. Zhou (2010) Effect of ultrafine grinding on hydration and antioxidant properties of wheat bran dietary fiber. *Food Research International,* 43**,** 943-948.

Ziani, K., Y. Fang & D. J. McClements (2012) Encapsulation of functional lipophilic components in surfactant-based colloidal delivery systems: Vitamin E, vitamin D, and lemon oil. *Food Chemistry,* 134**,** 1106-1112.

Zigoneanu, I. G., C. E. Astete & C. M. Sabliov (2008) Nanoparticles with entrapped alpha-tocopherol: synthesis, characterization, and controlled release. *Nanotechnology,* 19.

Zuckerman, B. M. & M. A. Geist (1983) Effects of vitamin E on the nematode Caenorhabditis elegans. *Age,* 6**,** 1-4.

VITA

Juan Li graduated from Hunan Agricultural University in Hunan, China, with a Bachelor of Science degree in Food Science and Engineering in June 2007. She earned her Master of Science in Food Science from Hunan Agricultural University, Hunan, China, in June 2010. She joined the Department of Food Science at Louisiana State University as a Ph.D. student under the direction of Dr. Subramaniam Sathivel in August 2010. She will receive her degree in Food Science in December, 2013. Juan published two refereed articles and 3 abstracts. Juan was awarded first place and $1000 at the 2013 IFT- Refrigerated and Frozen Foods division graduate student paper competition for presenting a paper entitled "Development of a combined osmotic dehydration and cryogenic freezing process for minimizing quality changes during freezing with application to fruits and vegetables".